Sediment pathways
in San Francisco South Bay

O.M. (Oxana) van Kempen

MSc Thesis

The cover picture shows a distinct stratification between the clear saline water from the Pacific and the more turbid freshwater in San Francisco Bay at the moment of peak flood velocity. The photograph was taken by the author at Angel Island, directed to San Pablo Bay, on 23^{th} of July 2017 at 11:00 PST.

Sediment pathways
in San Francisco South Bay

by

O.M. (Oxana) van Kempen

to obtain the degree of Master of Science in Hydraulic Engineering,
at the faculty of Civil Engineering and Geosciences at the Delft University of Technology,
to be defended publicly on Friday December 15, 2017 at 11:00 AM.

Student number:	4086996	
Project duration:	March 2, 2017 – December 15, 2017	
Thesis committee:	Prof. dr. J.D. Pietrzak,	TU Delft, supervisor
	Prof. dr. ir. Z.B. Wang,	TU Delft
	Dr. ir. B. van Maren,	TU Delft
	Dr. ir. M. van der Wegen,	Deltares, Unesco - IHE

TU Delft Deltares Enabling Delta Life SFEI San Francisco Estuary Institute & the Aquatic Science Center AQUATIC SCIENCE CENTER USGS science for a changing world UNESCO-IHE Institute for Water Education

Preface

This master thesis is the final product of my master Hydraulic engineering at the Technical University Delft. In this research, an analysis is performed on the sediment pathways in San Francisco South Bay. I have carried out the thesis in cooperation with Deltares, an institute for applied research in the field of water and subsurface, and the San Francisco Estuary Institute (SFEI), one of California's premier aquatic and ecosystem science institutes.

Researching the sediment pathways in San Francisco South Bay is part of a collaboration between USGS, SFEI, Deltares and Unesco-IHE. The focus of this partnership is to understand how coastal ecosystem functions and human disturbances alter those functions. One component of this program is directed toward following and understanding the water quality of San Francisco Bay. I hope this thesis will contribute to understanding the water quality by gaining more insight into the sediment pathways in South Bay.

I am very grateful that I had the opportunity to visit SFEI in Richmond during my research. In my three week stay, I had interesting discussions about the physics of the Bay Area with the SFEI colleagues and had the spare time to explore the Bay Area including San Francisco City. Additionally, I had the opportunity to join the scientific Peterson cruise for a two days field experiment as a visiting scientist. All combined, it was a pleasant experience, and I am thankful for everyone that made this trip possible and fun. Many thanks, Rusty, for inviting me to SFEI, for lending me your bike and for all the fruitful conversations during my stay at SFEI as well as during the plenty skype-calls we had last year.

I would also like to thank my academic supervisors for their guidance through the process of this research; Julie Pietrzak, Zheng Wang, Bas van Maren and Mick van der Wegen. Special thank you, Mick, for the extensive guidance from the beginning and for keeping me focused and enthusiastic throughout the process. I am very grateful that you created the opportunity for my stay in San Francisco.

I am also grateful to the Deltares employees who helped me and who were always there to answer my questions. Thank you, Arjen Markus, for all your help facing the challenges with DelwaQ.

And lastly, thanks to all my fellow graduate students at Deltares, thank you all for the great time we had and the many fruitful discussions, and thanks to everyone else who contributed in one or another way to this thesis.

O.M. (Oxana) van Kempen
Delft, December 2017

Abstract

This study aims for a better understanding of the sediment pathways in San Francisco South Bay (South Bay). Many issues relevant to the Bay Area community such as shipping, recreational and commercial fishing, habitat restoration, human health, and environmental water quality are reliant on understanding sediment pathways (McKee et al. [2006]). Existing theories suggest that the Sacramento-San Joaquin Delta deliver sediment to South Bay during periods of high river flows. Different hydrodynamic forces, such as the tide, wind and baroclinic flows, redistribute these sediments around South Bay.

In this research, trends are analysed using a new set of data (WY2015-WY2017) and sediment pathways in time and space are investigated using a 3D numerical model. In this model, the pathways of three sediment classes with different settling velocities are traced from their source throughout the Bay Area. No such study has yet been undertaken in the South Bay Area.

There is a high Delta sediment input to South Bay during periods of high river flow. The local tributaries contribute only marginally to the suspended sediment concentration of South Bay. With a decreasing sediment load from the Delta, the importance of the local tributaries as a sediment source for South Bay could increase.

In this research, three different types of sediment exchange between Central Bay and South Bay are observed. The first type is observed during periods of low river flows ($Q_{Delta} < 800 m^3/s$). A seaward directed residual flow is found in the channel at Bay Bridge. Sediments are slowly transported out of South Bay. The second type is observed after a period of moderate river flow ($Q_{Delta} > 800 m^3/s$). A pulsed sediment flux from the Delta increases the turbidity of Central Bay, resulting in a horizontal spatial variation in SSC from Central Bay to South Bay. The diffusive character of the tide transports the sediments slowly from the turbid Central Bay to the relatively clearer South Bay. The third sediment exchange type is observed after an extreme Delta river flow ($Q_{Delta} > 10,000 m^3/s$)). The extreme Delta flow refreshes a large part of Central Bay and South Bay. The salinity of Central Bay increases slowly, resulting in a substantially more saline Central Bay than South Bay for a couple of months. The resulting baroclinic flow transports the sediments from Central Bay into South Bay through the landward directed bottom current.

Two dominant pathways with opposite transport direction characterise the sediment transport in South Bay. One pathway is located in the channel and is directed southward during periods of high river runoff. The second pathway is located on the extensive east flat and is directed northward during periods of high river runoff. The transport in the channel is dominant during the wet period, resulting in a net transport landward. Besides these two dominant pathways, four re-circulations cells are found, facilitating the exchange between the channel and the shoals.

The next step in gaining more insight into the sediment physics is a model study which includes bed-interaction with the suspended sediments. A study like this could confirm the hypotheses opted in this research.

Contents

List of Figures

Nomenclature

Alameda	Alameda Creek
Cond	Conductance
Coyote	Coyote Creek
D-Flow FM	D-Flow Flexible Mesh
DelwaQ	D- Water Quality
Delta	Sacramento-San Joaquin Delta
Guadalupe	Guadalupe River
Lower South Bay	The sub-embayment south of Dumbarton Bridge
North Bay	northern reach of San Francisco South Bay (Central Bay, San Pablo Bay and Suisin Bay)
Pacific	Pacific Ocean
PSU	Practical Saliniy Unit
Sal	Salinity
SFEI	San Francisco Estuary Institute
South Bay	San Francisco South Bay (Reach between Bay Bridge and Dumbarton Bridge)
SSC	Suspended Sediment Concentration
SSF	Suspended Sediment Flux
Temp	Temperature
USGS	United Stated Geological Survey
WOCSS	Winds of Critical Streamline Surfaces
WWTP	Waste water treatment plant
WY	Water year

Symbols

Symbol	Description	Unit
c_f	Friction coefficient	-
c_b	Concentration of suspended matter near the bed	gm^{-3}
D	Deposition rate	$gm^{-2}d^{-1}$
d	Sediment diameter	μm
E	Erosion rate	$gm^{2}d^{-1}$
f_w	Johnsson's wave friction factor	-
Q	Discharge	m^3s^{-1}
M	Zero-order resuspension	$gm^{-2}d^{-1}$
u	Velocity	ms^{-1}
u_c^*	Shear velocity induced by the current	ms^{-1}
u_w^*	Shear velocity induced by the waves	ms^{-1}
u_{orb}	Orbital velocity	ms^{-1}
w_s	Settling velocity	mms^{-1}
ρ_w	Density of water	kgm^{-3}
τ_b	Bed shear stress	Nm^{-2}
τ_{ce}	Critical bed shear stress for erosion	Nm^{-2}
τ_{cs}	Critical bed shear stress for sedimentation	Nm^{-2}
τ_{cw}	Bed shear stress due to combined wave and current action	Nm^{-2}
τ_c	Bed shear stress due to current action	Nm^{-2}
τ_w	Bed shear stress due to wave action	Nm^{-2}

1

Research Introduction

Pritchard defined an estuary as a semi-enclosed body of water where fresh water from inland meets salt water from the marine environment [Pietrzak, 2016]. The tide, river discharge and the wind mix these waters with different densities within the estuary. The result is an exchange of water, substances and suspended particle matter (SPM) between the freshwater system and the marine environment [De Nijs, 2012, McCulloch et al., 1970]. These physical processes have a significant impact on the sedimentological processes within the estuary and its water quality [Pietrzak, 2016].

This chapter introduces the research. Firstly, a short introduction into San Francisco Bay and the motivation of this research is described in §1.1. In §1.2, the hydrodynamic conditions of San Francisco Bay are considered and lastly the existing theories on sediment transport in South Bay and the research questions are discussed in §1.3.

1.1. Introduction San Francisco Bay

The San Francisco Bay is the largest estuary on the California coast and the second largest in the United states [Barnard et al., 2013]. A major urban area surrounds it with a population of over seven million people [Barnard et al., 2013, Schellenbarger et al., 2013]. These people use the Bay for municipal and industrial sewage disposal, recreation, commerce, fishing, and as a source of aesthetic pleasure [McCulloch et al., 1970].

The southern reach of the estuary is threatened by elevated levels of several contaminants [Kimmerer, 2004]. The state of California has therefore issued health advisories recommending limits on the consumption of fish, drinking water and had to close beaches because of the pollution for some periods over the last years[San Francisco Bay conservation, 2017]. The contaminants originate from urban and agricultural runoff, treated industrial and municipal wastewater, atmospheric deposition, and chemicals applied directly to the surface water for invasive plants and pest control [Fong et al., 2016].

Fine suspended material acts as a carrier of these contaminants, due to the highly sorptive affinity of fine suspended material [Winterwerp and Prooijen, 2016]. The contaminants are transported into the Bay attached to suspended sediment particles [McKee et al., 2006] and are moved around within the estuary along the sediment pathways. Research into sediment dynamics can lead to better insight into the transport and fate of the contaminants in the Bay. Besides, the measurement of SSC and sediment fluxes are less costly and more easily measured than the contaminant particles [Bergamaschi et al., 2001, Schoellhamer et al., 2007].

Fine sediments characterise the southern reach of San Francisco Bay (South Bay). The average mean grain size found during bed sampling studies is 52 μm [Barnard et al., 2012, 2013, Brand et al., 2015, Buchanan and Schoellhamer, 1996, Schoellhamer et al., 2007]. The bed consist of 75 percent of silt particles and the remaining 25 percent are sand and clay particles. The average sediment concentration in the water column is between 10 and 200 mgL^{-1}. For the extreme cases, this concentration can vary between the 600 and 2000 mgL^{-1} [Cloern and Schraga, 2016a]. The concentration range at the shoals is higher than at the channel. The

concentration in the channels varies with the daily and spring-neap tidal cycles, with an elevated concentration during the wet periods. [Lacey et al., 2014, USGS, 2017]. During the winter, the sediment concentration in Central Bay is often higher than in South Bay, and this reverses in summer periods [Carlson and McCulloch, 1974].

The large rivers and tributaries are the primary sources of sediments for South Bay. A distinction can be made between the tributaries that flow directly into South Bay and the Sacramento-San Joaquin Delta that supplies sediment to South Bay through Central Bay. The wastewater treatment plants that distribute their sewage in South Bay do not discharge any sediments [SFEI, 2017]. The Pacific acts as a sink of the bay [Barnard et al., 2012, Conomos and Peterson, 1977, Schoellhamer et al., 2007].

This research focuses on understanding the sediment pathways in the southern reach of the Bay Area. Before describing the existing theories, a brief introduction of the hydrodynamic conditions is given.

1.2. Hydrodynamic conditions San Francisco Bay

The San Francisco Bay can be divided into two geographically and hydrologically distinct sub-estuaries. The northern reach lies between the connection to the Pacific Ocean at the Golden Gate and the confluence of the Sacramento-San Joaquin river system. The southern reach is the area between the Bay Bridge (linking San Francisco with Alameda) and the southern end of the Bay (Fig. 1.1) [Conomos, 1979].

In the northern reach, the river outflow of the Sacramento San-Joaquin Delta meets the salt water of the Pacific entering at the Golden Gate Bridge. The mixing of the waters of two different densities depends mainly

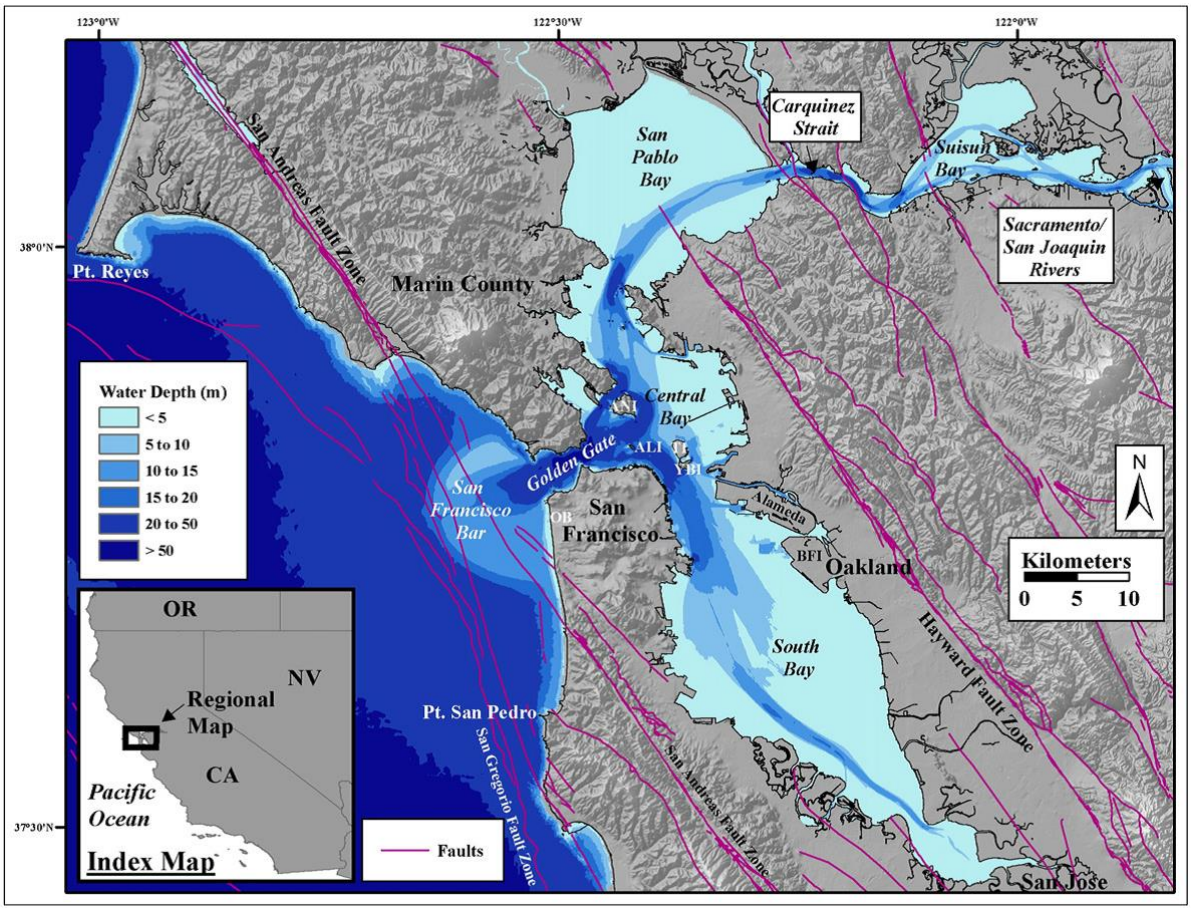

Figure 1.1: The general geographical overview of the San Francisco Bay. The Northern reach consists of Central Bay, San Pablo Bay and Suisun Bay. The southern reach only consists of South Bay. The different blue colours indicate the water depth. [Barnard et al., 2012].

on the seasonal varying river inflow, resulting in a partially mixed estuary[Conomos et al., 1985].

The outflow of the tributaries entering the southern reach (South Bay) is small. Therefore, South Bay does not have a normal estuarine pattern. Instead, South Bay is dependent upon water that enters from Central Bay for its circulation [McCulloch et al., 1970]. It is a tidally oscillating lagoon-type estuary which is mainly well mixed over time, with periods of stratification [Conomos et al., 1985, McCulloch et al., 1970, Pubben, 2017]. It has a channel-shoal morphology with narrow, deep channels surrounded by extensive areas of shallow water and mudflats (Fig. 1.1) [Schellenbarger et al., 2013] .

1.2.1. Tide

The tides propagate from the Pacific Ocean through the narrow opening at the Golden Gate, via Central Bay, into South Bay (Fig. 1.1). Here, the 'tide' refers to sea-level variation and 'tidal currents' is used to denote water movement. The tide is of mixed diurnal and semidiurnal type, with dominant M2, K1, O1 and S2 constituents. With a form factor of 0.85 the tide is primarily semi-diurnal, so two times a high water and two times a low water a day, with one high water higher than the other [Bosboom and Stive, 2013, Chengt and Gartner, 1985, Walters et al., 1985].

The highest tidal range is observed during spring tide (1.78 m) at the Golden gate [Kimmerer, 2004]). The daily inequality is high, and the tidal currents are significant with over 1 ms^{-1} in the channel and 0.4 ms^{-1} on the shoals. At neap tides the tidal height inequality is small, and the strength of the currents becomes moderate to 0.5 ms^{-1} in the channels [Barnard et al., 2013, Conomos, 1979, Conomos et al., 1985, Schoellhamer et al., 2016, Walters et al., 1985].

South Bay is an enclosed embayment. Therefore, the tides reflection from the South end of the Bay superimposes the incoming tides, and the tides become nearly standing waves. The mean range of the tide at the south end of the Bay is 2.2 m, which is 1.0 m greater than the 1.2 m range at the golden gate [Krone, 1993]. At the Southern tip of the Bay, the tidal currents precede the water levels by $1/4^{th}$ of the tidal cycle. The phase speed is higher in the deep channels than in the shoals. There is a tendency for the wave to propagate down the channels and then disperse into the shoals [Walters et al., 1985].

1.2.2. Freshwater inflow

The freshwater inflow by rivers is small compared to tidal flows in South Bay. There are 450 smaller drainages such as local streams and sewage that have a combined annual discharge of only 7.6 % of the volume of South Bay [Kimmerer, 2004, McCulloch et al., 1970]. The three biggest drainages deliver 55 % percent of the annual discharge; these are the Guadalupe River, the Coyote Creek and the Alameda Creek [Pubben, 2017].
South Bay receives its freshwater influx through Central Bay from the Sacramento-San Joaquin Delta, which is responsible for around 90 % of the freshwater supply to North Bay [Barnard et al., 2013, Cloern, 1984, Kimmerer, 2002, Schoellhamer et al., 2016]. Therefore, both the salt water and the fresh water enters the Bay through Central Bay, which is a special case for estuaries.

The Sacramento-San Joaquin Delta receives its fresh water from the Sacramento River (fed by its major tributary streams, the feather, Yuba and American Rivers) and the San Joaquin River (fed by the Merced, Tuolumne and Stanislaus Rivers). These rivers confluences in the Delta and enter in the eastern end of the San Fran-

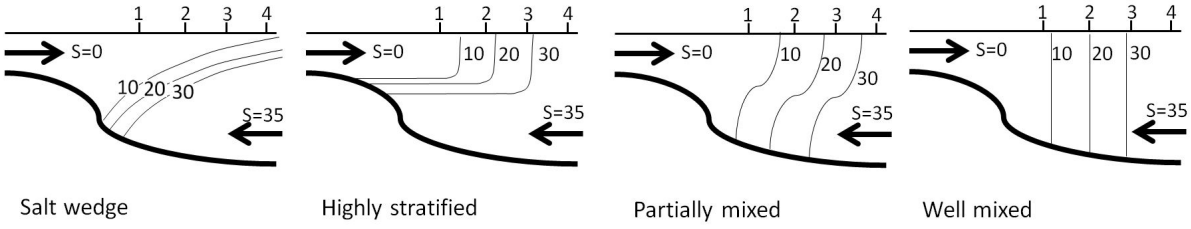

Figure 1.2: Estuary classification. The S indicates the salinity value, where zero is fresh water, and 35 is saline water. Figure redrawn based on [Pietrzak, 2016]

cisco Bay (Fig. 1.1). They encompass about 40 % of the State of California and thus rank among the world's 60 largest catchment areas (regarding both geographic areas of the drainage basin and flow rate) [Conomos et al., 1985]. The annual discharge rate into North Bay is 800 $m^3 s^{-1}$, with a record of 17,800 $m^3 s^{-1}$ in 1986. Sacramento river contributes 85 % of the sediment that enters North Bay, and 13 % from the San Joaquin river[Barnard et al., 2013]. Typically the Sacramento-San Joaquin river system has two periods of high discharge each year. The first high discharge occurs between December and February and is rainfall runoff. The second high discharge happens between March and June and is a result of the melting of snow in the Sierras. The small local streams entering South Bay only have the first rainfall peak. [Conomos, 1979, Conomos et al., 1985, McCulloch et al., 1970]

This seasonal pattern of winter precipitation, spring snow-melt runoff, and dry summers are fluctuating over the years. In some years there are two pronounced peak discharges including both the winter and the spring and in some only one of them is significant [Kimmerer, 2002, 2004]. The magnitude of the river runoff is highly varying over the years, resulting in significant dry and wet years.

1.2.3. Density driven flows

The degree of mixing between the fresh and salt water in an estuary depends on the density gradients in the longitudinal and vertical direction. Four types of estuaries can be defined, from a well-mixed estuary to a stratified estuary (Fig. 1.2). A well-mixed estuary is vertically mixed and continuously stratified along the estuary. In a highly stratified estuary, there is a sharp interface separating the fresh and salt water [Pietrzak, 2016].

South Bay does not enjoy the typical flushing pattern of an estuary. Instead, the Bay and its water properties are dependent upon the exchange of water with Central Bay [Conomos, 1979, McCulloch et al., 1970] and therefore seems to have the characteristics of an exchange flow [Conomos and Peterson, 1977]. The exchange between South and Central Bay is strongly affected by density differences due to differences in salinity[Kimmerer, 2004, Pubben, 2017].

The density of Central Bay is dependent on the magnitude of the river runoff of the Sacramento-San Joaquin Delta and the tide. The seasonally changing freshwater runoff results in a seasonally varying density of Central Bay and therefore in different stratified conditions in South Bay. Three types of stratification can be observed in South Bay (Fig. 1.3), each is further elaborated;

The first type is when the tidal prism exceeds the volume of freshwater flow by one or two orders of magnitude in the dry summer period [Barnard et al., 2013], resulting in a well-mixed estuary [Cloern, 1984, Conomos, 1979]. Both the density of South Bay as Central Bay are near-oceanic values [Conomos, 1979, Schoellhamer et al., 2016]. Gravitational flows are absent. Therefore, there is a balance between the resultant weak tidally driven and wind-driven flows. The residence time is relatively long, in the order of several months [Walters et al., 1985]. Only during significant dry years, the salinity can exceed those of the adjacent ocean, due to evaporation [Conomos, 1979, Kimmerer, 2004]. The dry summer period corresponds to stage one of figure 1.3.

The second type is when a high Delta outflow (less than eight o/oo) from the Sacramento river reduces the salinity in Central Bay, resulting in a horizontal density gradient from Central Bay to the tip of South Bay [Kimmerer, 2004, Walters et al., 1985]. A relatively pronounced stratification occurs, especially in the channels [Cloern, 1984, Conomos, 1979]. The resulting density differences drive a multi-layered flow (2 or 3) with bottom currents directed to Central Bay and surface currents directed to South Bay [McCulloch et al., 1970, Schoellhamer et al., 2016, Walters et al., 1985]. The strength of these currents depends on the magnitude of the freshwater inflow and the magnitude of the tide. This reverse estuarine circulation freshens South Bay to a relatively low salinity (20 o/oo), decreasing the residence time to less than a month [Kimmerer, 2004, Walters et al., 1985]. This phase corresponds to stage two of figure 1.3.

The third type is observed with a decline of river inflow, the density in Central Bay increases as its salinity reaches oceanic values. The circulation reverses, resulting in a classic estuarine circulation. The bottom currents are directed landwards, and surface currents are directed to Central Bay [Walters et al., 1985]. The more salty waters entering from Central Bay raises the salinity and therefore the density of South Bay until eventu-

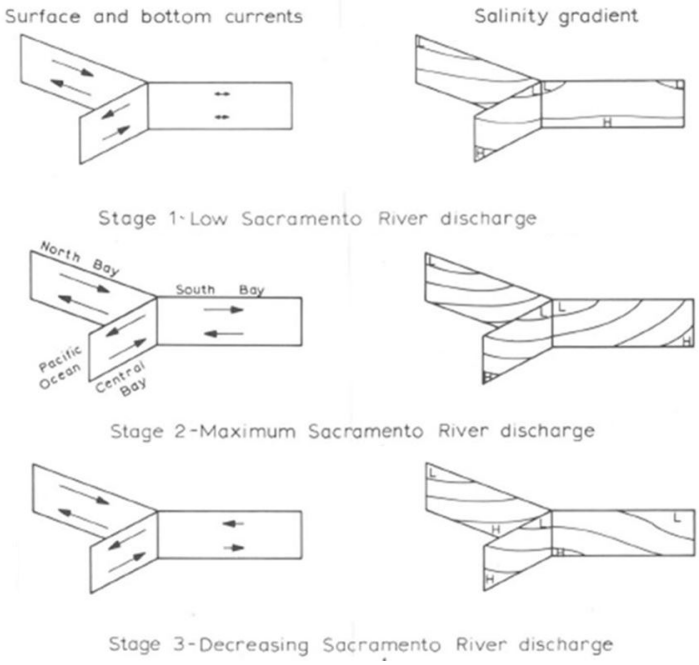

Figure 1.3: A highly diagrammatic model of the net surface and bottom currents and the salinity gradients during the major seasonal stages in the San Francisco Bay. The curved lines on the right-hand figures indicate salinity contours, where H indicates high, and L indicates low. Figure is redrawn based on [McCulloch et al., 1970]

ally there is little difference in density between Central and South Bay (stage 1) [McCulloch et al., 1970]. This phase corresponds to stage three of figure 1.3.

In general, South Bay can be seen as a well-mixed estuary with near-oceanic salinity values. This stage can be disturbed by a freshened Central Bay by high outflow from the Sacramento River. South Bay transforms into a partially stratified estuary, with a reversed estuarine circulation flushing the estuary. The Bay returns to its former state by a classic estuarine circulation, when the outflow decreases and the density of Central Bay increases. The duration of each phase fluctuates over the years, depending on the hydrograph of that specific year. In general, can be stated that the first phase is the dominant phase and often takes in between six to nine months. The duration of the two other stages depends on the height and the duration of the river outflow of the Sacramento River.

1.2.4. Wind

The wind speed and direction over South Bay vary seasonally. During summer there is a prevailing Westerly or North-westerly wind, generating wave heights exceeding one meter and having periods of 2 to 3 seconds. Whereas in the winter the winds are light, except during storms. The wind is then typically southeasterly and lasts 2-3 days. These winter storms can generate 5-sec waves in areas with long fetch [Chengt and Gartner, 1985, Conomos, 1979]. Waves generated by winds originated from the Pacific Ocean do not significantly affect South Bay, due to the sheltering of the Bay [Barnard et al., 2013].

1.3. Existing theories and research questions

In order to better understand sediment transport in South Bay, a number of studies have focused on the erosional/depositional behaviour of South Bay [Jaffe and Foxgrover, 2006a,b, Krone, 1993, Schellenbarger et al., 2013], on the estuarine sediment budgets [Achete et al., 2015, Carlson and McCulloch, 1974, McKee et al., 2006, 2012, Schoellhamer et al., 2007, Wright and Schoellhamer, 2004], on sediment transport fluxes [Barnard et al., 2012, Conomos and Peterson, 1977, Downing-Kunz et al., 2016, Erikson et al., 2013, Lacey et al., 2014, Lacy et al., 1996, Schellenbarger et al., 2013] and on re-suspension rates of the bed [Brand et al., 2010, 2015]. These studies opt the following statement;

The Sacramento-San Joaquin Delta delivers sediments to South Bay during periods of high river flows. Hydrodynamic forcings such as the tide, wind and baroclinic flows redistribute these sediments around South Bay

It is often thought that the Sacramento-San Joaquin Delta is the primary source of sediments [Carlson and McCulloch, 1974, Conomos and Peterson, 1977, Erikson et al., 2013, Jaffe and Foxgrover, 2006a, Schoellhamer et al., 2007]. Recently, researchers advocate that the Delta is not the only source of sediments of South Bay. Schoellhamer et al .(2007) estimated that by the end of the 20th century the sediment supply from the Delta would decrease and become roughly equal to the sediment supply from the local tributaries. This theory is reinforced by a sediment budget study by Mckee et al.(2006, 2012). They found that the local tributaries directly out-flowing into South Bay discharges significant amounts of sediment. The sediment load from the local rivers was roughly equal to the sediment load from the Delta during the dry years but was significantly lower during wet years.

Previous studies found the tide and the baroclinic flows to be the governing forces for the exchange of water between Central Bay and South Bay at Bay Bridge [Conomos, 1979, McCulloch et al., 1970, Pubben, 2017]. However, it is unknown what the driving forces are of the sediment exchange between Central Bay and South Bay at Bay Bridge. Studies suggest that the Delta sediments are delivered to South Bay during periods of high Delta flow [Carlson and McCulloch, 1974, Downing-Kunz et al., 2016]

A combination of tidal advection, seasonal winds and baroclinic flows, generates the suspended sediment transports in San Francisco South Bay [Schoellhamer et al., 2007]. These different forces vary in time. This result in spatially and time-varying suspended sediment pathways. Suspended Sediment Flux (SSF) studies on location-specific sites in South Bay suggested that the sediments are transported up-estuary in the channel during the wet period, and down-estuary during the dry period [Lacy et al., 1996]. The opposite holds for the sediment transport on the flats. Researchers found that the net transport of sediments is seaward directed in the wet season and landward during the dry season. [Lacey et al., 2014, Schoellhamer et al., 2007].

Prior studies were based on data analysis and conceptual hind-cast models. Although the region has an extensive network of surveying stations, there are many areas without measuring stations. Most data analysis focus on a small region in South Bay, with just one or two measurement points. Often these studies have recorded measurements for a short period. The research results and conclusions so far are therefore very location specific in South Bay and account for a small period of time. This might lead to knowledge deficits since no integral study of the complete sediment pathways in time and space is done. This knowledge gap can be filled using a 3D numerical sediment transport model. No such study has yet been undertaken in the total South Bay Area.

This research reviews the sediment sources as well as how these sediments are transported in South Bay with the use of a numerical model and by analysing a new set of data. This research will focus on gaining more insight in sediment transport mechanisms, by answering four research questions;

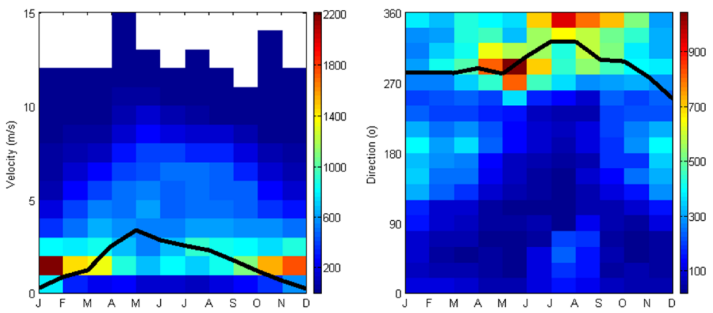

Figure 1.4: Wind speed (left) and direction (right) in Redwood City. The colours indicate the times of occurrence during period 1969-2016. [Schettini et al., 2017]

Research questions

1) What are the sediment sources of San Francisco South Bay?

2) What are the primary sediment pathways in the Northern reach of San Francisco Bay and how do they change over time and space?

3) What are the dominant physical processes affecting the sediment exchange between Central Bay and South Bay at Bay Bridge?

4) What are the primary sediment pathways in San Francisco South Bay and how do they change over time and space?

In which the following are specified to define the scope of this research:

Sediment	Considering only fine sediments
Sediment pathways	Considering suspended sediment transport
San Francisco South Bay	The southern reach of the San Francisco Bay (figure 1.1)
Physical processes	Physical processes regarding hydrodynamic forces as wind, wind-waves, tides and freshwater flows
South Bay	Reach between Bay Bridge and Dumbarton Bridge

Before presenting the observations and conclusions, in §two the fundamental theories on the physics of excellent sediment transport are discussed, to make a distinction between several theories and which of these theories is chosen here to follow. Further the influence of hydrodynamic forces such as the tide and density gradients on the sediment transport are discussed, to get a better understanding of how transport can be affected by several hydrodynamic components.

In §3, the methods used are described. For a suspended sediment study it is essential to characterise advection, mixing, flocculation, and settling of sediment particles in the water column as well as the resuspension of sediment from the bed. Many of the parameters controlling these processes are difficult to measure. In situ measurements of the sediment properties and settling velocities require complex analytically devices. Laboratory studies cannot reproduce in situ conditions and therefore may change sediment properties. An alternative approach is observing the measured suspended sediment concentration (SSC) and analyse these with a numerical model. In this research, the software Delft3D FM is used to get a bettering insight into the sediment pathways of San Francisco South Bay. Additionally, a new set of in situ data is analysed.

The results of the data analysis and the numerical model simulations are outlined in §4. The trends observed in time series and the found correlations between these trends and hydrodynamic forcing are described. Several insights are given in the hydrodynamic and sediment characteristics of South Bay.

In §5, the interpretation of the results are discussed for each research question, followed by a discussion on the limitation of the methods used.

The conclusions and recommendations of this research are stated in §6.

2

Physics of fine sediment transport

This chapter outlines some fundamental theories on sediment transport. The influence of hydrodynamic forces on the sediment transport are described, to get a better understanding of how transport can be affected by several hydrodynamic components. The underlying theories are restricted to fine sediments, with a sediment diameter of d < 60 μm, (British Standards and M.I.T.) and d < 1/16 mm (American Geophysical Union). Furthermore is the discussion restricted to suspended sediment transport which is according to mechanisms classification defined according to as sediment which is suspended in the fluid for some time. Its origin can be both bed material transport as well as wash load [Jansen et al., 1997]. The effect of mixing and sediment properties on sediment transport is described in §2.1 and §2.2 considers the effect of the tide on sediment transport. In §2.3, the effect of density gradients on sediment transport are touched upon.

2.1. Mixing and sediment properties

The sediment particle in the water is prone to several forces, resulting in different sediment movements (Fig 2.2). The gravity acting on the particle is causing the falling of the particle. The sediment characteristics control the fall velocity of the particle. The turbulent mixing brings the sediment up in the water column. The combination of these two determines the shape of the suspended sediment concentration profile (Fig. 2.1). The sediment particle can leave or enter a certain water body by exchange of the bed or advection (Fig 2.2). The sediment transport profile can be obtained by multiplying the sediment concentration profile with the velocity profile (Fig. 2.1) [Rijn, 1993].

Hydrodynamic forces play a significant role in the suspended sediment transport. Its role is two folded. Firstly, the hydrodynamic forces shape the velocity profile, determining the direction of the transport. Sec-

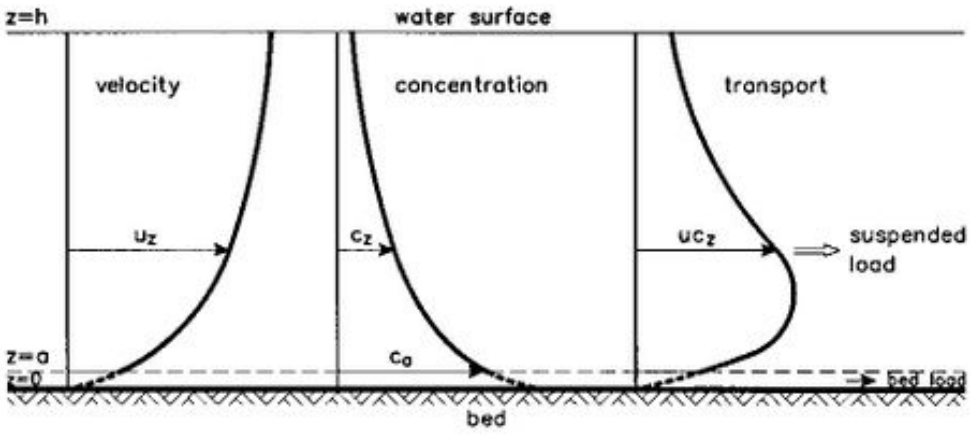

Figure 2.1: The vertical suspended sediment transport profile (right) depends on the velocity profile (left) and the concentration profile(middle) [van Rijn, 2006]

ondly, the hydrodynamic forces determine the concentration profile by increasing or decreasing the turbulence mixing. A hydrodynamic force can, therefore, influence the sediment transport in several ways, which makes it more complicated. The different impacts of the tide and density gradients on sediment transport are shortly stated to get more insight into the sediment dynamics.

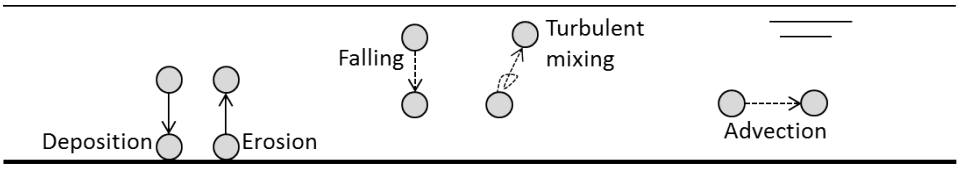

Figure 2.2: Particle motions in the water column. Figure redrawn based on River Engineering class notes by Prooijen (2016

2.2. The tide

Tidal processes are periodic. There must be some spatial of temporal asymmetry present for the tidal processes to induce net sediment transport. No net transport would occur if the processes subjected to a flood and ebb were the same. For practical purposes are the asymmetries that lead to net sediment transport dived into spatial and local asymmetries. The relative importance of the asymmetries will vary as function of sediment type, hydrodynamic energy, sediment supply, local tidal flat shape and surrounding coastal morphology.

Net transport due to spatial asymmetries
Net sediment transport due to horizontal asymmetries is a sort of dispersion in that it drives suspended sediment from areas of higher concentration towards areas of lower concentration. Tidal currents that are moving away from areas with a high sediment concentration are likely to carry more sediments than tidal currents that are moving away from areas with a low sediment concentration. For example, a suspended sediment source, such as local river runoff or an easily eroded bed region can cause a horizontal spatial variation in suspended concentration. Additionally, a horizontal difference in high-energy waves or tides can induce a horizontal spatial variation in suspended sediment concentration [Friedrichs, 2011].

A net sediment transport can be induced by vertical asymmetries in the suspended sediment concentration flow in combination with an asymmetry in the flow velocity profile. For example, the vertical mixing is stronger during flood peak velocities than during ebb peak velocities. Sediments are brought higher into the water column due to stronger vertical mixing. The horizontal velocity is larger higher up in the water column. Therefore, sediments are travelling longer during flood tide than during ebb tide, resulting in a net sediment transport [Maren and van Winterwerp, 2013].

Net transport due to local asymmetries
A distortion of periodic tidal velocity is often the most important local asymmetry for net transport in a well-mixed estuary. A local asymmetry in maximum peak velocity results in a flood or ebb dominant current [Maren and van Winterwerp, 2013]. The sediment suspension and transport increases with a bed shear stress, which has a non-linearly relation with the current velocity. A dominant flood current will produce more stress during the flood current than the ebb current, resulting in a net sediment transport [Friedrichs, 2011]. Coarser sediment are more sensitive for this type of asymmetry, but it can still be relevant for finer sediments [Maren and van Winterwerp, 2013].

A net transport occurs when there is asymmetry in the slack tidal periods. If the slack tidal period is longer around high water than low water, a land water sediment transport is present. Sediment has more time to settle out after the flood period than after the ebb period. Fine sediments are very sensitive for this type of asymmetry [Friedrichs, 2011, Maren and van Winterwerp, 2013].

The re-suspension due to wind-waves increases as the depth decreases. The water depth is smaller at ebb than during flood. Therefore, more sediments are in re-suspension after ebb. More sediments are in suspension during flood tide than during the ebb tide, resulting in a net sediment movement Brand et al. [2010].

2.3. Density gradients

Density gradients (horizontal and vertical) can be induced by a gradient in salt and fresh water/temperature or suspended sediment concentration. These gradients affect the flow structure and therefore the transport of sediment in the water. Therefore the influences of these gradients are discussed. Firstly, the effects of a density gradient over the vertical is outlined. Secondly, the effect of a horizontal gradient on suspended sediment transport is described.

Vertical mixing in stratification

Considering shallow water conditions, the mixing over the vertical is induced by the near-bed velocity gradients. In a well-developed flow, this mixing is pronounced of the whole water column. Density gradients over the vertical of the water column can reduce this vertical mixing. The vertical mixing in dampened by the reduction in mixing of both momentum and sediment[Winterwerp and Prooijen, 2016].

Vertical densities differences can either be gentle, such as the right figure in 2.3 or have a sharp interface, such as the left figure in 2.3. At the bottom a relatively high densities are presents due to the salt water. At the surface, relatively low densities are found due to fresh water. The turbulent mixing between the different densities includes that a more massive particle needs to be transported up in the water column against the action of gravity. This process consumes more turbulent energy than for a flow with uniform densities. Therefore, the stratification will dampen the turbulence [Rijn, 1993].

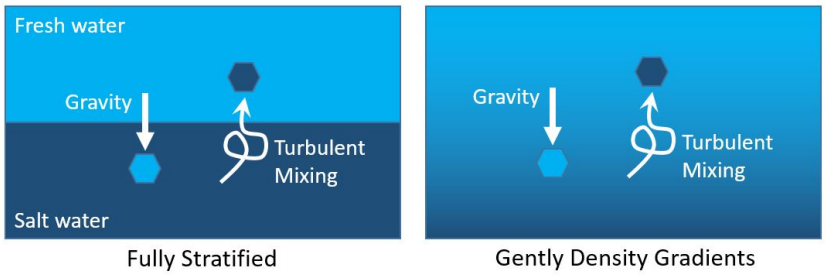

Figure 2.3: A schematic presentation of the effects of vertical density gradients on turbulent mixing for fully stratified conditions (left) and for gently density gradients (right). The dark blue colour represents the higher density water and the light blue colour the lighter density water. Damping of turbulent mixing by vertical density gradients figure redrawn [Winterwerp and Prooijen, 2016]

The usual method to account for is the reduction of the fluid mixing coefficient by introducing a dampening factor related to the Richardson number. Therefore, the vertical stratification induces a loss-term in the balance of the kinetic energy [Rijn, 1993, Winterwerp and Prooijen, 2016]. For a k-ε turbulence model (incl. buoyancy effects), the following equation (2.1) can be introduced;

$$\frac{Dk}{Dt} = \frac{\delta}{\delta z}\left\{(\upsilon + \upsilon_T)\frac{\delta k}{\delta z}\right\} + \upsilon_T\left(\frac{\delta u}{\delta z}\right)^2 - \varepsilon - \frac{g}{\rho}\varepsilon_T\frac{\delta \rho}{\delta z} \tag{2.1}$$

The last term of the equation is the dampening factor as result of the stratification. The result of this reduction is that less sediment gets transported over the water column. Therefore, there is a considerable reduction of the concentration at the top of the water column [Rijn, 1993]

Gravitational circulation (estuarine circulation)

Consider a horizontal density gradient due to salinity, such as in figure 2.4. Fresh water with low salinity is on the left side, whereas salt water with a high salinity is on the right side. The pressure increases linearly over depth. The difference in the densities on both sides results in a different pressure over depth. The hydrostatic pressure near the bed is higher in salt water than in fresh water. Therefore is the hydrostatic pressure profile over depth different for both waters. A slope in water level needs to compensate this hydrostatic pressure

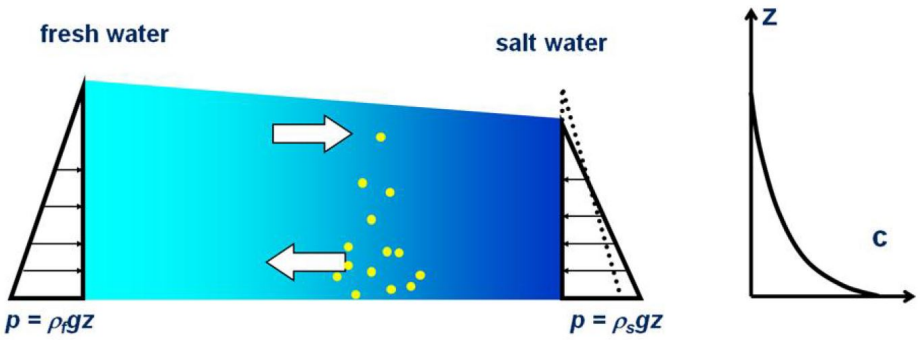

Figure 2.4: A schematic presentation of the effect of the gravitational circulation on suspended sediment transport. The suspended sediment concentration profile is shown on the right. ([Winterwerp and Prooijen, 2016])

gradient. The result is a near-bed flow from the saline water to the fresh water, and a near-surface flows from fresh water to the saline water. These currents form the gravitational circulation.

The depth mean net transport of the water is zero. However, due to suspended sediment gradient over the water column, there is a net transport of fine sediment [Winterwerp and Prooijen, 2016]. Therefore, the horizontal gradient induces the gravitational circulation, but it is magnitude is affected by the vertical stratification.

Strain induced Periodic Stratification /Tidal straining
On top of the horizontal density gradient is the effect of the tide, which can be separated in two-phase the flood and the ebb. Consider a water body such as the top of figure2.5 with only horizontal salinity gradients. During ebb, the fresher water flows over the saline water, as depicted with the light blue arrows in figure 2.5. This is a stable situation because the denser water is below the fresh water imposing stratification. During flood, the denser water flows over the fresh water. This is an unstable situation, resulting in extra mixing in the area, breaking down the stratification. [Winterwerp and Prooijen, 2016]

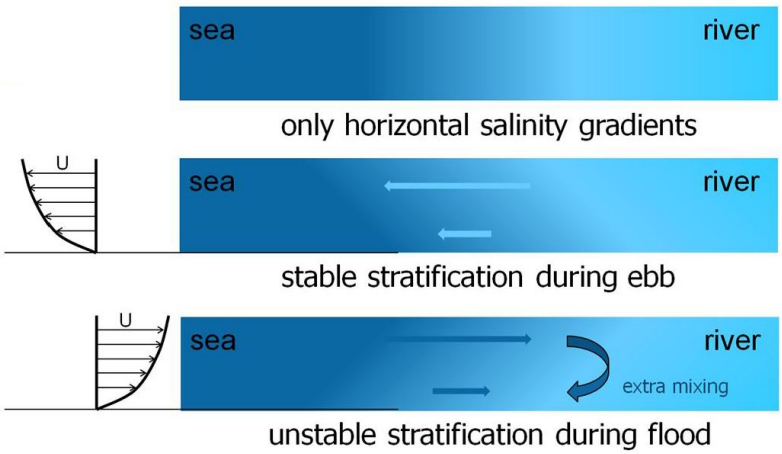

Figure 2.5: A schematic presentation of tidal straining over a tidal cycle. ([Winterwerp and Prooijen, 2016])

The process described above can be seen as periodic stratification due to tidal straining. During ebb, there is a stable stratification, during flood there is de-stratification. When the stratification during ebb is sufficiently well-developed, it can suppress the de-stratification part of the cycle, resulting in persistent stratification. This can occur because the stratification impedes the vertical transport of momentum. Therefore, the tendency for stratification overcomes the tendency for vertical mixing by the tidal shear stresses. Monismith (1996) proposed a horizontal Richardson number to identify the transition between periodically and persis-

tently stratification, see equation 2.2. This number is dimensionless and is the ratio of potential energy of the longitudinal density gradient over the tidal kinetic energy. [Kimmerer, 2004]

$$Ri_x = \frac{g\beta\Gamma H^2}{C_D U_m a x^2} \tag{2.2}$$

When Ri_x is greater than 0.25 the tidal energy is not sufficient to overcome the stratifying effects of the baroclinic pressure gradients [Stacey et al., 1999], Therefore, the water column will stratify. When Ri_x is less than 0.25 the turbulence is not affected by the stratification, Therefore, not persistent stratification [Stacey et al., 1999]. The ratio increases linearly with increasing density gradient and the square of the water depth and the square of the tidal energy. Therefore,this persistent stratification will be found in deep locations with strong salinity gradients and weak tides [Kimmerer, 2004].

3

Methods

To study the suspended sediment dynamics in a system, it is important to account for advection, mixing, flocculation, and settling of sediment particles in the water column as well as the re-suspension of sediment from the bed. Many of the parameters controlling these processes are difficult to measure. In situ measurements of the sediment properties and settling velocities require complex analytically devices. Laboratory studies cannot reproduce in situ conditions and therefore may change sediment properties. An alternative approach is observing the measured suspended sediment concentration (SSC) and analyse these with a numerical model.

This chapter outlines how a new set of SSC time series (WY2015-WY2017) in San Francisco South Bay (South Bay) are observed and analysed with a 3D numerical model. Firstly, the analysis of the data is described in §3.1. Secondly, the 3D numerical model is introduced in §3.2.

3.1. Data analysis

The U.S. Geological Survey (USGS) sustains a research program, since 1988, to understand how coastal ecosystem functions and how human disturbances alter those functions [USGS, 2017]. One component of this program is directed toward following and understanding the water quality of San Francisco Bay. Since 2014, this program includes a new SSC monitoring network which is designed to capture the spatial and temporal variability of SSC. This study analyses this new set of SSC data. First the measurement stations are described in §3.1.1. Second, the approach of the data analysis is discussed in §3.1.1. The results of the data analysis are stated in §4.1.

3.1.1. Measurement stations

At some locations a high frequency (15-minute sampling) water quality measurement device is installed to create instantaneous time series (Fig. 3.1). Some regular measurements (at least once a month) along a transect of the Bay with the Peterson cruise takes place to create a 2D view (Fig. 3.1).

High frequency interval monitoring locations

Continuous water-quality measurements are recorded at one or two water depths every 15 minutes at each station using multiparameter water quality sondes. They are retrieved either real-time via cellular telemetry or by manual download during routine station visits. The sondes are equipped with sensors to measure water level, temperature, specific conductance, turbidity (optical), and dissolved oxygen(optical). All data undergo a review process that includes editing, quality assurance, and approval. Some data-gaps are possible due to either construction projects, instrument failures or by biological activity and growth [Wagner et al., 2006]. A detailed description of the measurement station and its measurements are stated in appendix A.

To construct instantaneous time series of SSC first the turbidity sensor readings are related to in situ SSC determined from periodic water samples. Then the SSC time series are obtained by linking turbidity to SSC using either a simple linear regression model to the log-transformed data or the nonparametric repeated median method [Rasmussen et al., 2013].

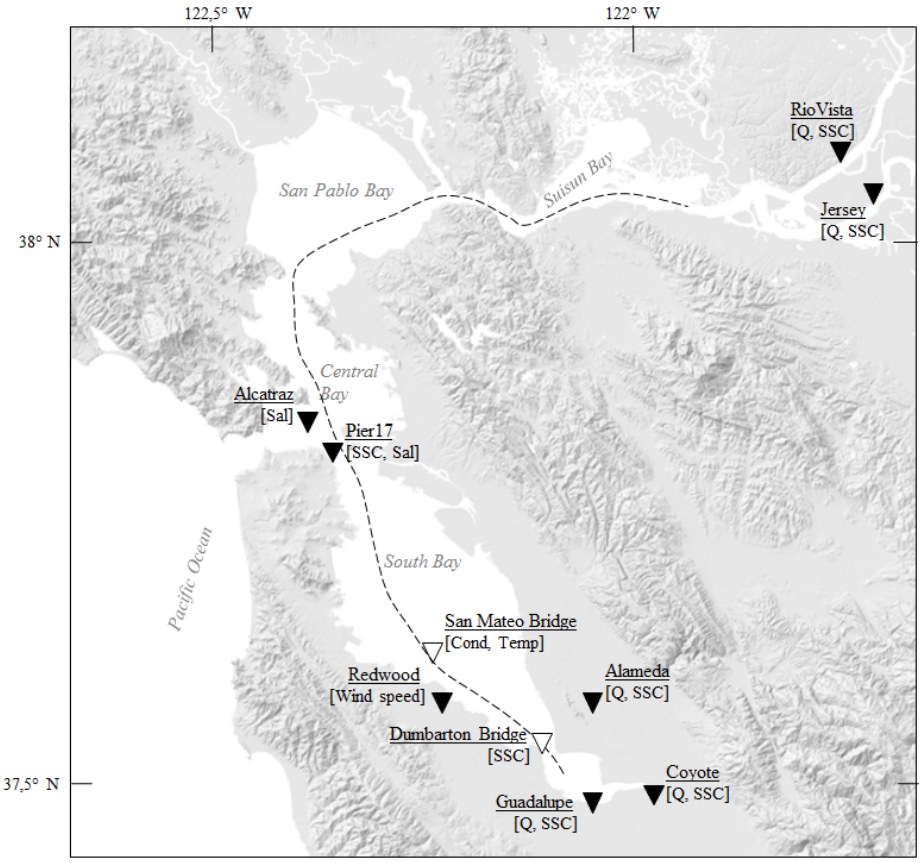

Figure 3.1: The data measurement locations are depicted with a triangle. A black triangle indicates that the parameters measured are at one level in the water column. A white triangle indicates that the parameters measured at this station are at two different depths in the water column. The abbreviations below the underlined station name state the measured parameters. SSC = Suspended Sediment Concentration, Sal= Salinity, Q= Discharge, Cond= Conductance, Temp = Temperature. A detailed description of the observation locations is stated in appendix A. The two-dimensional profile is obtained by sampling a station located along the intermittent black line.

Data can be obtained from site; *https://maps.waterdata.usgs.gov/mapper/index.html?state=ca.*

Monthly measurements Polaris cruise
Multiple water quality parameters (depth, conductivity, temperature, suspended solids, chlorophyll, light penetration, and dissolved oxygen) are obtained at a series of fixed stations along the broken black line in figure 3.1 using a submersible instrument package. Once every month a vertical profile is obtained at each location to get a two-dimensional (longitudinal and vertical) description of water quality. This sampling was done on the Polaris cruise vessel until 2015, from 2016 it is the R/V David H. Peterson. At each location, a discrete water sample of suspended particle matter is collected, to compare the discrete values and the sensor volts. It is possible to calculate the suspended solids at each station with a regression equation. [Cloern and Schraga, 2016b].

Data can be obtained from the site; *https://sfbay.wr.usgs.gov/access/wqdata/query/index.html.*

3.1.2. Approach data analysis
The time series of both the SSC as the hydrodynamic conditions are analysed to notify possible trends. Observed trends in SSC and hydrodynamic forces are compared to find correlations. The following adjustments to the data are made to find the trends and correlations.

- The time series are daily averaged.
- The time series of the two Delta rivers (Sacramento River and San Joaquin river) are combined to account for the total influence of the Delta. The time series of the Delta is constructed by merging the

time series of the measurement station RioVista and the measurement station Jersey.

- The sediment load of the river is constructed by multiplying the instantaneous discharge data with the instantaneous SSC data at a specific location.

- The salinity at San Mateo Bridge is computed according to the Practical Salinity Scale 1987 [Fofonoff and Millard, 1983, Lewis and Perkin, 1981].

3.2. Numerical model

The use of the numerical model is described in this paragraph. It is not the aim of this research to mimic the found SSC time series but to understand how different processes are affecting the sediment pathways in South Bay. First, the used software is discussed in the section model selection (§3.2.1). Second, the set up of the model is described (§3.2.2). Third, the model simulations are outlined (§3.2.3). Fourth, the model output locations are given (§3.2.4). The results of the analysis of the numerical model are outlined in §4.2.

3.2.1. Model selection

The software used is Delft3D Flexible Mesh (Delft3D FM). The software is the latest hydrodynamical software program developed by Deltares for 1D, 2D and 3D computations for coastal, river and estuarine areas. It can carry out simulations of flows, waves, water quality and ecology and contains several modelling suites [Deltares, 2017]. For this research, an offline coupling is used between the hydrodynamic module D-Flow Flexible Mesh (D-Flow FM) and the water quality module D-Water Quality (DelwaQ).

The D-Flow FM module is a multi-dimensional hydrodynamic simulation program which calculates non-steady flow and transport phenomena that result from tidal and meteorological forcing on structured and unstructured, boundary-fitted grids. It solves the one, two and three-dimensional Navier Stokes equation for an incompressible fluid, under the shallow water assumption (hydrostatic pressure) and the Boussinesq assumption (constant density)[Deltares, 2016b].

The DelwaQ module is a mathematical water quality model that delivers an approximate quantitative description of one or more water quality state variables. It calculates the concentrations of substances as resulting from mass transport and water quality processes. It derives the water flow and dispersion coefficients from the D-Flow FM module [Deltares, 2016a]. The sediment concentrations and transport are calculated with the diffusion-advection equation.

For a technical description of both D-Flow FM and DelwaQ and their coupling is referred to the manuals of Deltares [Deltares, 2016a,b, 2017, 2014].

Prior San Francisco Bay modeling efforts

Previous numerical model studies showed that a D-Flow FM model could accurately represent the hydrodynamic conditions of San Francisco Bay. A collaboration of USGS, University of California-San Diego, UNESCO-IHE, and Deltares [Martyr-Koller et al., 2017] developed a hydrodynamic D-Flow FM model of the area. The model contains the San Francisco Bay and the Sacramento-San Joaquin rivers and their connected Delta system. It is a three-dimensional model and accounts for salinity and temperature. The software of Delft3D-FM was chosen for its following distinguishing features [Martyr-Koller et al., 2017]:

- The software's unstructured grid framework to create a single model domain of the Bay-Delta's highly complex geometry and perform year-long simulations at relatively low computational cost

- Its unique momentum conservation scheme which can be applied in 1D channels, 2D overland flows, and 3D stratified flows

- 3D numerics supporting salinity and temperature dynamics.

- a loosely-coupled framework for sediment, water-quality, phytoplankton, and habitat suitability models.

This model can accurately represent hydrodynamic, salinity and temperature conditions throughout Central Bay, North Bay and Delta over a wide range of tidal and fluvial conditions [Martyr-Koller et al., 2017].

Pubben (2017) adjusted the model developed by Martyr-Koller et al. (2017) for a detailed study on the hydrodynamic conditions of South Bay. The model is reduced to only the San Francisco Bay by simplifying the Delta-system, increasing the computational efficiency. This model can accurately represent the hydrodynamic, salinity and temperature conditions for South Bay. The D-Flow FM model of Pubben (2017) is used as a reference for constructing the D-Flow FM module in this research. Most physical parameters and computational parameters are adopted.

Adjustments to the software
The stirring of the wind-waves is an important force controlling the movement of suspended sediments [Sanfoord and Maa, 2001]. However, this force is yet not incorporated in D-FLOW FM. The DelwaQ module can account for an increased bed shear stress due to wind-waves. However, the wind field of San Francisco Bay varies each square kilometre every hour, and this level of accuracy cannot be obtained in DelwaQ. Hence, the effect of the stirring of the wind waves on the bed shear stress is incorporated in the software of D-FLOW FM. .

The new calculation of the bed shear stress is based on the theory of Swart (1974), with the following equations;

$$\tau_{cw} = \tau_c + \tau_w \tag{3.1}$$

where τ_c is determined as;

$$\begin{aligned} \tau_c &= \rho_w * u_c^* 2 \\ u_c^* &= \sqrt{c_f} * u \end{aligned} \tag{3.2}$$

and τ_w is determined as;

$$\begin{aligned} \tau_w &= \rho * {u_w^*}^2 \\ u_w^* &= 0.5 * f_w * u_{orb} \end{aligned} \tag{3.3}$$

Where τ_{cw} is the bed shear stress due to combined wave and current action $[Nm^{-2}]$, τ_c is the bed shear stress due to current action $[Nm^{-2}]$, τ_w the bed shear stress due to wave action $[Nm^{-2}]$, ρ_w the density of water $[kgm^{-3}]$, u_c^* is the shear velocity induced by the current $[ms^{-1}]$, c_f the friction coefficient [-], u the depth averaged velocity $[ms^{-1}]$, u_w^* is the shear velocity induced by the waves $[ms^{-1}]$, f_w the Johnsson's wave friction factor [-]and u_{orb} orbital velocity $[ms^{-1}]$. In appendix B, the calculation of the Johnsson's wave friction is further elaborated.

The new calculation of the bed shear stress is tested with several computational runs. The results of these simulations are outlined in detail in appendix B. The computation of the bed shear stress is sufficiently for wind speeds between 0 ms^{-1} and 6 ms^{-1}. Since the wind speed in San Francisco South Bay is on average between 0 ms^{-1} and 6 ms^{-1}, the new calculation is sufficient for calculating the bed shear stress in this research.

3.2.2. Set up of the model

Grid and Bathymetry
The model area extends from the Pacific Ocean to the confluence of the Sacramento River and San Joaquin river. It contains South Bay, Central Bay, San Pablo Bay and Suisun Bay. The model accounts for the two major Delta rivers (Sacramento River and San Joaquin River) and the three major local tributaries (Alameda River, Guadalupe River and Coyote Creek). The contribution of the other local tributaries is neglected in the model. It is assumed that this will not influence the behaviour of the sediments in South Bay, as the outflow of these tributaries is low in comparison to the three major tributaries. Additionally, previous research opted that the Delta is the major source of sediments. It is expected that the local tributaries only contribute marginally to the sediment input of South Bay.

The grid covering this area is shown in blue in figure 3.2 and is constructed of rectangles and triangles. This allows for a proper alignment along main flow directions and more natural depictions of irregular coastlines

and increases the numerical efficiency. The model has three dimensions to correctly model sediment processes over the horizontal as well as over the vertical. The vertical structure is discretized using σ layers. The model contains 10 σ layers; each contains 10% of the depth. The bathymetry data is provided by SFEI and Unesco-IHE [personal communication, van der Wegen, M.]

Time periods modelled

The D-Flow FM models developed by Martyr-Koller et al. (2017) and Pubben (2017) are calibrated and validated for the period 2011-2013. There is no sediment data available for this period since the operator USGS started collecting sediment data begin 2014. Therefore the hydrodynamic module is adjusted for the water year 2015 (01/10/2014-01/10/2015) and water year 2017 (01/10/2016-01/07/2017). A water year (WY) is defined from 1 October to 30 September of the next year to keep the entire wet season on one hydrological year [Achete et al., 2015]. The first water year is a typical dry year with relatively low discharges during the wet period. The second water year is an extremely wet year with a period of extreme high discharges, which occurs infrequently. Some of the extreme wet years in the past coincided with El Nino years. However, an El Nino/La Nina event on its own does not result in high precipitation rates in California and therefore does such an event not immediately result in a wet year. A complex combination of different meteorological components leads to an extremely wet year, such as WY 2017 [Yuan and Yamagat, 2014].

For each year a model spin-up for two months was performed with data between 01/08/2014 and 01/10/2014 and 01/08/2016 and 01/10/2016 respectively for the model suites.

The model set-up takes approximately ten days to run the D-Flow FM module for the period of interest (a complete water year with two months spin-up time included) and one day for the DelwaQ module. This computational time is significant due to the [Pubben, 2017];

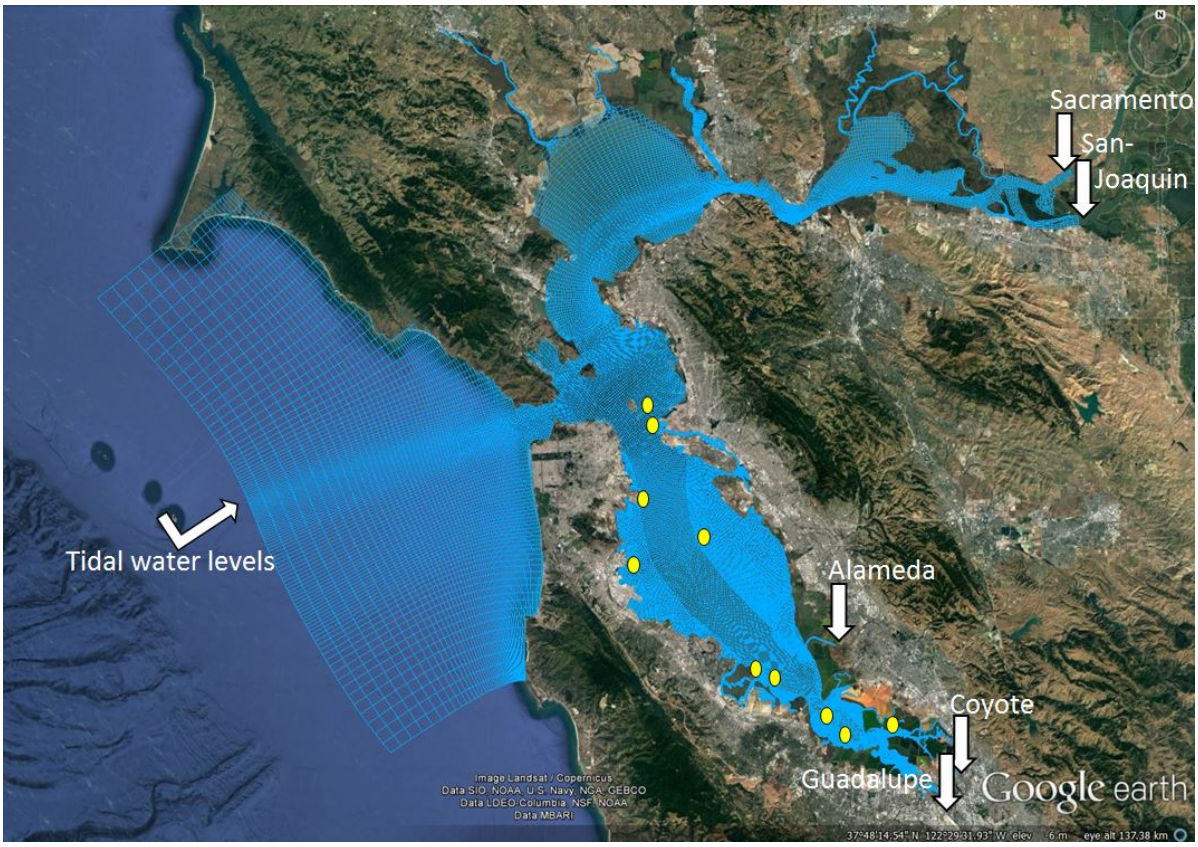

Figure 3.2: Model grid of D-Flow FM of San Francisco Bay is shown in blue. The model is driven by tidal water levels at the Pacific boundary and discharges at the five river boundaries, both displayed with the with arrows. The outflow locations of the waste-water treatment plants are shown with yellow dots.

- The large model domain
- The large period of interest (14 months)
- The small computational time step based on the maximum CFL-value of 0.5
- Applying a 3D model with ten sigma layers instead of a 2D model
- The number of modelled constituents (hydrodynamics, salinity, sediments)
- The output interval of the desired output data and the amount of desired output locations

Linear Erosion model
Erosion of the bed occurs when the shear stress τ_b exceeds the critical shear stress τ_{crit}. [Brand et al., 2015]. There is little agreement about the appropriate mathematical formulation for erosion rate. Some researchers advocate the power law erosion formulations, others favour the exponential form, and others opt for the simple linear relationship [Sanfoord and Maa, 2001]. Brand (2015) found that the use of the linear sediment erosion model in bottom shear stress was the most appropriate choice to describe the field observations in South Bay when the critical shear stress and the proportionality factor M were kept constant.

The erosion rate is therefore calculated in the model according to the linear erosion model. This equation is presented by Ariathurai (1974) for cohesive sediment erosion and attributed it to Partheniades work. This equation has been widely and successfully used to characterise surface erosion of cohesive sediments [MacAnally and Mehta, 2001].

$$\begin{aligned} &\textit{Ariathurai-Parheniades erosion equation} \\ &E = M(\tau_b - \tau_{ce}) \qquad for \quad \tau_b > \tau_{ce} \\ &E = 0 \end{aligned} \tag{3.4}$$

Where E is the erosion rate [$gm^{-2}d^{-1}$], M the zero-order re-suspension rate [$gm^{-2}d^{-1}$], τ_b the bed shear stress [Nm^{-2}] and τ_{ce} the critical shear stress for erosion bed shear stress [Nm^{-2}] [Deltares, 2016a].
The erosion rate is zero, when the ambient shear stress is less than the critical shear stress.

Parameters
The parameters for D-Flow FM module are stated in table 3.1 . They are adopted from the previous model studies, where these parameters are extensively calibrated [Martyr-Koller et al., 2017, Pubben, 2017]. The parameters for the DelwaQ module are stated in table 3.2. The parameters of the DelwaQ module are discussed below.

The Fall velocity (W_s)
Researches opt that the sediments in South Bay can be sub-dived into several sediment classes. Brand et al. (2015) suggest the existence of a class with fast settling velocities (w_s of $0,9\ mms^{-1}$ in spring and $0.58 * 10{-}2\ mms^{-1}$ in fall) and a slowly settling particle fraction (w_s of $1 * 10^{-4}\ mms^{-1}$ in spring and $1,4 * 10^{-2}\ mms^{-1}$ in fall) in a particle class model study. They suggest that the fall velocities are seasonally varying. This variation is neglected in this research. It is expected that this variation has limited influence on the sediment pathways. Achete (2015) used a fall velocity of 0.25 mms^{-1} during a 2D model study on the sediment dynamics in

D-Flow FM module settings

Parameter	Value
Version	1.1.231.50878M
Cells	51.658
Vertical layer type	σ
Number of layers	10
turbulence closure model	k - ϵ
total bed shear stress	According to Swart

Table 3.1: Several settings of the D-Flow FM module

North Bay. She suggests three sediment classes for a 3D model simulation of the Bay. One class with high fall velocities (w_s of 1.5 mms^{-1}) and two classes of intermediate fall velocities (w_s of 0.24mms^{-1} and w_s of 0.49 mms^{-1}) [personal communcation, Achete, F.]

Three sediment classes are defined in the model, to incorporate the suggestions of both Brand and Achete. There is a sediment class with a high fall velocity (w_s of 1.62 mms^{-1} (130 md^{-1})), an intermediate fall velocity (w_s of 0.49 mms^{-1} (50 md^{-1})) and a slow fall velocity(w_s of 0.011 mms^{-1} (1 md^{-1})). A thorough calibration requires more time than available for this research.

Critical shear stress for erosion (τ_{ce})
One uniform critical shear stress for erosion is applied in the model. In literature, the range of sediment erosion in South Bay is in between 0.1 Pa and 0.4 Pa [Brand et al., 2015, Zimmerman et al., 2008]. Achete (2015) used a critical shear stress of 0.25 for a 2D model study of the northern reach of San Francisco Bay. Therefore, the critical shear stress is set to 0.25 Pa.

Critical shear stress for sedimentation (τ_{cs})
Krone (1962) defines the deposition rate as;

$$\begin{aligned} D &= w_s c(1-\tau_b/\tau_d) \qquad for \quad \tau_b < \tau_d \\ D &= 0 \qquad for \quad \tau_b > \tau_d \end{aligned} \tag{3.5}$$

With D is the deposition rate [$gm^{-2}d^{-1}$], c_b the concentration of suspended matter near the bed [g^{-3}], w_s the fall velocity [ms^{-1}], τ_b the bed shear stress [Nm^{-2}] and τ_{ce} the critical shear stress for deposition [Nm^{-2}] [Deltares, 2016a].

The equation of Krone is approximated by Eq. 3.6 under the assumption that deposition takes places regardless of the prevailing bed shear stress [Winterwerp et al., 2006]. The deposition bed shear stress is observed in laboratory experiments, but its existence in natural systems is still questioned. Therefore, we assume that simultaneous erosion and deposition occurs such that the net influx into the water column is the difference between erosion E and the deposition D [Brand et al., 2015].

The critical shear stress for deposition is set to 1000 [Nm^{-2}], so that the equation (3.5) reduces to equation (3.6).

$$D = w_s c_b \tag{3.6}$$

Dry Cell threshold
The dry cell threshold is set to 0.01 m to establish numerical correctness and stability of the simulation. The establishment of numerical correctness and stability is further elaborated in the next paragraph 'Continuity'.

Continuity
A continuity tracer analysis is done to establish the numerical correctness and stability of the simulation. It

DelwaQ module settings

Parameter	Value
Version	Delft3D FM suite 2017 HMWQ 1.2.2.36603
Cells	51.658
Fall velocity w_s [Class 1, 2, 3]	0.011 [mm^{-1}], 0.49 [mm^{-1}], 1,62 [mm^{-1}]
Critical bed shear stress for erosion (τ_{ce})	0.25 [Pa]
Critical bed shear stress for sedimentation (τ_{cs})	1000 [Nm^{-2}]
Dry Cell threshold	0.01 [m]

Table 3.2: Several settings of the DelwaQ module

is a conservative tracer that is only subjected to transport. By assigning a concentration of 1 gm^{-3} to all water sources (initial condition and boundary conditions), the continuity concentration should remain 1 gm^{-3} during the whole simulation, as there are no processes that dilute or concentrate it [Deltares, 2016a]. If for example the continuity concentration is equal tot 1.1 gm^{-3}, the concentration is overestimated by 10 %.

On average is the deviation of the continuity concentration in this research maximum 1 %. Only in the southern area of South Bay is the deviation 4 %. As a result, the SSC in the model simulation is deviating on average for 1 %. This is sufficient to establish the numerical correctness and stability of the model [personal communication, Markus, A.]. The results of the concentration tracer analysis are outlined in appendix C.

Initial and boundary conditions
The model is driven by one sea boundary and five river boundaries, displayed by the white arrows in figure 3.2. The model time is set to UTC/GMT, and the water levels are set with reference to North American Vertical Datum of 1988 (NAVD88). The data locations are shown in figure 3.1. More details about the measured data and locations referred to in this section, are found in appendix A. The San Francisco Bay is a well-measured system. Therefore, all the input data are in situ measurement data.

Sea Boundary
The tidal boundary contains hourly water levels and depth dependent, daily-varying salinity and temperature information. The water level data are based on data retrieved from data station 'Point Reyes'[NOAA, 2017b]. Since the salinity and temperature hardly fluctuate over the years, the data are adopted from the model study of Pubben (2017) (van der Wegen, personal communication). The suspended sediment concentration is set to zero (van der Wegen, personal communication).

Sacramento River boundary
The Sacramento river boundary contains information on the discharge, temperature and suspended sediment concentration with an interval of 15 minutes. The data are retrieved from the data station 'RioVista' [USGS, 2017]. The salinity at this boundary can be compared with station 657 of the Polaris Cruise [USGS, 2017]. The maximum measured salinity was 0.8 PSU. Therefore, the salinity was set to zero for the complete year.

San Joaquin River boundary
The San Joaquin river boundary contains information on the discharge and temperature and suspended sediment concentration with an interval of 15 minutes The data are retrieved from the data station 'Jersey'[USGS, 2017]. The salinity at this boundary can be compared with station 657 of the Polaris Cruise [USGS, 2017]. The maximum measured salinity was 0.8 PSU. Therefore, the salinity was set to zero for the complete year.

Alameda River boundary
The Alameda river boundary contains information on the discharge and temperature with an interval of 15 minutes. It contains as well information on suspended sediment concentration with a daily interval. The data are retrieved from the data station 'Alameda' [USGS, 2017]. The information on the salinity values are retrieved from data station 31 of the Polaris Cruise and has a monthly interval [USGS, 2017]

Coyote River boundary
The Coyote river boundary contains information on the discharge, temperature and suspended sediment concentration with an interval of respectively 15 minutes, monthly and daily. The data are retrieved from the data station 'Coyote' [USGS, 2017]. The salinity was set to zero for the complete year since the boundary location is situated sufficiently far upstream the river branch, where the salinity intrusion from the ocean is not noticeable.

Guadalupe River boundary
The Guadalupe river boundary contains information on the discharge, temperature and suspended sediment concentration with an interval of respectively 15 minutes, monthly and daily. The data are retrieved from the data station 'Guadalupe' [USGS, 2017]. The salinity was set to zero for the complete year since the boundary location is situated sufficiently far upstream the river branch, where the salinity intrusion from the ocean is not noticeable.

Hydrodynamic scenarios

Scenario	Freshwater inflow	Wind forcing	Density gradients	characteristic year
1	moderate	seasonal	baroclinic	WY2015
2	***extreme wet period***	seasonal	baroclinic	WY2017
3	moderate	***no wind forcing***	baroclinic	WY2015
4	***extreme wet period***	seasonal	***barotropic***	WY2017

Table 3.3: Caption

Water waste treatment plants sources
The small yellow dots in figure 3.2, are the locations where the outflow of the water waste treatment plants is located. Their discharge into South Bay is modelled as a source because the magnitude of the discharge can be significant. The outflow from the water waste treatments plants do not contain sediments [SFEI, 2017].

Wind profile
A two-dimensional wind field is imposed on the complete area, containing hourly data for each square kilometre of the area. The wind field is constructed with the Winds of Critical Streamline Surfaces (WOCSS) analysis scheme, developed by Dr Frank Ludwig. It was developed to produce high-resolution three dimensional gridded wind analyses and is especially suitable for areas with complex terrain geometry such as the San Francisco Bay Area [Bridger et al., 1994]. The model converts the wind data retrieved from 20 to 43 stations (see appendix A) to a two-dimensional field with a wind component for the x and y-direction [Cheng et al., 1998]. The wind drag coefficient is considered to depend linearly according to Smith and Banke. [Deltares, 2016b]

3.2.3. Model simulations
To get more insight into the sediment pathways in South Bay a set of model scenarios were carried out to investigate the effect of different hydrodynamic conditions on the sediment processes. A set of four scenarios is carefully chosen since the computational time is long and the disk space to store the extensive model output is limited.

The 'base' mode represents the most common hydrodynamic conditions in South Bay, which is a dry year with averaged freshwater inflow during the wet period and seasonal varying wind forces (Sim. 1 in table 3.3). The other modes each represent a separate hydrodynamic scenario to investigate the influence of an extremely wet period (Sim. 2 in table 3.3), the influence of the wind forcing (Sim. 3 in table 3.3) and the influence of the density gradients (Sim. 4 in table 3.3).

Both the hydrodynamics and sediment transport particles were analysed through numerical tracers. In three different DelwaQ setups, the complexity is build up to get a better comprehension of the physics. The first DelwaQ set up consists of hydrodynamic tracers. The hydrodynamic traces are only subjected to transport (Fig. 3.3a). The second DelwaQ set up traces sediment particles in the water. In this setup, the bed interaction

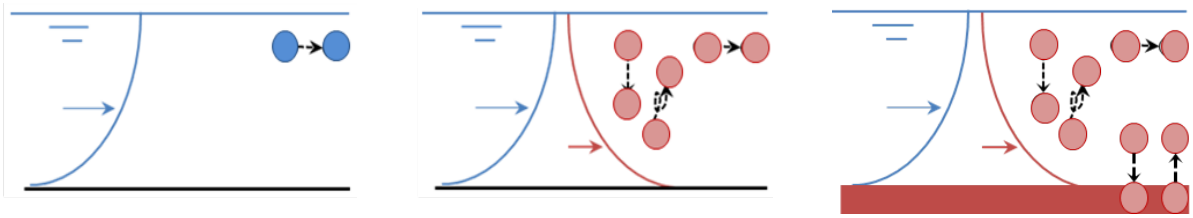

(a) DelwaQ set-up 1; Hydrodynamic tracers

(b) DelwaQ set-up 2; Sediment tracers, with no bed interaction

(c) DelwaQ set-up 3; Sediment tracers, with bed interaction

Figure 3.3: Three DelwaQ set-ups

is excluded (Fig. 3.3b). The third DelwaQ set up consists of sediment tracers. The bed interaction is included in this set up (Fig. 3.3c).

DelwaQ set-up 1; Hydrodynamic tracer (Fig. 3.3a)
A conservative tracer is assigned to each water boundary. The conservative tracers indicate where the water entering over the model boundaries is going to. In area's of interest, it is possible to determine the fraction of water originating from a certain source and its residence times. The tracer is only subjected to horizontal water transport. [Deltares, 2016a].

DelwaQ set-up 2; Sediment tracer, with no bed interaction (Fig. 3.3b)
A sediment tracer is assigned to the river boundaries. The sediment tracers indicate where the sediment entering over the river boundaries is going to. The label 'Delta sediment' is assigned to the sediment tracer assigned to the Sacramento River boundary and San Joaquin River boundary. The label 'local sediment' is attached to the sediment tracers assigned to the three major local tributary boundaries (Alameda, Coyote and Guadalupe). The sediment tracer follows the horizontal and vertical movement of the sediment particle in the water (Fig 3.4). This simulation starts empty. The sediment tracers enter the boundaries according to tot the set boundaries as stated in §3.2.2.

The advective sediment transport induced by river flow or baroclinic flow can be analysed with this simulation. Additionally, it is possible to analyse the net transport due to tidal dispersion, which drives suspended sediment concentration towards areas of lower concentrations. The benefit of this DelwaQ set-up is the small spin-up time.

However, this DelwaQ set-up does not include all essential processes for sediment transport, due to the exclusion of the bed-interaction. Therefore, the model does not account for net sediment transport due to slack duration asymmetry, peak velocity asymmetry and wind-wave induced re-suspension (§2). Additionally, sediments end up in the lowest layer of the water column instead of the bed since there is no bed-interaction. Bottom currents, such as baroclinic flows, transport these sediments (Fig. 3.4c). Therefore, this model set-up overestimates sediment transport due to bottom currents.

DelwaQ set-up 3; Sediment tracers, with bed interaction (Fig. 3.3c)
A sediment tracer is assigned to the river boundaries. The sediment tracers indicate where the sediment entering over the river boundaries is going to. The label 'Delta sediment' is assigned to the sediment tracer assigned to the Sacramento River boundary and San Joaquin River boundary. The label 'local sediment' is attached to the sediment tracers assigned to the three major tributary boundaries (Alameda, Coyote and Guadalupe). The sediment tracer follows the horizontal and vertical movement of the sediment particle in the water, as well as its interaction with the bed (Fig 3.3c). The DelwaQ setup accounts for essential processes, such as net sediment transport due to slack duration asymmetry, peak velocity asymmetry and wind-wave induced re-suspension.

However, the interaction of suspended sediment particles with the bed are not modelled in this research. Fine sediment is usually (and also here) supply-limited. Including the water-bed interaction requires a sed-

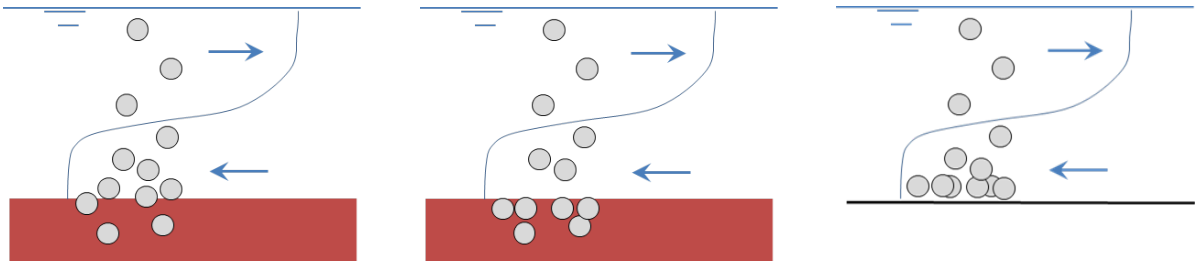

(a) A schematisation of the bed interaction in the field

(b) DelwaQ set up with bed interaction

(c) DelwaQ set up with no bed interaction

Figure 3.4: A schematisation of the implication of modelling of the bed interaction in DelwaQ

iment bed in equilibrium with the hydrodynamics, which requires more time than available for this study. Even more, fine sediment particles are subject to consolidation (a gradual increase in density and therefore of resistance against erosion). Such processes are not implemented in D-WAQ.

3.2.4. Model output locations

The model output locations consist of five observation points, sub-areas and several transects in the San Francisco Bay Area (Fig. 3.5). The observation points, Pier17 and Dumbarton Bridge, are specified at the exact location as the measurement stations with the same name. At the transects in the northern reach and South Bay, the cumulative transport is calculated. In South Bay, these transects are subdivided into different parts to make distinction between the distinct geological areas (Fig. 3.5b).

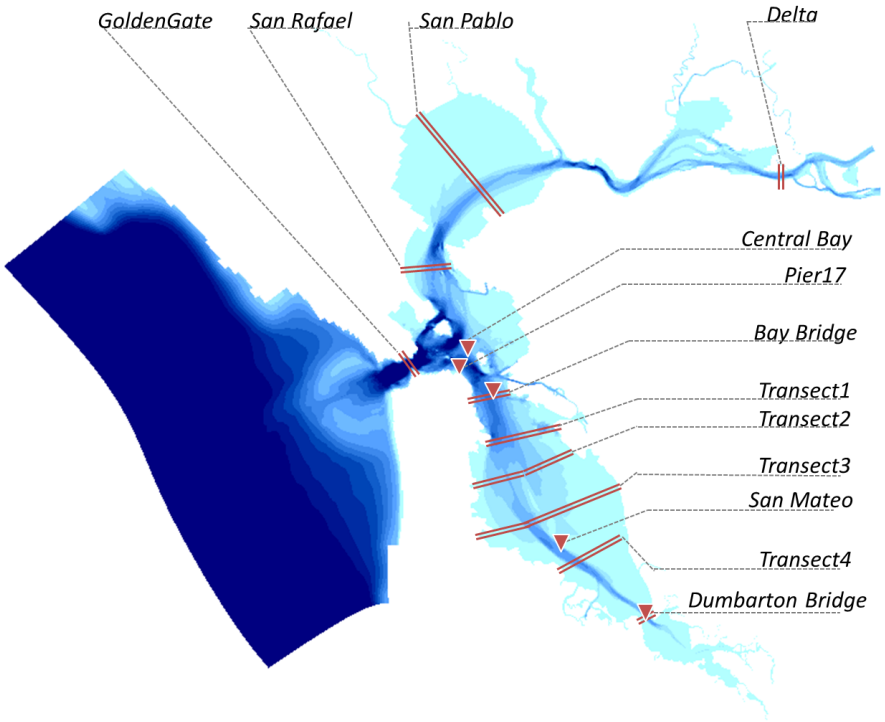

(a) San Francisco Bay Area

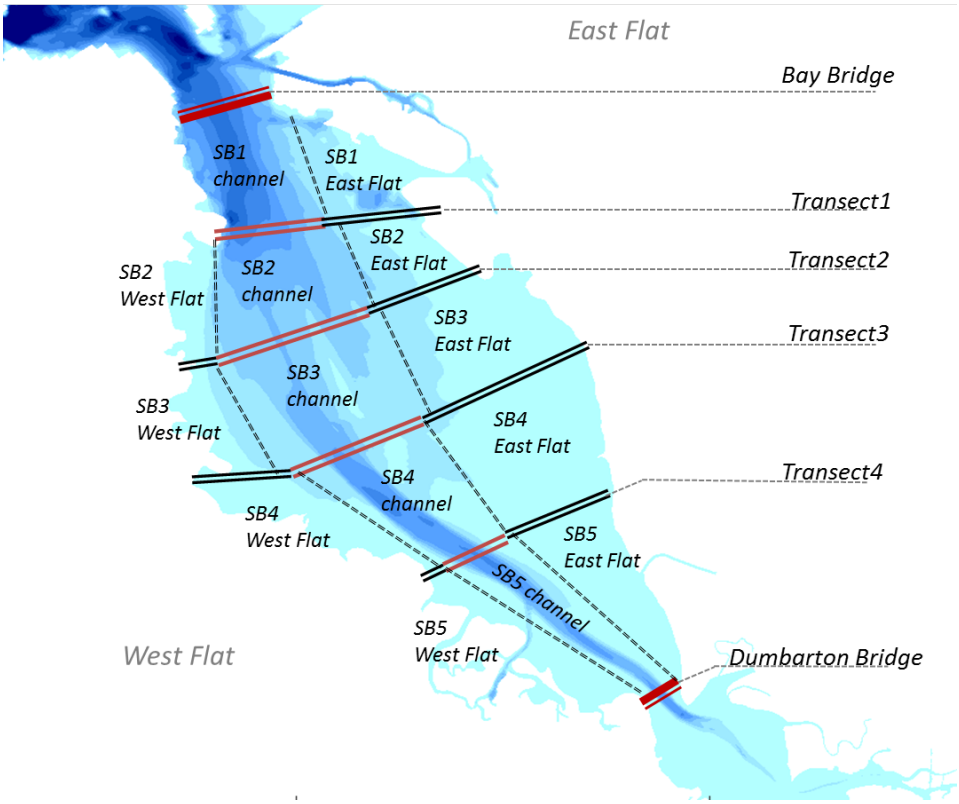

(b) San Francisco South Bay

Figure 3.5: The output locations of the model. The different blue colours indicate the water depth. Light blue represents shallow water (< 4 m) and dark blue water deeper water (>10 m) The transects are shown with a double line. The transects are divided into a west flat transect (black double line), a channel transect (red double line) and an east flat transect (black double line). The dotted grey line indicates the transect separating the channel from the flat.

4

Results

This chapter describes the results of both the data analysis and the numerical model simulations. Firstly, the results of the data analysis are presented in §4.1. Secondly, the results of the numerical model simulations are given in §4.2.

4.1. Results Data Analysis

A new set of data (WY2015-WY2017) are observed in this research. Firstly, the observed trends in the times series are outlined in §4.1.1. Firstly, the correlations found between observed trends in SSC and hydrodynamic forces are stated in §4.1.2. Paragraph 3.1 outlines the characteristics of the dataset and how these are analysed.

4.1.1. Observed trends

Observed river trends

The five substantially rivers that influence South Bay can be subdivided into two rivers that confluence in the northern reach of the estuary (Sacramento-San Joaquin Delta) and three smaller local rivers sources (Alameda Cr, Guadalupe and Coyote CR) discharging directly into South Bay. Each year has at least one small period of high discharges and the rest of the year a longer period of low discharges, respectively the wet and dry period. Some years contain several high discharge peaks during the wet period (§1.2.2).

The magnitude of the wet periods varies over the years. The average wet periods are the standard, with once every five to six years an extremely wet year. The years 1998, 2006 and 2017 are extreme wet years (Fig 4.1). Some intermediately wet years are 1999, 2000, 2004 and 2011. The wet years of 1998 and 2017 coincide with strong El Nino years. An El Nino/La Nina event on its own does not result in high precipitation rates in California and therefore does not immediately result in high river discharges. A complex combination of different meteorological components leads to a wet year [Yuan and Yamagat, 2014].

With an average discharge of 800 m^3s^{-1}, the Delta is substantial in comparison to the average discharges of around 30 m^3s^{-1} of the rivers out flowing directly into South Bay. During an extremely wet period, the Delta discharge increases to 10.000 m^3s^{-1} and for the smaller rivers only to 400 m^3s^{-1} (Fig 4.1). The Delta outflow is significant in comparison to the total discharge out-flowing from the local river sources.

The sediment load from the Delta as well as the local river source Alameda is substantial. The contribution of the local river sources Guadalupe and CoyoteCR are insignificant. The sediment load from the Delta is $2,5 * 10^5 gs^{-1}$ during a moderately wet period. The sediment load from the Alameda is between the $0,5 * 10^5 gs^{-1}$ and $1,2 * 10^5 gs^{-1}$ during this period. The sediment load from the Delta increases to $18 * 10^5 gs^{-1}$ in an extremely wet period.

There is limited data on sediment load available. There are no time series on sediment characteristics during an exceptionally wet year. Therefore,a comparison between the rivers, based on only data, is insufficient.

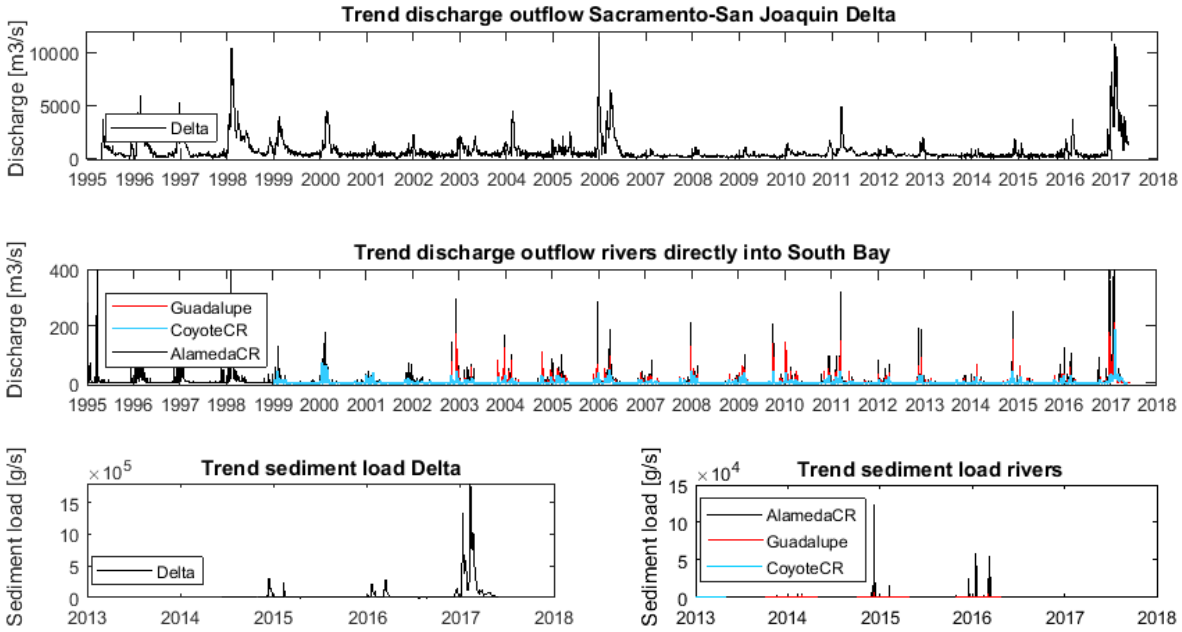

Figure 4.1: This figure shows the trends of discharge and sediment load of the five major rivers. The discharge of the Delta is discharge of the Sacramento river (RioVista station, §A.1) combined with the discharge of the San Joaquin river (Jersey station §A.1) from 1885 to 2017. It concerns the tide filtered discharge. The discharge of the Guadalupe, Alameda, Coyote (With the same name stations, §A.1) is instantaneous, since the tide does not act at this point in the rivers. The sediment load is constructed by multiplying the discharge with the SSC at that moment at the same station. SSC data is only available since midway 2014.

The cumulative sediment transport of both the Delta as the Alameda show a pulse-like behaviour of the rivers. On average, both the Delta as well as the Alameda Creek has two or three sediment pulses each year.

The Delta discharges approximately 0.42 Mty^{-1} and 0.53 Mty^{-1} in respectively WY2015 and WY2016 (Fig. 4.2). In a remarkably wet year such as WY2017, the Delta discharges 3.6 Mty^{-1}. The Alameda discharges fewer sediments than the Delta. The sediment load is 0.02 Mty^{-1} and 0.03 Mty^{-1} in respectively WY2015 and WY2016.

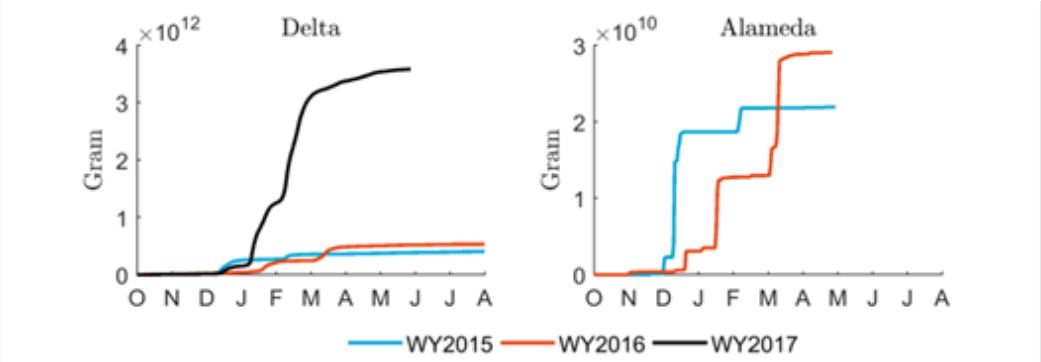

Figure 4.2: Cumulative sediment transport of the Delta and the Alameda Creek for three different Water Years. Sediment transporting downstream is positive defined.

Observed density gradients trends

Relation Delta discharge and Bay Bridge salinity

The salinity in San Francisco Bay varies throughout the year. The salinity in Central Bay and South Bay has a value of approximate 32 PSU. The salinity reduces one or twice every year during the wet season. The reduction of the lower embayments salinity's is non-linearly related to the discharge from the Delta. An increase in discharge from the Delta leads to a decrease of salinity at Bay Bridge (Fig.4.3).

A moderate high Delta discharge ($Q_{Delta} > 800 m^3 s^{-1}$) results in a lowering of 2 to 4 PSU at Bay Bridge. The lowering is a reduction of 20 percent, suggesting that 20 percent of the water gets diluted by the Delta water. The reduction is even higher during a period of extreme high Delta discharge ($Q_{Delta} > 10,00 m^3 s^{-1}$). The water at Bay Bridge is then for 50 percent refreshed by Delta water.

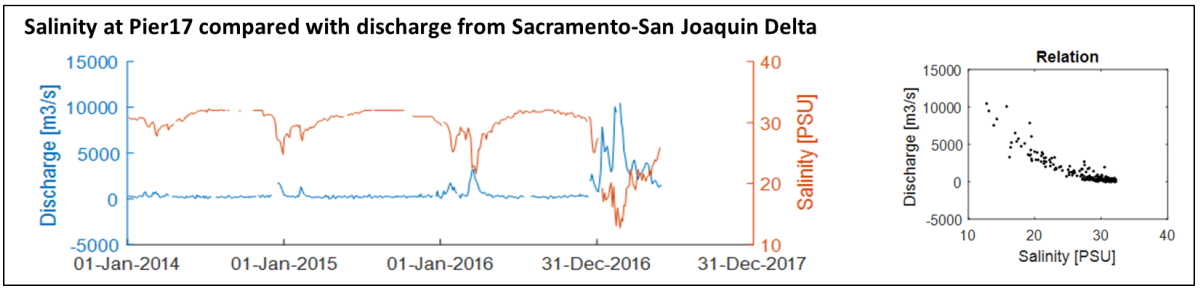

Figure 4.3: The time series of the salinity at measurement location Pier17 (right axis) and the time series of the discharge from the Sacramento-San Joaquin Delta (left axis) are shown. On the right, the relation between the two parameters is displayed.

Horizontal salinity differences Central Bay and South Bay
The refreshment of Central Bay and South Bay occurs almost simultaneously during the Delta high river runoff (around Jan-2015, Jan-2016, Jan-2017 in Fig 4.4). The dilution of South Bay (San Mateo Bridge) lacks behind Central Bay (Alcatraz), resulting in a higher surface salinity in South Bay than in Central Bay. The horizontal salinity difference is just for a short period because the refreshment of South Bay happens fast and the salinity reaches eventually the same salinity value.

The surface salinity in Central Bay increases due to the interaction with the more saline water of the Pacific, resulting in a slow increase of salinity until it reaches the same value as before the refreshment. The surface salinity of South Bay increases more gradual than at Central Bay, resulting in horizontal salinity difference between the Bays. The maximum difference observed is 5 PSU during a dry year and 10 PSU during a wet year (Fig. 4.4).

The salinity difference approach zero and eventually reverse in the dry summer period. The salinity of South Bay can reach very high values during summer due to evaporation. Then, the surface salinity of South Bay is higher than Central Bay, resulting in a negative salinity difference.

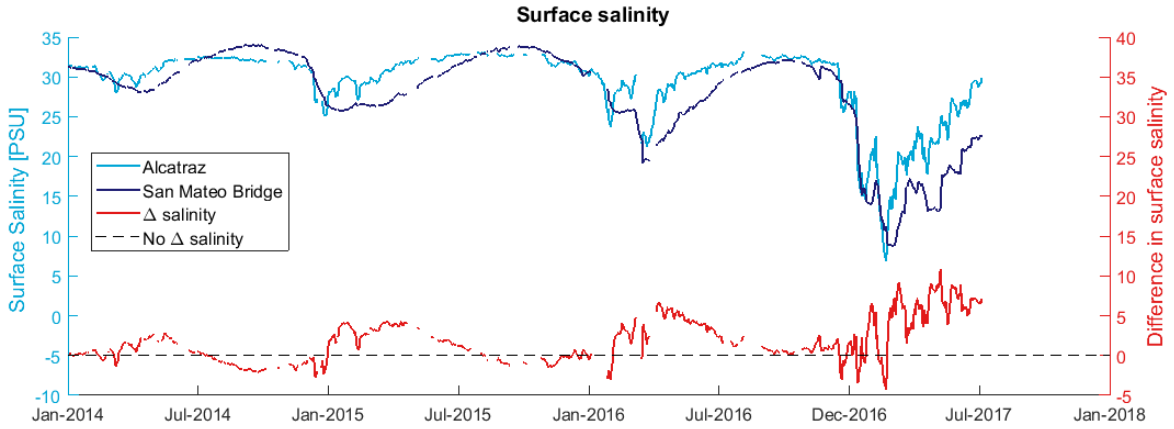

Figure 4.4: Surface salinity at measurement location Alcatraz (left axis) and San Mateo Bridge (left axis). The difference in surface salinity is shown with the red line (right axis). Positive salinity differences (red line is above the black dotted line) is a higher salinity at Alcatraz than at San Mateo Bridge.

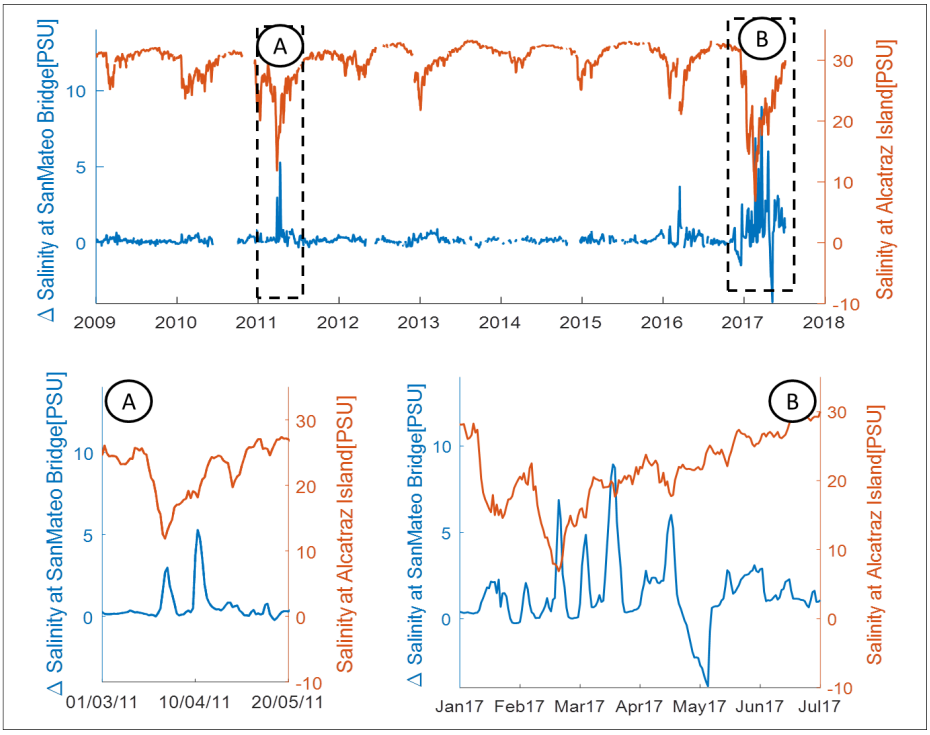

Figure 4.5: Salinity differences between bottom and surface salinity at measurement location San Mateo Bridge compared with salinity at measurement location Alcatraz Island. The vertical distance between the two measurement stations at San Mateo Bridge is 10 meter. Positive salinity difference means that the surface is fresher than the bottom

Three stages of surface salinity differences can be observed. The first stage is the refreshment of Central Bay and South Bay by Delta water. The surface salinity at South Bay is higher than at Central Bay. The second stage marks the period just after the refreshment of South Bay. The surface salinity of Central Bay is higher than South Bay. The third stage is where the surface salinity of South Bay is higher than Central Bay, due to high evaporation rates.

Vertical salinity differences in South Bay
In general, South Bay is a well-mixed estuary, where the difference between the bottom and surface salinity's are minimal. The mean difference is 0.26 PSU, with a standard deviation of 0.66 PSU (Fig. 4.5). Significant salinity differences are observed when the salinity in Central Bay (Alcatraz) drops below 20 PSU, which is noticed in WY2011 and WY2017.

For 2011, two distinct salinity difference peaks can be observed. The first one corresponds to the declining of the salinity in Central Bay. This peak is observed as well in figure D.3 on 29th of March. The surface is fresher than the bottom, and stratification is observed. The second peak corresponds to 12th of April in figure D.3, with some pronounced observed stratification. In between, there is indeed a period of uniform salinity over the depth. The uniform salinity might indicate the effect of a spring tide.

In spring of 2017 some distinct stratification periods are observed, fluctuating along the spring-neap tidal cycle, with remarkable a negative salinity difference, which indicates that there is more dense water on top of the fresher water, resulting in instabilities.

4.1.2. Observed relations between SSC and hydrodynamic forcing

The SSC data at measurement station 'Dumbarton Bridge' and 'Pier17' (Fig. 3.1) are reviewed with time series of several hydrodynamic forcing. Firstly, the SSC time series are compared with the sediment loads from the rivers. Firstly, the SSC time series are compared with the wind speed.

Correlations SSC time series and river outflow
The sediment load discharged by the rivers has each year a period with high sediment loads and a longer period of low sediment loads. The rivers discharge insignificant amount of sediment loads during the dry periods. These sediment loads do not show any correlation with the SSC time series measured in South Bay (Fig 4.6). The rivers have no direct influence on the SSC in South Bay during dry periods. Some correlations are observed during wet periods, suggesting that the rivers have a direct effect during these periods.

Pier 17
A distinct correlation (r=0.63) between the wet periods and the sediment load from the Delta is observed. The moderate positive correlation indicates that the SSC is positively related to an increase in sediment load from the Delta. This dependency is different for separate wet periods. Intermediate sediment pulses from the Delta has less impact on the SSC than an extreme sediment pulse. During an extreme sediment pulse of 2017, a strong positive correlation (r=0.75) was found. It is suggested that the SSC at Pier17 is strongly related to the sediment load from the Delta.

The sediment load from the other two rivers are hardly related to the SSC at Pier17, according to the correlations. However, a substantial peak in sediment load is just observed before an increase in SSC at Pier 17. The data of the sediment discharge from the local rivers are very discrete. The rivers discharge almost their yearly sediment budget in just one day. This discrete peak is hard to correlate. An option is that the sediments do influence this raised SSC during 2015. Besides, a weak positive correlation (r=0.27) was observed for the sediment load from the Alameda and SSC in 2016. The sediment load of the river is highly varying inter-annual, which might lead to different dependencies each year.

Dumbarton Bridge
The SSC at Dumbarton Bridge is weakly related to the sediment load from the Delta during the wet periods. This dependency is varying inter-annually. The sediment concentration shows a very weak correlation (r=0.045, r=0.22) with the sediment load in the wet periods of 2015 and 2016. In contrast, there is a moderate correlation (r=0.52) found for the wet period of 2017. The moderate correlation implies that the Delta sediments only influence the SSC at Dumbarton Bridge during very wet periods.

The sediment load from the other two rivers does not relate to the SSC concentration. Here, high SSC peak is observed just after the high discharge of sediments of both the Alameda Creek as the Guadalupe River in 2015. It could be possible that these peaks do influence the SSC at Dumbarton Bridge. However, the sediment load from Alameda Creek would be significant in comparison to the load from the Guadalupe River.

The time-lag in which the sediment needs time to travel down is accounted for in these plots with a time lag of 24 hours for Bay Bridge and 48 for Dumbarton bridge. A deviation in this time-lag did not result in a significant difference in correlation. Except for the first wet peak of the Dumbarton plot, which shows a correlation (r=0.29) when the time-lag is 70 hours. Apparently did it took longer for the sediment load to be transported.

Correlations with wind speed
The wind speed has a strong seasonal pattern in South Bay. In the summer period, the wind speed is constantly strong, whereas in the winter it is more episodic (1.2.4).

Pier17
The wind speed is weakly correlated with the SSC measured at location Pier17. The correlation coefficient found for the daily averaged time series is 0.31 and for the monthly averaged data is 0.46. This weak correlation implies that the SSC at Pier17 has a weak dependency on the wind.

Dumbarton Bridge
The SSC at measurement location Dumbarton Bridge correlates with wind speed at Redwood city (Fig B.2). The daily averaged times series show a weak positive correlation (r=0.46) and the monthly averaged time series show a strong positive correlation (r=0.76). The SSC time series follows the periodically wind speed variations. These correlation coefficients suggest a strong seasonal dependence of the SSC on the wind speed at Lower South Bay.

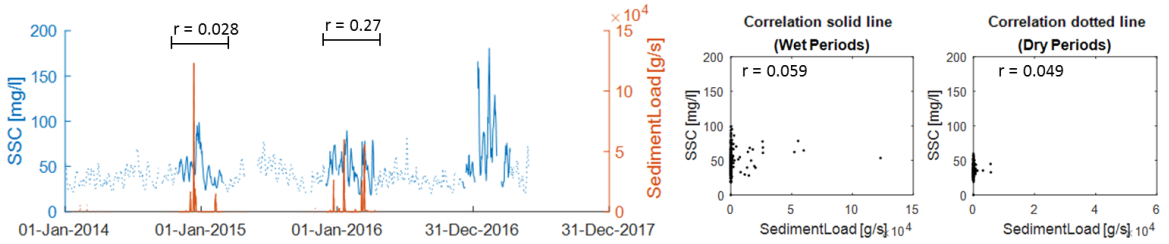

(a) SSC time series at measurement location **Pier17** compared with sediment load from the **Alameda river**

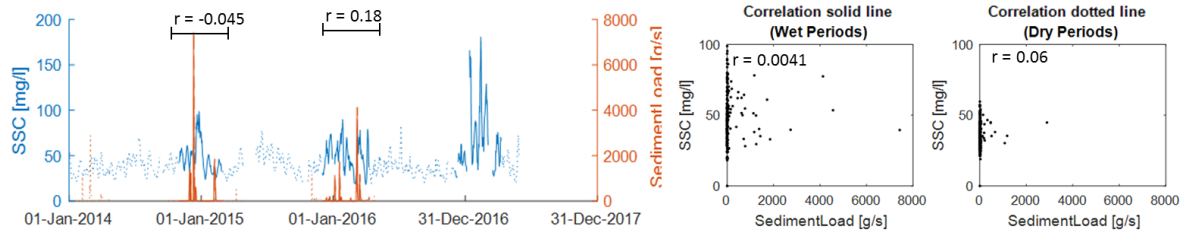

(b) SSC time series at measurement location **Pier17** compared with sediment load from the **Guadalupe river**

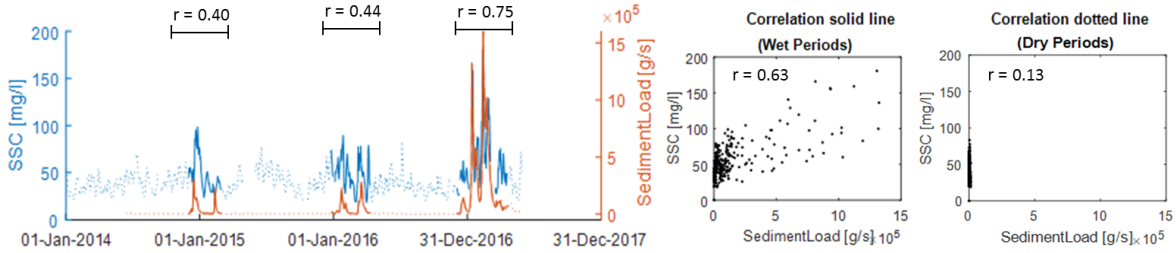

(c) SSC time series at measurement location **Pier17** compared with sediment load from the **Delta**

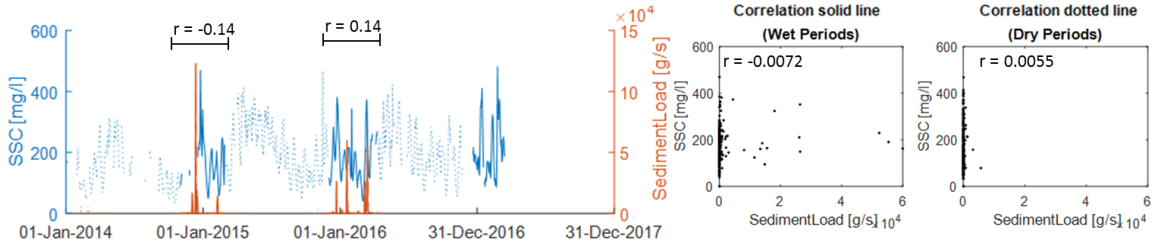

(d) SSC time series at measurement location **Dumbarton Bridge** compared with sediment load from the **Alameda river**

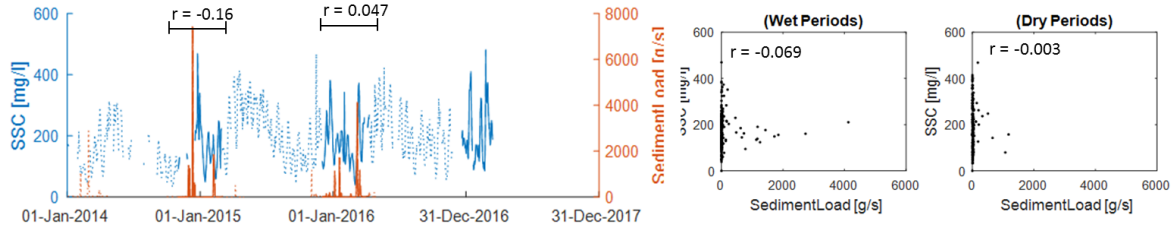

(e) Time series compared for measurement location **Dumbarton Bridge** and **Guadalupe river**

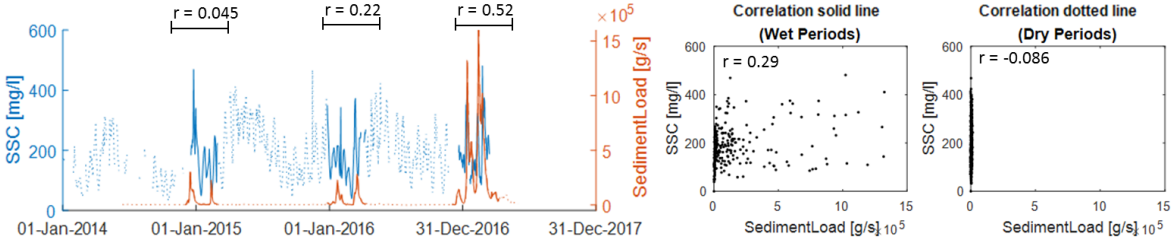

(f) SSC time series at measurement location **Dumbarton Bridge** compared with sediment load from the **Delta**

Figure 4.6: The SSC time series of South Bay are compared with sediment load from the major rivers. The two parameters are plotted over time; the blue line indicates the SSC [mg/l] and the orange line the sediment load [g/s]. The solid line represents the wet periods of the year. The dotted line represents the dry periods. The correlation coefficient for each wet period is displayed above the wet period. The correlation coefficients and plots for the combined wet periods and combined dry periods are plotted next to the time series.

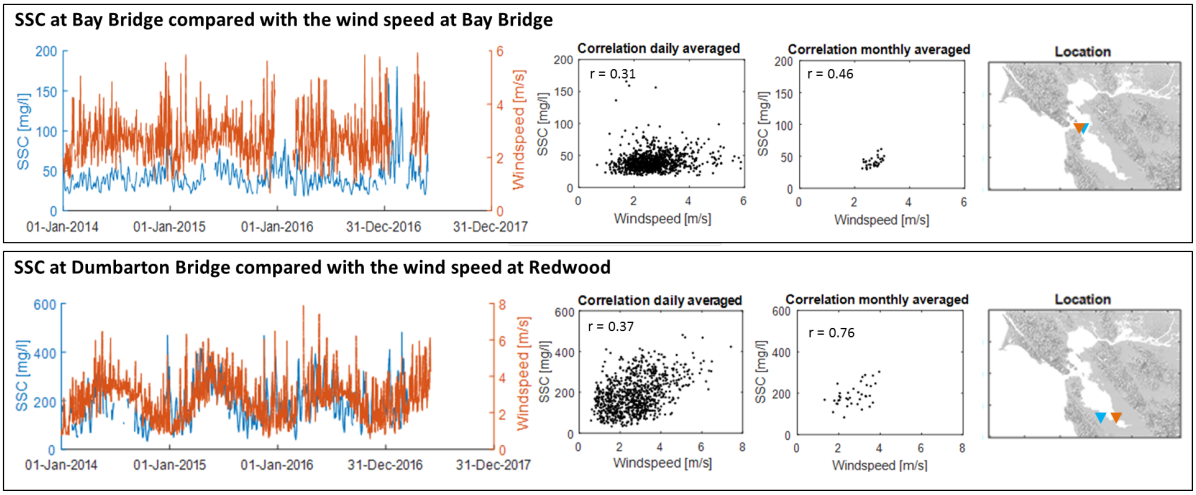

Figure 4.7: The correlation of SSC measurements and wind speed measurements at Bay Bridge and Dumbarton Bridge. The SSC at the two locations is shown in blue (left axis) and the winds speed in orange (right axis). The correlation of the daily averaged and monthly averaged values are displayed in the middle. The plot on the right shows the locations of the measurement stations.

4.2. Results Numerical model

The sediment pathways in time and space are investigated using a 3D numerical model. The model selection and the set-up of the numerical model are described in §3.2. The results of the different model simulations stated in §3.2.3, are outlined in this paragraph. Firstly, the results of the hydrodynamic tracer simulation are outlined. Firstly, the results of the sediment tracer simulations are described.

4.2.1. Hydrodynamic tracer; Water fraction at Pier17 and Dumbarton Bridge

The hydrodynamic tracer indicates where the water entering over the model boundaries is going to. At observation station Pier17 and Dumbarton Bridge, the fractions of water originated from the sea or one of the five river boundaries are distinguished (Fig. 4.8). The results of each hydrodynamic scenario are stated below.

WY2015

The main fraction of water originates from the sea at Bay Bridge throughout a dry year such as WY2015. A period of moderate Delta river flow is present in December. It is within this period that a fraction of water from the sea is partially replaced by water from the Delta rivers at Bay Bridge. At the start of January, the water consists of 20 percent of Delta water and around 80 percent of seawater (Fig 4.8(1)). The fraction of Delta river water is slowly replaced by sea water after the period of high river runoff. This decrease in Delta water at Bay Bridge occurs from January until June. The refreshment of water by Delta water happens fast in contrast to its replacement by sea water.

The fraction test shows the same water movement behaviour at Dumbarton Bridge as Bay Bridge. The differences between the refreshment at Bay Bridge and Dumbarton Bridge are insignificant (Fig 4.8(2)).

The fractions of water from the local tributaries (Alameda, Coyote and Guadalupe) are insignificant throughout the year at both Bay Bridge and Dumbarton Bridge. This suggests that there is almost no influence of local tributaries on the horizontal water movement at the two locations.

The initial condition is replaced by sea water in the first three months of the simulation. This suggests that the residence time of this seawater is in the order of months during lower river flows.

WY2015 with no wind forcing

The results of the dry year WY2015 with no wind forcing (Fig 4.8(3),4.8(4)) follow the same refreshment pattern as WY 2015 with wind forcing (Fig 4.8(1),4.8(2)). This suggests that the wind force has no significant influence on the horizontal water movement at the two locations.

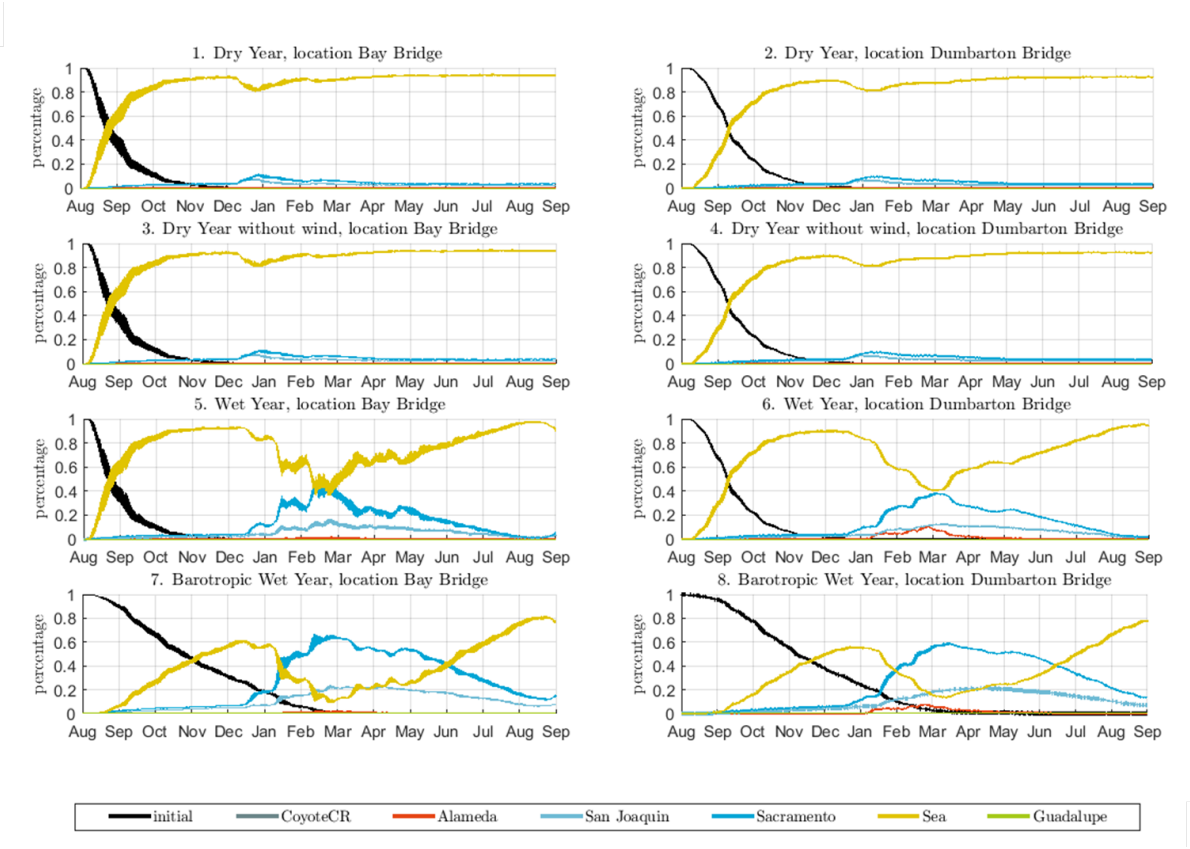

Figure 4.8: The plot shows the fractions of water originating from a certain source throughout the year at Pier17 (four left plots) and at Dumbarton Bridge (four right plots) for the four different hydrodynamic model scenarios (§3.2.3). Plot 1 and 2 show the fractions for hydrodynamic scenario WY2015, plot 3 and 4 for WY2015 with no wind forcing, plot 5 and 6 for WY2017 and plot 7 and 8 for a barotropic WY2017.

WY2017, baroclinic simulation

The main fraction of water originates from the sea at Bay Bridge for the bigger part of a wet year such as WY2017. A period of extreme Delta river flow lasts from December until March. Within this period, three Delta river runoff pluses are observed (§4.1.1). The first pulse is small and occurs in December. The following two are extreme and occur in January and February. For each of the water pulses a sharp increase can be observed in the percentage of water that originates from the Delta at Bay Bridge (Fig 4.8(5)). At the end of February, the water consists of 55 percent of Delta water and around 45 percent of seawater (Fig 4.8(5)). In the period from March until August, the water originated from the Delta is slowly replaced by seawater. This suggests that the residence time of water in the Bay is in the order of months during the dry period.

The dilution at Dumbarton Bridge happens almost simultaneously with the refreshment at Bay Bridge (Fig 4.8(6)). The first difference is that the refreshment is more gradual. The second difference is the significant fraction of water originates from the Alameda Creek. This suggests that this river could have an influence on the processes in the southern part of South Bay during extreme wet years.

WY2017, barotropic simulation

The refreshment pattern for the barotropic simulation (Fig 4.8(7),4.8(8)) is different than the baroclinic simulation of a wet year such as WY2017 (Fig 4.8(5),4.8(6)). The dilution of both Bay Bridge and Dumbarton bridge is more gradual. Additionally, more fresh water from the Delta is transported into South Bay. The fraction of water originated from the sea is around March almost 15 percent, whereas this is 45 percent in the baroclinic simulation. The replacement of the refreshed water by sea water takes as well a longer period. This suggests that the baroclinic flows have an impact on the horizontal movement of Delta water into South Bay.

The influence of the Alameda remains the same in the barotropic simulation (Fig 4.8(7),4.8(8)) as for the baro-

clinic simulation (Fig 4.8(5),4.8(6)). This may suggests that the baroclinic flows have minimum effect on the horizontal water movement in the southern part of South Bay.

The replenishment of the initial condition takes six months in the barotropic simulation in contrast to the three months in the baroclinic simulation. The residence time of water in South Bay is increased. This suggests that the density differences accelerate the refreshment of South Bay. Only the tide and wind forcing do not lead to a small residence time.

4.2.2. Sediment tracer; SSC at Pier17 and Dumbarton Bridge

This paragraph outlines the computed suspended sediment concentration (SSC) of the three different settling velocities sediment classes at Pier17 and Dumbarton Bridge. In situ data are available at the two locations. Therefore, it is possible to compare the field SSC with the computed SSC for different hydrodynamic scenarios.

A distinction is made between sediments originated from the Delta and sediments originated from the local tributaries. The Delta sediments enter South Bay from Central Bay through the channel at Bay Bridge, whereas the local sediments directly enter the flat at South Bay.

SSC at Pier 17

The averaged measured SSC at station Pier 17 is 70 gm^{-3}. The in situ measured SSC is higher for a short period in after periods off high river flow.

WY2015

The in situ measured SSC is 250 gm^{-3} for a short period in the month December in WY2015. This first peak in measured SSC corresponds to a computed small peak in SSC of local river sediments and a more significant increase in SSC of Delta sediments. The increase in SSC of Delta sediments is substantial in comparison to the increase of local sediments in December. This suggests that the SSC at Pier17 mainly reflects sediment input from the Delta. The input sediment input from the local tributaries is limited throughout the year.

The magnitude of computed SSC is not in same order of magnitude as the measured SSC. The computed SSC is too low. The sediment input of only the rivers does not result in the correct SSC profile. The SSC might be masked by other sources, like re-suspended material, sediment that is kept in suspension and transported due to persistent tidal and other currents.

WY2015, with no wind forcing

The model scenario with no wind forcing shows the same behaviour as the model scenario with wind forcing. This result indicates that the wind force does not lead to an elevated SSC during the wet summer.

WY2017

The in situ measured SSC is 400 gm^{-3} for a more extended period during the period of high river flow in WY2017. The peak period in measured SSC corresponds to the computed peak period in SSC. This suggests that the SSC at Pier17 reflects sediment input from the Delta.

The computed SSC are substantially higher for WY2017 than WY2015. This suggests that more Delta sediments enter South Bay in an extremely wet year than in an averaged dry year.

The in situ measured SSC shows a high inter-tidal SSC range from the month January until March. This inter-tidal range seems to correspond to a spring-neap tidal cycle. The computed SSC displays as well a high inter-tidal SSC from the month January until Marc. This inter-tidal range of SSC suggests that the spring-neap tidal cycle is an essential aspect at Pier17.

SSC at Dumbarton Bridge

The averaged in situ measured SSC at one meter from the bed at Dumbarton Bridge is 200 (gm^3)]. The in situ measured SSC is higher for a short period in the month December or January and a longer period in the summer months.

WY2015

The in situ measured SSC is 600 gm^{-3} for a short period in the month December in WY2015. This first peak in measured SSC corresponds to a computed small peak in SSC of local river sediments. This small peak of local river sediments is observed just after the high sediment load pulse of the Alameda Creek in December. This observation suggests that the sediment load from the Alameda contributes little to the SSC at Dumbarton Bridge. This contribution holds for the three different sediment classes.

The in situ measured SSC is 500 gm^{-3} for a more extended period during the summer months in WY2015. The higher field-measured SSC corresponds to a raised level of computed Delta SSC of the sediment with the larger settling fall velocities (Ws=0.49 mms^{-1} and Ws=1.62 mms^{-1}) at Dumbarton Bridge in the same period. This suggests that the elevated SSC in the dry summer is a lagged response of Delta sediments with larger settling velocities entering South Bay. The computed SSC of the sediment with smaller fall velocity (Ws=0.011 mms^{-1}) does not exhibit the elevated values during the dry summer months.

The magnitude of computed SSC is not in same order of magnitude as the measured SSC. The computed SSC is too low. The sediment input of only the rivers does not result in the correct SSC profile. The SSC might be masked by other sources, like re-suspended material, sediment that is kept in suspension and transported due to persistent tidal and other currents.

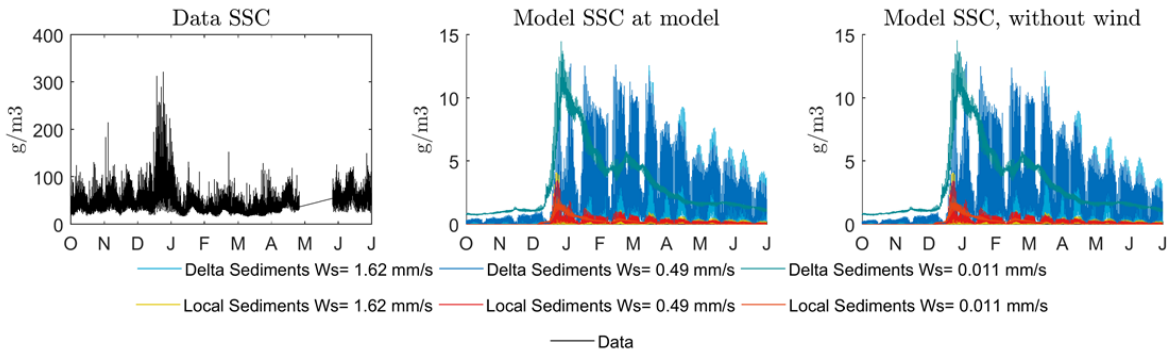

(a) The in situ measured SSC in WY2015 is displayed left, the computed SSC for WY2015 is shown in the centre, and the computed SSC for WY2015 with no wind forcing in the model is displayed right.

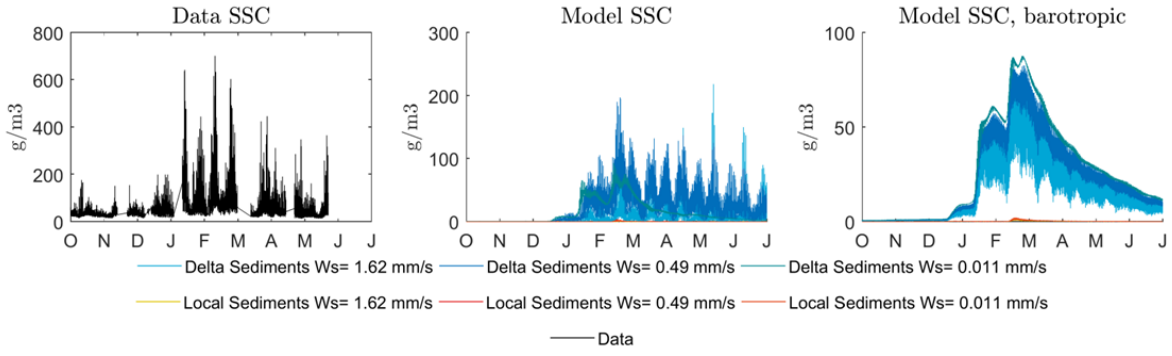

(b) The in situ measured SSC in WY2017 is displayed left, the computed SSC for WY2017 is shown in the centre, and the computed SSC for a barotropic simulation of WY2017 is displayed right.

Figure 4.9: In situ measured and computed surface SSC at observation location Pier17

WY2015, no wind forcing
The model scenario with no wind forcing shows the same behaviour as the model scenario with wind forcing. This result indicates that the wind force does not lead to an elevated SSC during the dry summer. This result may indicate that the elevated SSC during the summer months is not due to re-suspension on the shoals due to wind-waves.

WY2017
The in situ measured SSC is 500-1000 gm^{-3} for a more extended period during the summer months in WY2017. The higher field-measured SSC corresponds to a raised level of computed Delta SSC of the sediment with the larger settling fall velocities (Ws=0.49 mms^{-1} and Ws=1.62 mms^{-1}) at Dumbarton Bridge in the same period. This suggests that the elevated SSC in the dry summer is a lagged response of Delta sediments with larger settling velocities entering South Bay. The computed SSC of the sediment with smaller fall velocity (Ws=0.011 mms^{-1}) does not exhibit the elevated values during the dry summer months.

The computed SSC are substantially higher for WY2017 than WY2015. This suggests that more Delta sediments enter South Bay in an extremely wet year than in an averaged dry year.

The in situ measured SSC shows a high inter-tidal SSC range from the month March until July. This inter-tidal range seems to correspond to a spring-neap tidal cycle. The computed SSC displays as well a high inter-tidal SSC from the month March until July. The high inter-tidal SSC range is profound for the middle settling velocity sediment class (Ws=0.49 mms^{-1}). This inter-tidal range of SSC suggests that the spring-neap tidal cycle is an important aspect at Dumbarton Bridge.

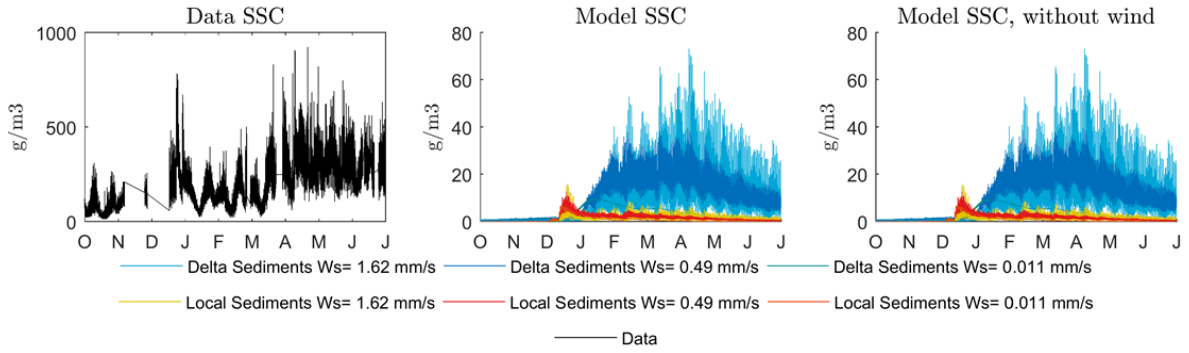

(a) The in situ measured SSC in WY2015 is displayed left, the computed SSC for WY2015 is shown in the centre, and the computed SSC for WY2015 with no wind forcing in the model is displayed right.

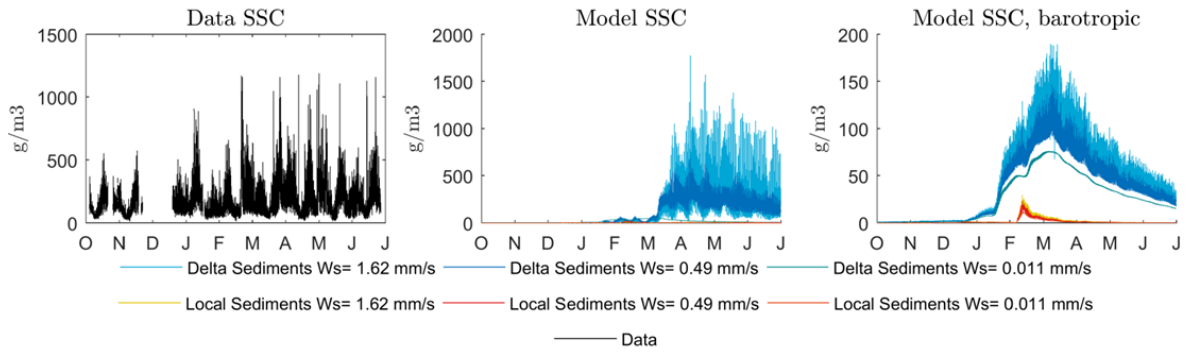

(b) The in situ measured SSC in WY2017 is displayed left, the computed SSC for WY2017 is shown in the centre, and the computed SSC for a barotropic simulation of WY2017 is displayed right.

Figure 4.10: In situ measured and computed near bed SSC at observation location Dumbarton Bridge. The measurements and the observation point in the model is one meter from the bed

WY2017, barotropic simulation
The computed SSC in the barotropic simulation shows a different behaviour than the computed SSC in the baroclinic simulation. The SSC is increasing at Dumbarton Bridge from January until March for the barotropic simulation, whereas the SSC increases only from March in the baroclinic simulation. This difference indicates the importance of density gradients in the system. It suggests that the density gradients cause the lagged response at Dumbarton Bridge.

4.2.3. Sediment tracer; SSC at South Bay sub-areas

This paragraph outlines the computed suspended sediment concentration (SSC) of the three different settling velocities sediment classes at several South Bay sub-areas. A distinction is made between sediments originated from the Delta and sediments originated from the local tributaries. The Delta sediments enter South Bay from Central Bay through the channel at Bay Bridge, whereas the local sediments directly enter the flat at South Bay.

South bay can be divided into three different geometrical sub-areas; the west flat, the channel and the east flat. The flats have a maximum depth of five meters whereas the channel has depths between five and twenty meters. The west flat is split into four sub-areas. The channel and east flat are both divided into five sub-areas. Therefore, South Bay is divided into 14 sub-areas in the model simulation (Fig. 3.5b). For the sake of brevity, the midsection of South Bay is only outlined in this text-section. The results of the fourteen South Bay sub-areas are shown in the appendix (D).

WY2015
The SSC in the channel and on the west flat contain mainly sediments from the Delta throughout the year. The SSC on the east flat contains sediments from the local sources as well as the Delta. A high concentration of local sediments on the east flat can be found, just after the high river outflow of the Alameda Creek in De-

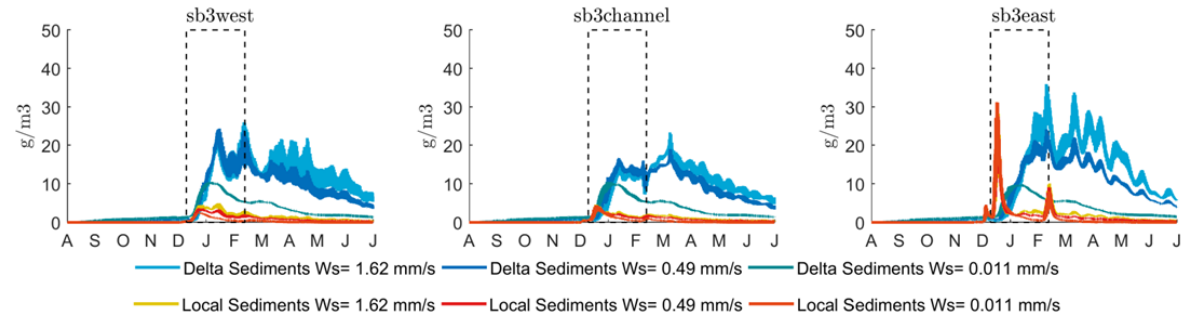

(a) WY2015

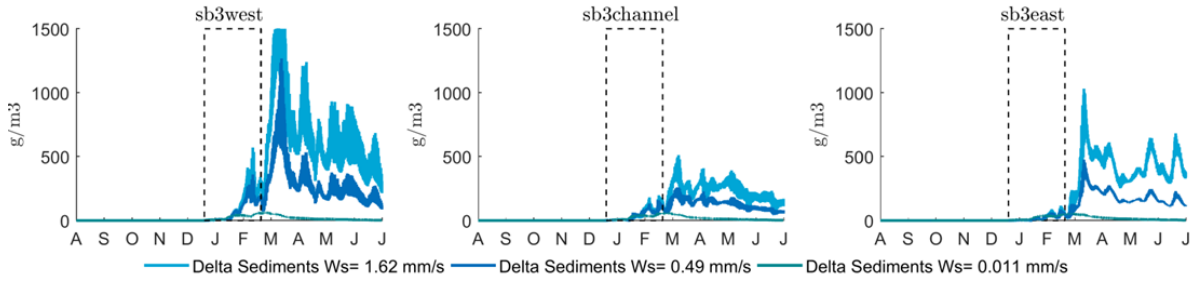

(b) WY2017

Figure 4.11: The SSC at three sub areas in South Bay in a dry year such as WY2015(a) and in a wet year such as WY2017(b) are shown in the figure. The SSC is area- and depth averaged. The subareas are marked in Fig(3.5b). The dotted rectangle reflects the period of high river flows. The sediments from the Sacramento-San Joaquin Delta are labelled as Delta sediments. The sediments from the local tributaries are labelled as the local sediments. There is no sediment data available for the local sediments during the WY2017. Therefore, the are no local sediments included in the simulation of WY2017.

cember 2015. The short peak suggests that the sediments have a short stay on the east flat(Fig. (4.11a). The short peak indicates that the sediments coming from local sources are only significant for a minimal period on the east flat.

The SSC of the Delta sediments at the three sub-areas only increases during periods of high river outflow in WY2015 (Fig. (4.11a). The increase during periods of high river outflow suggests that the Delta sediments are delivered to South Bay during the wet period. Only the concentration of the lower fall velocity particles is both increasing as decreasing in the wet period. This may indicate that lower fall velocities sediments have a small residence time in South Bay. The sediment concentration is decreasing for all Delta sediments in the dry period.

A peak of SSC of the local sediments at the east flat is visible during the period of high river runoff. This indicates that the local sediments are delivered to South Bay during the wet periods.

WY2017
The SSC of Delta sediment at the three sub-areas in WY2017 are higher than the SSC of Delta sediment in WY2015. Therefore, a larger amount of Delta sediment enters South Bay in an extremely wet year such as WY2017 than in a dry year such as WY2015. The large difference between WY2015 and WY2017 holds especially for the two larger settling velocities (Ws = 0.49 mms^{-1} and Ws = 1.62 mms^{-1}). The sediment class with the smallest settling velocity (Ws = 0.011 mms^{-1}) shows a minimal increase in SSC in the WY2017. Therefore, the results suggest that the sediment with the larger settling velocities are more affected by the differences between the dry and wet year.

The SSC of the Delta sediments increases only marginally at the three sub-areas during the period of high river flow. The SSC increases substantially just after the period of high river flow. This substantial increase after the period of high river flow indicates that the sediments do not enter South Bay during periods of high river flow in an exceptionally wet year.

The concentrations are on average higher on the flats than on the shoals. This suggests that the Delta sediments end up on the shoals in South Bay.

There is no data of the local sediments available during WY2017. The data could not be constructed out of other, due to the high inter-annual variability of the hydrodynamics in South Bay. Therefore, it was not possible to compute the local sediments during WY2017.

4.2.4. Sediment tracer; Pathways in the northern reach

San Francisco Bay can be divided into two geographically and hydrologically distinct sub-estuaries; the northern reach lying between the connection to the Pacific Ocean at the Golden Gate and the confluence of the Sacramento-San Joaquin river system, and the southern reach between Bay Bridge and the southern end of the Bay [Conomos et al., 1985]. The characteristics of the sediment transport between the two sub-estuaries are different, but depending on each other.

This paragraph outlines the sediment pathways of the sediments in the northern reach, by reviewing the computed cumulative transport at several transects in the northern reach (§3.2.4). Firstly, the transport of Delta sediments is stated. Firstly, the transport of local sediments are described.

Transport of Delta sediments in the Northern reach
Sediment pulses propagating from the Delta towards Central Bay characterise the sediment transport in the northern reach. The Sacramento - San Joaquin Delta discharges circa two times a year a high sediment pulse. These sediments move quickly down the northern reach in a pulselike behaviour. The sediment load entering the northern reach is small for the rest of the year. The small fall velocity particles are slowly moving down the estuary in the period of low river discharge. The higher settling velocity particles are slowly moving up the estuary in this stage (Fig. 4.12).

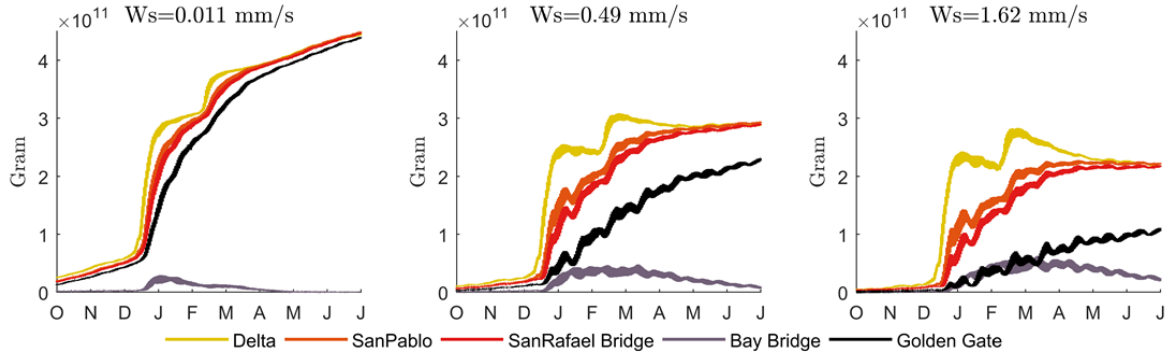

(a) Dry Year WY2015

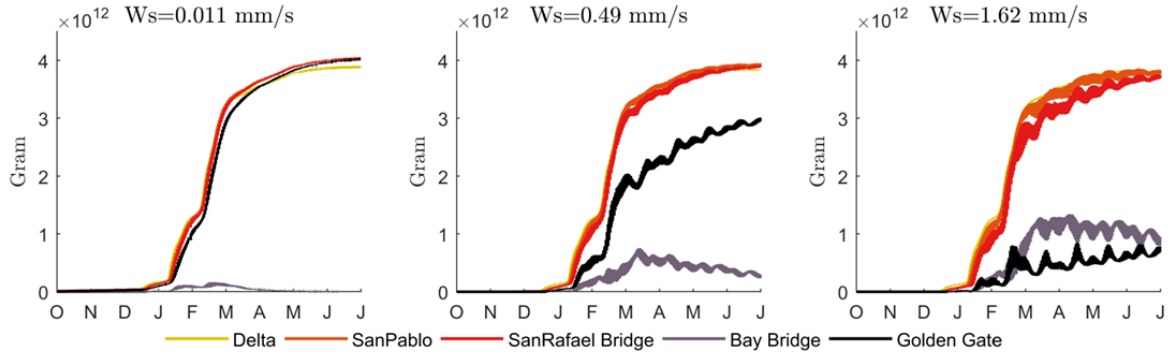

(b) Wet Year WY2017

Figure 4.12: The figure displays the cumulative sediment transport curves for the three settling velocity Delta sediment classes (ws=0.011 mms^{-1}, ws=0.49 mms^{-1}, ws=1.62mms^{-1}) in the Northern reach for a dry year such as WY2015 (a) and a wet year such as WY2017 (b). Each graph displays the cumulative transport for several transects in the northern reach (§3.2.4). Downstream transport is positive defined. Transport from Central Bay to the Pacific is defined positive at the Golden Gate transect.

WY2015

The Sacramento - San Joaquin Delta has two sediment pulses in WY 2015. These sediment pulses propagate down the northern estuary to Central Bay (Fig. 4.12). The smaller settling velocity sediments (Ws = 0.011 mms^{-1}) are transported quickly down, within days the sediments enter Central Bay. From there, the predominant sediment pathway is from Central Bay to the Pacific through the Golden Gate. Just a small fraction of this sediment class enters South Bay through Bay Bridge. Soon the transport flux at Bay Bridge reverses, and the net sediment transport is from South Bay to Central Bay.

The sediment pulses for the larger settling velocities (Ws = 0.49 mms^{-1} & Ws=1.62 mms^{-1}) have a slightly different behaviour than the smaller settling velocity particles. The sediments are transported down the northern reach more slowly and more diffusive till they enter Central Bay. A fair amount of sediments remain in Central Bay, increasing the SSC. A fraction of sediments is transported either towards the Pacific or South Bay. Sediment is transported gradually from Central Bay to South Bay until February/March(Fig. 4.12). The sediment flux at Bay Bride reverses around March, and the net sediment transport is then from South Bay to Central Bay for the rest of the year. The cumulative transport approaches zero at the end of the water year. Therefore, South Bay almost does not accumulate sediments. The transport of sediments from Central Bay to the Pacific is almost constant over time and does not show a pulse-like behaviour.

WY2017

An extremely wet period characterises WY2017. Three sediment pulses enter North Bay, of which the last two are significantly bigger than observed sediment pulses in a dry year such as WY2015. The propagation of the sediments down the northern reach is faster in WY2017 than in WY2015. All three sediment classes show the same transport behaviour without a distinctive diffusion while transporting down the northern reach. Within days the sediments enter Central Bay. From there, sediment with a smaller settling velocity (Ws=0.011

mms^{-1}) is transported directly into the Pacific. Only a tiny fraction of the sediment moves into South Bay. All these sediments eventually flow out of South Bay to Central Bay. Therefore, South Bay does not accumulate sediments with a slow settling velocity.

Sediment with the larger settling velocities (Ws=0.49 mms^{-1} & Ws=1.62 mms^{-1}) is mainly remaining in Central Bay. A fraction of these sediments moves either to South Bay or the Pacific. The cumulative transport curves into South Bay show a sharp increase at Bay Bridge in March. From March on, the direction of the net transport is from South Bay to Central Bay. The net transport from South Bay to Central Bay is more gradual in the months from March than the net transport from Central Bay to South Bay in the prior months. South Bay accumulates sediments with larger settling velocities in WY2017.

Transport of Local river sediments in Northern reach
The primary sediment pathway of Local river sediments in the Northern reach is from Central Bay to the Pacific. One smaller pathway of local sediments is upstream from Central Bay to the Delta.

WY 2015
The Alameda Creek discharges three sediment pulses directly into South Bay in WY 2015. These sediment pulses propagate quickly to Central Bay, trough the Bay Bridge. The second sediment pulse is predominant (Fig. 4.13) for all three sediment classes.

The smaller settling fall velocity particles (Ws=0.011 mms^{-1}) move directly from Central Bay through the Golden Gate Bridge to the Pacific after entering Central Bay from South Bay. Therefore, the residence time in Central Bay of this sediment is tiny. No sediments move upstream up to the Delta in the northern reach.

The larger settling fall velocity particles (Ws=0.49 mms^{-1} & Ws=1.62 mms^{-1}) move more gradual to the Pacific than the smaller settling fall velocity. The net sediment transport at the Golden Gate Bridge is constant throughout the year. The cumulative transport curve shows some wiggles at the Golden Gate, which might indicate the spring-neap variation. A small fraction of the larger settling fall velocity moves upstream up to the Delta in the northern reach.

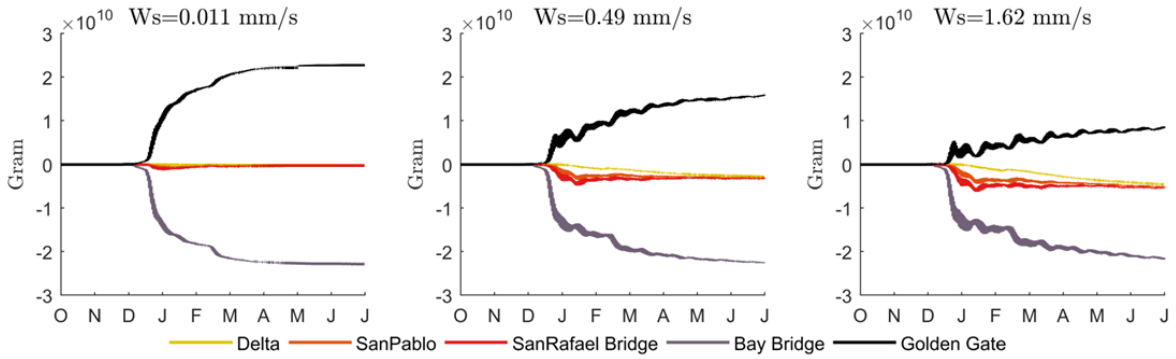

Figure 4.13: The figure displays the cumulative sediment transport curves for the three settling velocity local sediment classes (ws=0.011 mms^{-1}, ws=0.49 mms^{-1}, ws=1.62mms^{-1}) in the Northern reach for a dry year such as WY2015 (a) and a wet year such as WY2017 (b). Each graph displays the cumulative transport for several transects in the northern reach (§3.2.4). Downstream transport is positive defined. Transport from Central Bay to the Pacific is defined positive at the Golden Gate transect.

4.2.5. Sediment tracer; Sediment exchange at Bay Bridge

San Francisco Bay can be divided into two geographically and hydrologically distinct sub-estuaries; the northern reach lying between the connection to the Pacific Ocean at the Golden Gate and the confluence of the Sacramento-San Joaquin river system, and the southern reach between Bay Bridge and the south end of the Bay [Conomos et al., 1985]. The two sub-estuaries exchange water and sediment at Bay Bridge (§1.2).

This paragraph outlines the sediment exchange at Bay Bridge transect (§3.2.4), by reviewing the cumulative transport at Bay Bridge. Possible forces that influence this sediment exchange are analysed. Firstly, the sediment exchange at Bay Bridge induced by a horizontal spatial variation in SSC is reviewed. Secondly, the sediment exchange at Bay Bridge induced by residual flows is analysed.

Sediment exchange at Bay Bridge induced by a horizontal spatial variation in SSC
The computed cumulative transport of the three different Delta sediment classes are compared to the horizontal spatial variation in SSC for the three different sediment classes. Each year, a sediment pulse from the Delta arrives in Central Bay, increasing the turbidity.

Dry Year
A sediment pulse from the Delta arrives half December in Central Bay in WY2015 (Fig. 4.2). The SSC increases for the three Delta sediment classes with different fall velocities at Bay Bridge from mid-December. The increase of SSC at Dumbarton Bridge lags behind for all three the sediment classes, resulting in a horizontal spatial variation of SSC from Central Bay to South Bay (Fig. 4.14).

The computed SSC of the smallest settling velocity (Ws=0.011 mms^{-1}) is fastly increasing from mid-December until January at Bay Bridge. The SSC increases gradually from mid-December until half-January at Dumbarton Bridge (Fig. 4.14). The increase of SSC at Dumbarton Bridge lags a week behind, resulting in a horizontal spatial variation between Central Bay and the southern end of South Bay between half December and half January. Within this month, the cumulative transport at Bay Bridge is increasing, implying net sediment transport into South Bay. Around mid-January, the computed SSC at the two observation points are equal,

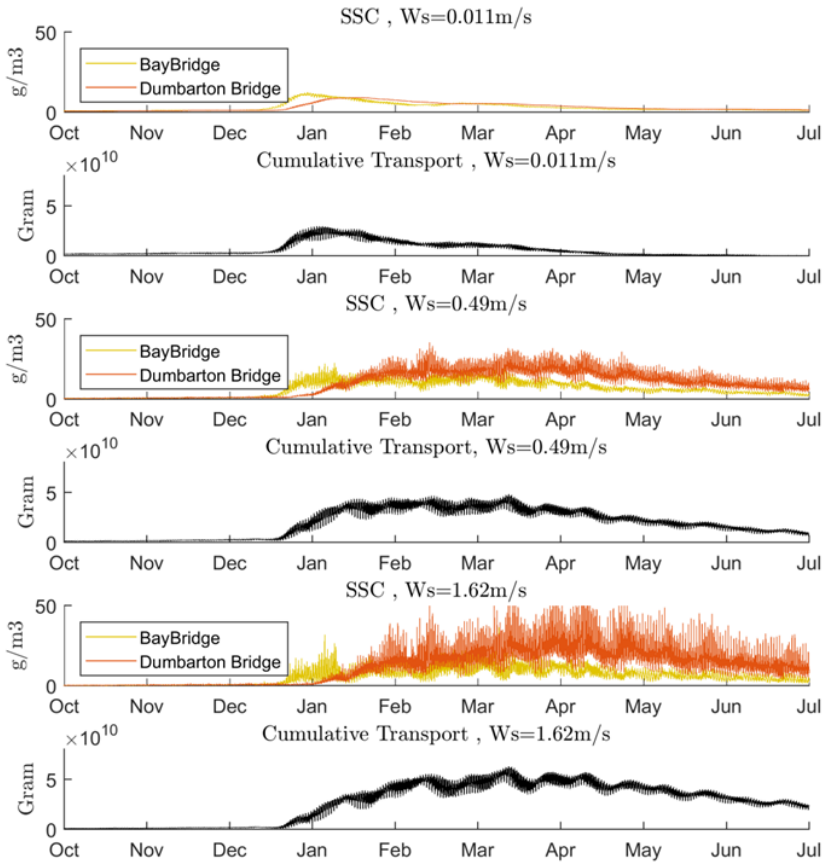

Figure 4.14: The figure shows the SSC of the three Delta sediment classes with different settling velocities at Bay Bridge (yellow) and Dumbarton Bridge (red) in WY2015. The cumulative transport is shown for each sediment class at Bay Bridge. Transport directed into South Bay has positive values, whereas transport directed out of South Bay has negative values. Therefore, an increasing cumulative transport curve indicates transport into South Bay and a decreasing transport curve indicates transport out of South Bay. A constant cumulative transport implies no net transport

and the cumulative transport is constant(Fig. 4.14), indicating zero net transport. After January, the cumulative transport is decreasing, implying that the net transport is directed from South Bay to Central Bay. Within these months after January, the SSC is slightly higher at Dumbarton Bridge than at Bay Bridge. The horizontal gradient is minimal, as well as the net sediment transport to the Central Bay. These model results could suggest that the horizontal spatial variation in SSC between Central Bay and South Bay induces net transport of the sediment with the smallest settling velocity.

The computed SSC of the middle sediment class (mms^{-1}) is increasing from mid-December to mid-January at Bay Bridge (Fig. 4.14). The SSC increases gradually from begin January until the end of January. The increase of SSC lags at Dumbarton Bridge a couple of weeks behind, resulting in a horizontal spatial variation in SSC for a few weeks. It is during this period that the direction of net sediment transport is into South Bay. From the end of January to the beginning of March the concentration at Dumbarton Bridge is slightly higher than the concentration a Bay Bridge. The cumulative transport is constant in these months (Fig. 4.14), implying no substantial net transport. The horizontal spatial variation increases after March, with higher SSC at Dumbarton Bridge than at Bay Bridge. The net transport is directed to Central Bay at Bay Bridge in the months after March. These model results could suggest that the horizontal spatial variation in SSC between Central Bay and South Bay induces net transport of the sediment with the middle settling velocity.

The computed SSC of the largest selling velocity sediments (Ws=1.62 mms^{-1}) is increasing from mid-December until the begin of February at Bay Bridge (Fig. 4.14). The SSC increases gradually from begin January until the end the begin of March. The increase of SSC lags at Dumbarton Bridge a couple of weeks behind, resulting in a horizontal spatial variation in SSC for almost two months. The net sediment transport is directed to South

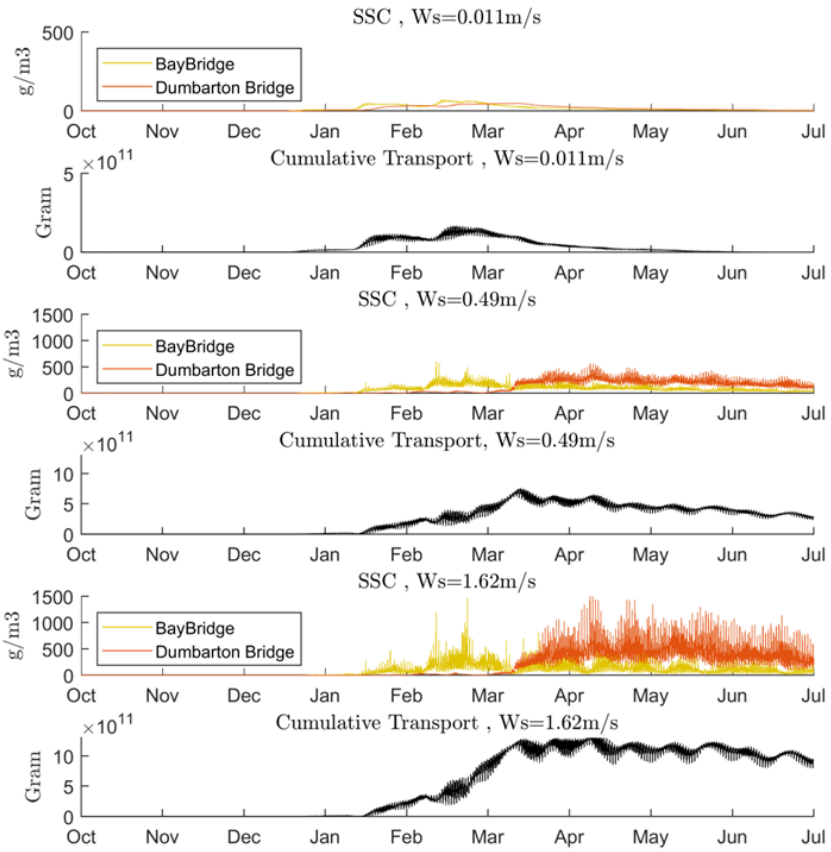

Figure 4.15: The figure shows the SSC of the three Delta sediment classes with different settling velocities at Bay Bridge (yellow) and Dumbarton Bridge (red) in WY2017. The cumulative transport is shown for each sediment class at Bay Bridge. Transport directed into South Bay has positive values, whereas transport directed out of South Bay has negative values. Therefore, an increasing cumulative transport curve indicates transport into South Bay and a decreasing transport curve indicates transport out of South Bay. A constant cumulative transport implies no net transport

Bay from January until mid-January (Fig. 4.14). From mid-January until March, the sediment transport is still directed to South Bay, but the magnitude is less than in the previous weeks. The horizontal spatial variation reverses from March. A higher SSC is found at Dumbarton Bridge instead of Bay Bridge. The cumulative transport is decreasing, indicating a sediment transport out of South Bay towards Central Bay. these model results could suggest that the horizontal spatial variation in SSC between Central Bay and South Bay induces net transport. Additionally, it is noted that the increase of SSC at Dumbarton Bridge lags more behind the increase of SSC at Bay Bridge for the sediment with the largest settling fall velocities.

Wet Year
Three sediment pulses from the Delta arrives respectively mid-December, mid-January and mid-February in Central Bay in WY2017. The SSC increases for the three Delta sediment classes with different fall velocities at Bay Bridge after each pulse has arrived Central Bay. The increase of SSC at Dumbarton Bridge lags behind for all three the sediment classes, resulting in a horizontal spatial variation of SSC from Central Bay to South Bay.

The SSC of the sediments with the smallest settling velocity (Ws= 0.011 mms^{-1}) Dumbarton Bridge and Bay Bridge are almost equal throughout the year (Fig. 4.15). At Mid January and mid-February, the SSC at Bay Bridge is higher than at Dumbarton Bridge for a week, implying a horizontal spatial variation in SSC. The cumulative transport only increases in these two weeks. Therefore, the net sediment transport is directed into South Bay only in the small periods where the SSC is higher at Bay Bridge than at Dumbarton Bridge. These model results could indicate that the horizontal spatial variation in SSC between Central Bay and South Bay induces net transport of the smallest settling velocity.

The computed SSC of the larger selling velocity sediments (Ws= 0.49 mms^{-1}, Ws= 1.62 mms^{-1}) is higher at Bay Bridge than at Dumbarton Bridge from mid-January until mid-March, resulting in a substantial horizontal spatial variation (Fig. 4.15). In the months after February, the SSC is increasing at Dumbarton Bridge. The increase in SSC at Dumbarton Bridge lags two months of the increase of SSC at Bay Bridge. The cumulative transport plot shows that a net transport of sediment directed to South Bay during these months. In the months after March, the sediment concentration is higher at Dumbarton Bridge than at Bay Bridge. The cumulative transport curve shows a net transport directed out of South Bay during these months. These model results could indicate that the horizontal spatial variation in SSC between Central Bay and South Bay induces net transport of the smallest settling velocity.

Sediment exchange at Bay Bridge induced by residual flows
The computed cumulative transport of the three different Delta sediment classes are compared to residual flow at an observation point in the channel at Bay Bridge in the model.

WY2015
The computed residual flow in the channel at Bay Bridge is seaward directed over the total water depth in WY2015. Varying residual flow profiles are found for different time periods. Just after a moderate water pulse has arrived at Central Bay, the residual flow at Bay Bridge displays a small net surface flow directed to South Bay and at mid-depth a net surface flow directed to Central Bay for a week in December (Fig. 4.16). The salinity of Central Bay is higher than the salinity at South Bay, from mid-December until January (Fig. D.4). In these three weeks, a stronger surface flow directed to Central Bay is observed and a reduced bottom flow directed to Central Bay (Fig. 4.16). This could be the result of a baroclinic flow induced by the horizontal density gradients. However, the baroclinic flow is not strong enough to induce a bottom current directed to South Bay. Therefore, the residual flow is over the total depth is directed to Central Bay. In the months after January, a small horizontal gradient is observed (Fig. D.4). However, the residual flow does not reflect any baroclinic flows. The residual flow is directed to Central Bay over depth. This suggest that the flow is governed by tidally driven and wind driven flows in WY2015.

The computed cumulative transport curve implicates that the sediments are transported into South Bay from mid-December until March (Fig. 4.16). During this period, the residual flow observed in the channel at Bay Bridge is directed to Central Bay. These model results could implicate that the sediments are not entering South Bay due to an advective flow.

The computed cumulative sediment transport is increasing and decreasing throughout the year at Bay Bride

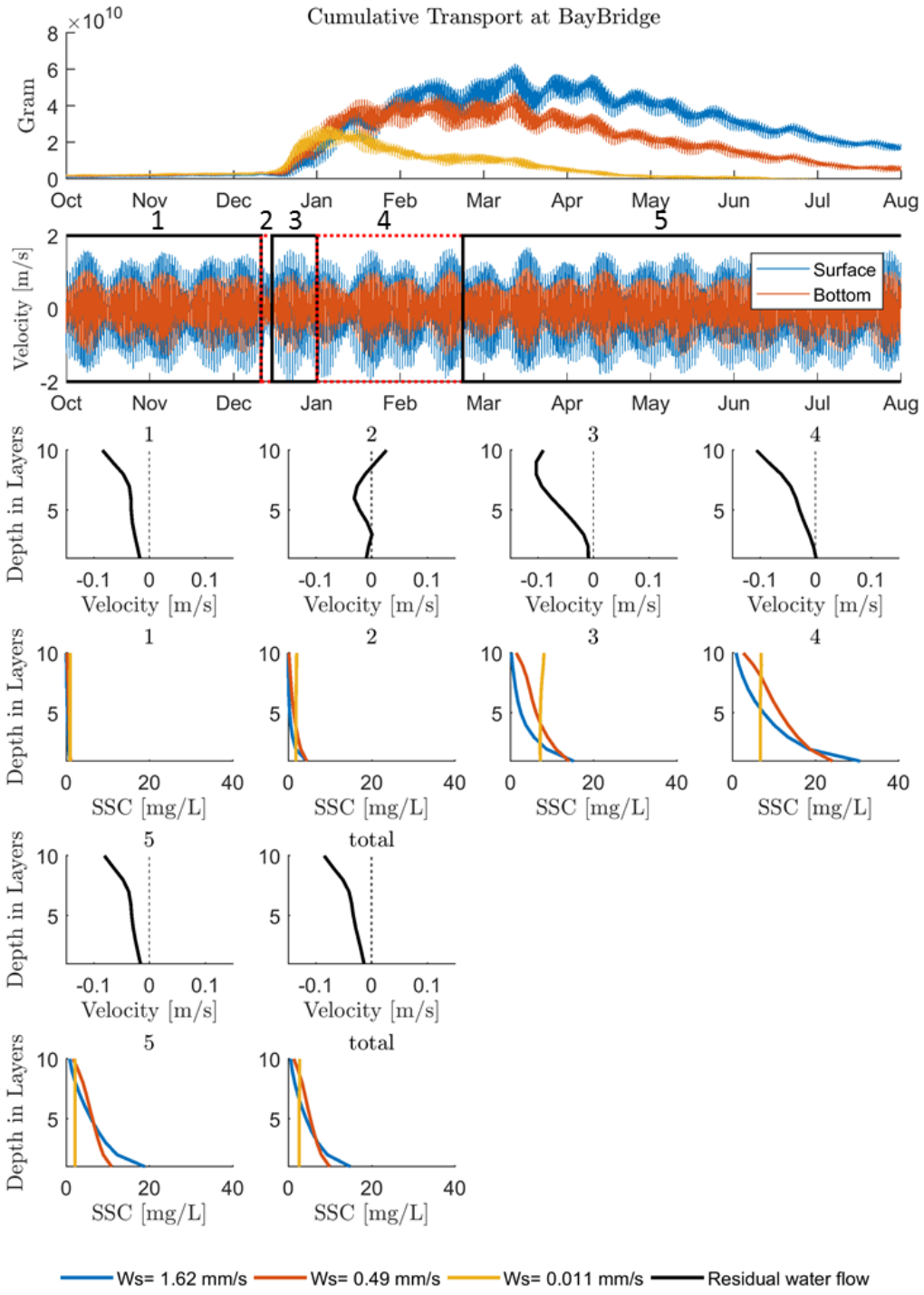

Figure 4.16: The figures shows the computed cumulative transport of three different sediment classed at the Bay Bridge transect (top plot) and the surface (blue line) and bottom (red line) velocities at Bay Bridge for WY2015. The computed residual flow and the averaged concentration profile at the Bay Bridge observation point is plotted for five periods over the year. Each period is marked by either a black or red intermittent line in the velocity plot. Period 1 is from October until mid-December, period 2 represents a week in December, period 3 represent the last two weeks in January and the first week in February, period 4 represents the period from January until March and period 5 represent the dry summer months. The total residual flow and averaged concentration profile of WY2015 are as well represented. Layer 10 implies the surface layer, and layer 1 the bottom layer. A positive value for the velocity implies a velocity direct to South Bay and a negative value indicates a velocity directed to Central Bay.

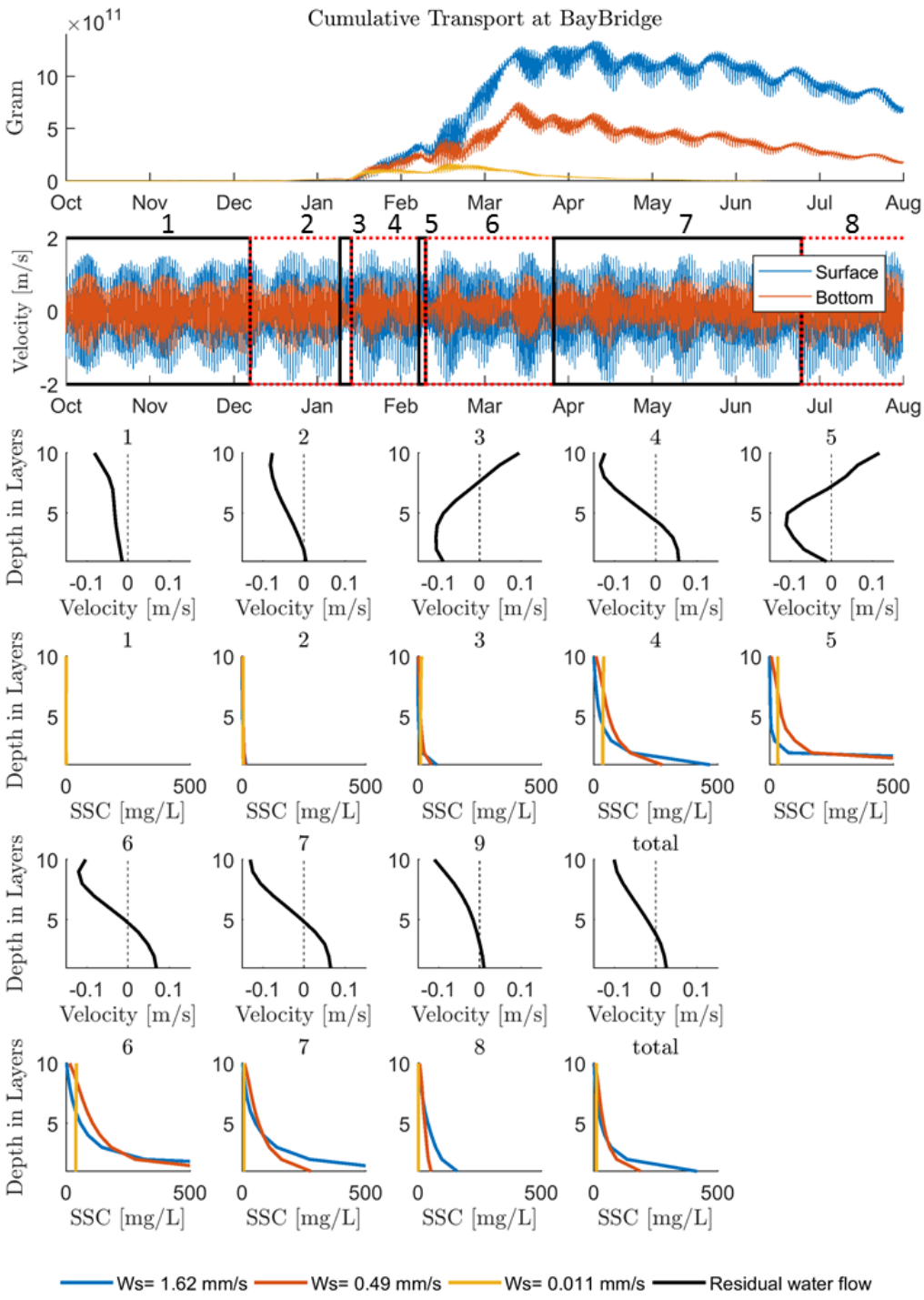

Figure 4.17: The figures shows the computed cumulative transport of three different sediment classed at the Bay Bridge transect (top plot) and the surface (blue line) and bottom (red line) velocities at Bay Bridge for WY2017. The computed residual flow and the averaged concentration profile at the Bay Bridge observation point is plotted for five periods over the year. Each period is marked by either a black or red intermittent line in the velocity plot. Period 1 is from October until mid-December, period 2 represents a month, period 3 represent a week in January, period 4 represents the month February, period 5 represent a week in February, period 6 represent almost two months, period 7 represent the period from April till July and period 8 represents the dry summer months. Layer 10 implies the surface layer, and layer 1 the bottom layer. A positive value for the velocity implies a velocity direct to South Bay and a negative value indicates a velocity directed to Central Bay.

in WY2015 (Fig. 4.16). An increasing sediment transport indicates that sediments enter South Bay and a decreasing sediment transport implies that sediments leave South Bay. Therefore, South Bay accumulates and loses sediments throughout WY2015. The cumulative transport is positive for sediments with larger settling velocities (Ws= 0.49 mms^{-1} & Ws= 1.62 mms^{-1}) and zero for sediments with the smallest settling velocities (Ws= 0.011 mms^{-1}). This indicates that South Bay accumulates sediments with larger settling velocities in WY2015.

WY2017
The computed residual flow in the channel at Bay Bridge has a small bottom flow directed to South Bay and a surface flow directed to Central Bay in WY2017 (Fig. 4.17). Varying residual flow profiles are found for different time periods. In the period from October until December and from July until August, a residual flow directed to Central Bay is found over depth. This suggest that the flow is governed by tidally driven and wind driven flows these two periods.

In the month December, the salinity of Central Bay is slightly higher than the salinity at South Bay. In this period, an enhanced residual surface flow directed to Central Bay is found, and the residual bottom flow is almost zero (Fig. 4.17). This could be the result of the baroclinic flows induced by the horizontal density gradients. However, the baroclinic flow is not strong enough to induce a bottom current directed to South Bay. Therefore, the residual flow is directed to Central Bay over the total water depth. The averaged SSC is insignificant in this period, so no substantial sediment transport takes place.

A residual flow is found to correspond a reversed estuarine circulation during a week in January and a week in February, with surface currents directed to South Bay and bottom currents directed to Central Bay (Fig. 4.17). Within this week it is found that South Bay is more saline than South Bay (Fig. D.5). For the week of January, the SSC over depth is insignificant, therefore is the net sediment transport as well insignificant. During the week in February, the SSC profile at Bay Bridge indicates that the concentration is higher near the bed than at the surface. More sediments are therefore transported with the bottom current towards Central Bay than with a surface current towards South Bay. The cumulative transport is decreasing in this week, indicating that the net sediment transport is directed to Central bay.

From February until April, a classic estuarine circulation can be observed, with bottom currents directed to South Bay and surface currents directed to South Bay (Fig. 4.17). The substantial horizontal gradient, with fresher water in South Bay than Central Bay, induced this baroclinic flows (Fig. D.5). The suspended sediment concentration profile of the sediment with the larger settling velocities (Ws= 0.49 mms^{-1} & Ws= 1.62 mms^{-1}) shows that the sediments are not uniformly distributed over the depth. The concentration is substantially higher near the bed than near the surface. This asymmetry of SSC over depth results that more sediments are affected by the bottom current than the surface current. It is during this period that the cumulative sediment transport is directed to South Bay for the sediments with larger settling velocities. According to these results, sediments are transported by a bottom current into South Bay induced by horizontal density gradients. The suspended sediment concentration of the sediment with the smallest settling velocity is uniform over depth at Bay Bridge during this period. Therefore, the surface currents transport almost the same amount of sediments as the bottom currents, resulting in a very small net sediment transport. Therefore, the net sediment transport of the sediment with the smallest settling velocity is not likely to be transported by baroclinic flows.

A baroclinic flow can be observed as well from April until July, with stronger surface currents than bottom currents. However, the SSC profile in this period is more uniformly distributed over depth than from February until April (Fig. 4.17). The latter holds especially for the sediment with a settling velocity of Ws= 0.49mms^{-1}. This results could indicate that more sediments are transported to the Central Bay along the surface current than into South Bay along the bottom current. It is in this period that the net sediment transport of this sediment class is directed to Central Bay.

The computed cumulative sediment transport is increasing and decreasing throughout the year at Bay Bride in WY2017 (Fig. 4.17). An increasing sediment transport indicates that sediments enter South Bay and a decreasing sediment transport implies that sediments leave South Bay. Therefore, South Bay accumulates and loses sediments throughout WY2017. The cumulative transport is positive for sediments with larger settling velocities (Ws= 0.49 mms^{-1} & Ws= 1.62 mms^{-1}) and zero for sediments with the smallest settling velocities

(Ws= 0.011 mms^{-1}). This indicates that South Bay accumulates sediments with larger settling velocities in WY2017. The cumulative transport at the end of WY2017 is substantially larger than the cumulative transport at the end of WY2015. Therefore, more sediments are transported into South Bay during WY2017 than WY2015.

4.2.6. Sediment tracer; Pathways in South Bay

San Francisco Bay can be divided into two geographically and hydrologically distinct sub-estuaries; the northern reach lying between the connection to the Pacific Ocean at the Golden Gate and the confluence of the Sacramento-San Joaquin river system, and the southern reach between Bay Bridge and the southern end of the Bay [Conomos et al., 1985]. The characteristics of the sediment transport between the two sub-estuaries are different, but depending on each other.

This paragraph outlines the sediment pathways of the sediments in South Bay, by reviewing the computed cumulative transport at several transects South Bay (§3.2.4). Firstly, the transport of Delta sediments is stated. Firstly, the transport of local sediments are described.

Transport of Delta sediments in South Bay

Delta sediments move from the Delta to Central Bay through the northern reach of San Francisco Bay. A sediment exchange between Central Bay and South Bay facilitates the transport of Delta sediments in and out of South Bay. The exchange takes places at Bay Bridge, which is the connecting channel between the two sub-embayments. After sediments entered South Bay at Bay Bridge, the sediments redistribute around South Bay.

WY2015

The Delta discharges two sediment pulses in WY 2015. These sediments reach Central Bay, from where a fraction of sediments enter South Bay (Fig. 4.12). The Delta discharge the first sediment pulse half December. This pulse crosses Bay Bridge from December until January (4.18a). The observed pulse at Bay Bridge is visible for the three different sediment settling velocities. However, more sediment with larger settling velocity crosses Bay Bridge than sediments with the smaller settling velocity. The Delta discharge the second pulse of sediments half February. However, after this moment no significant sediment pulse crosses Bay Bridge.

The net transport at Bay Bridge stagnates after a few weeks, meaning that around the same amount of sediments are transport south as north. The net transport of sediments reverses almost directly after it stagnated for the smaller fall velocity particles. The net transport is from South Bay to Central Bay from February until the end of the year. The net transport of sediment with the larger settling velocity reverses in April. The net transport of these sediments is from South Bay to Central Bay from April to the end of the year.

The sediments are slowly transported from Bay Bridge south towards Dumbarton bridge in the channel (Fig. 4.18c). The maximum cumulative transport of each transect is delayed, suggesting that the sediments are slowly transported down the channel. The transport of sediment decreases from Bay Bridge towards Dumbarton Bridge. Less than 20 percent of the sediments that cross Bay Bridge passes the Dumbarton Bridge cross-section. These sediments remain in Lower South Bay since the sediment flux at Dumbarton Bridge is always directed south (Fig. 4.18a). The sediment with smaller fall velocity does not reach the Dumbarton Cross-section. These sediments, together with the other 80 percent of the sediment with higher fall velocity disperse to the shoals. On the east shoal, a transport north brings the sediments back to Bay Bridge (Fig. 4.18d). On the southwest shoal, sediment transport is directed north, whereas the sediment transport on the mid-west shoals is directed south.

The two dominant pathways are the sediment pathway directed south in the channel, and the sediment pathway directed north on the east flat. These two have a significantly higher cumulative sediment transport in respect with the sediment transport on the west flat (Fig. 4.18b & 4.18c &4.18d).

The relation between the two dominant pathways determine if the direction of the net transport over the entire cross-section. The sediments enter first South Bay through the channel. The sediment transport over the flats lags behind, creating a net transport to the south. At some point the transport at the shoals is getting

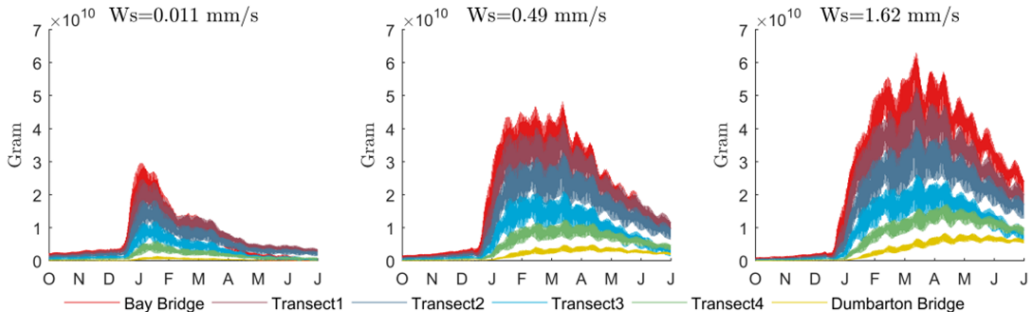

(a) The computed cumulative transport is shown for the transects that account for north/south transport over the complete transect in South Bay

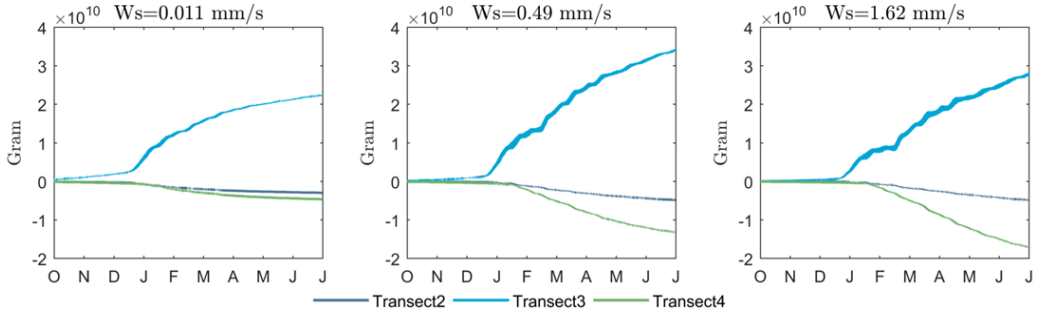

(b) The computed cumulative transport is shown for the transects that account for north/south transport over at west flat of South Bay

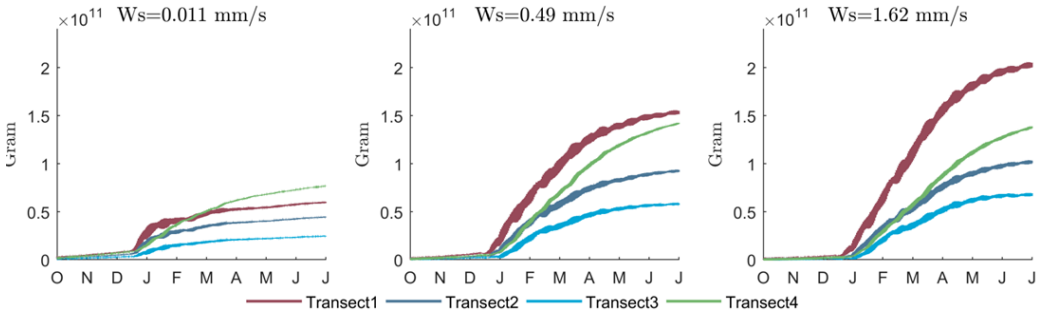

(c) The computed cumulative transport is shown for the transects that account for north/south transport over at the channel of South Bay

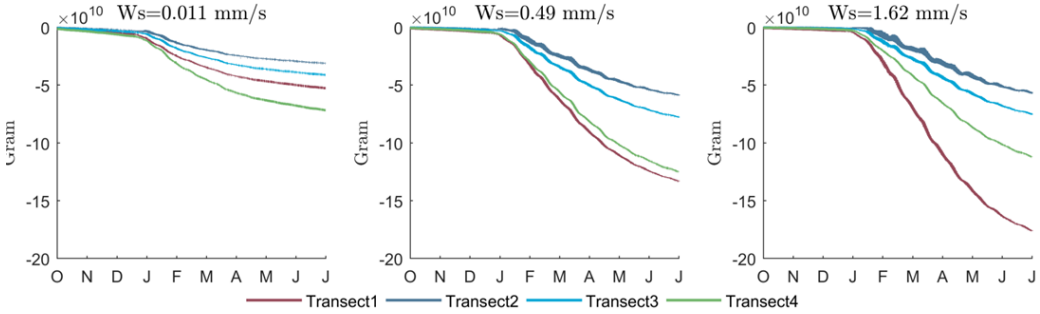

(d) The computed cumulative transport is shown for the transects that account for north/south transport over at the east flat of South Bay

Figure 4.18: The computed cumulative transport is shown for three Delta sediment classes at several transects in South Bay in WY2015. Transport directed south has positive values, whereas transport directed north has negative values. Therefore, an increasing cumulative transport curve indicates transport south and a decreasing transport curve indicates transport north. A constant cumulative transport implies no net transport

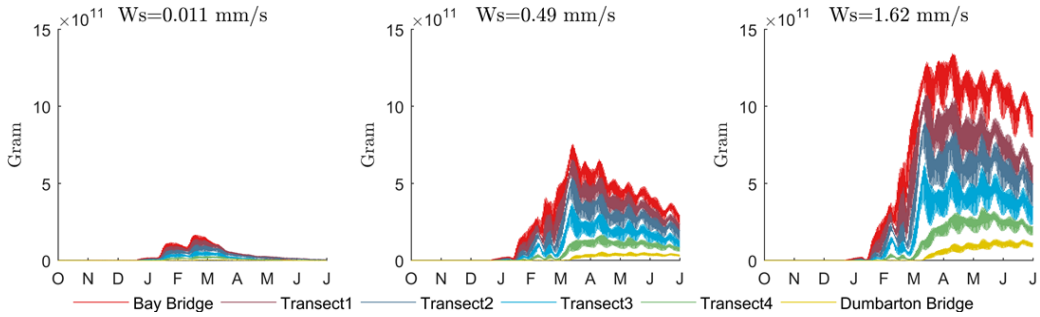

(a) The computed cumulative transport is shown for the transects that account for north/south transport over the complete transect in South Bay

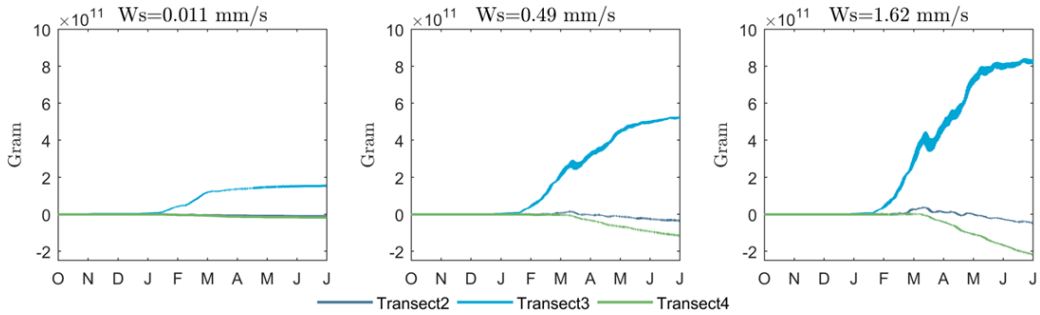

(b) The computed cumulative transport is shown for the transects that account for north/south transport over at west flat of South Bay

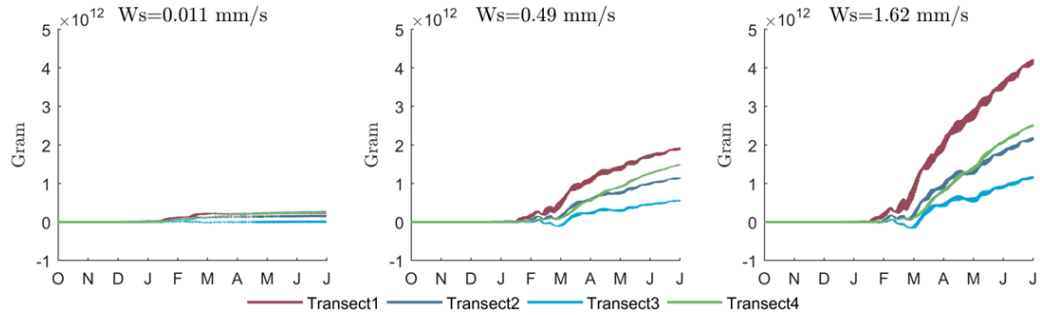

(c) The computed cumulative transport is shown for the transects that account for north/south transport over at the channel of South Bay

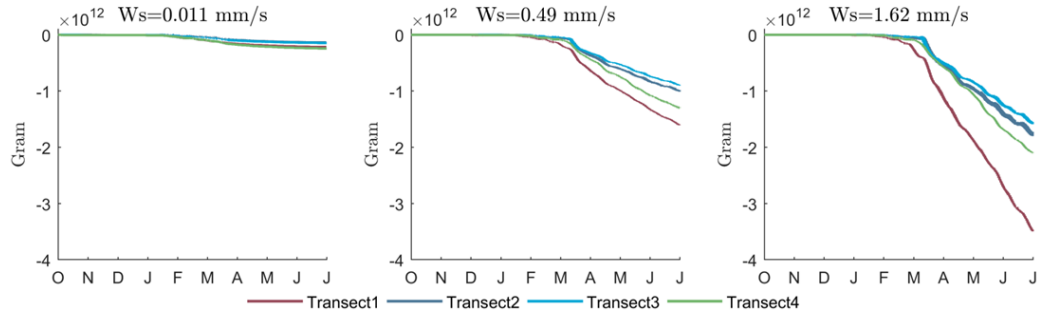

(d) The computed cumulative transport is shown for the transects that account for north/south transport over at the east flat of South Bay

Figure 4.19: The computed cumulative transport is shown for three Delta sediment classes at several transects in South Bay in WY2017. Transport directed south has positive values, whereas transport directed north has negative values. Therefore, an increasing cumulative transport curve indicates transport south and a decreasing transport curve indicates transport north. A constant cumulative transport implies no net transport

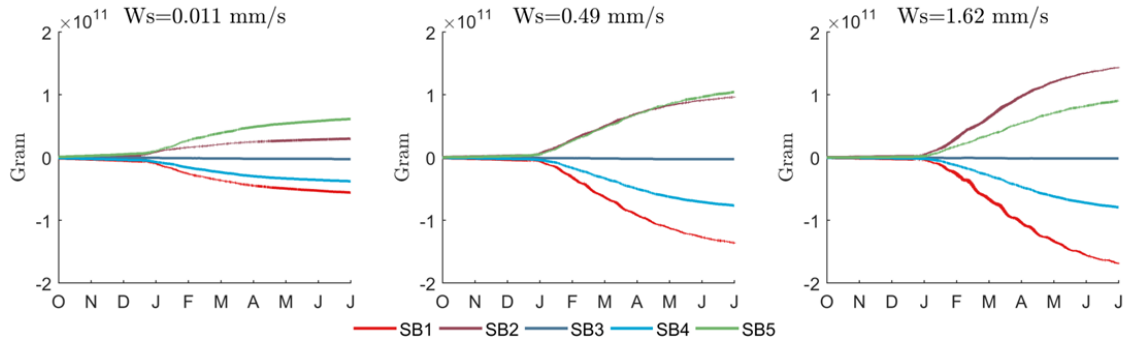

(a) The cumulative transport is shown for the transects between the channel and the east flat for WY2015

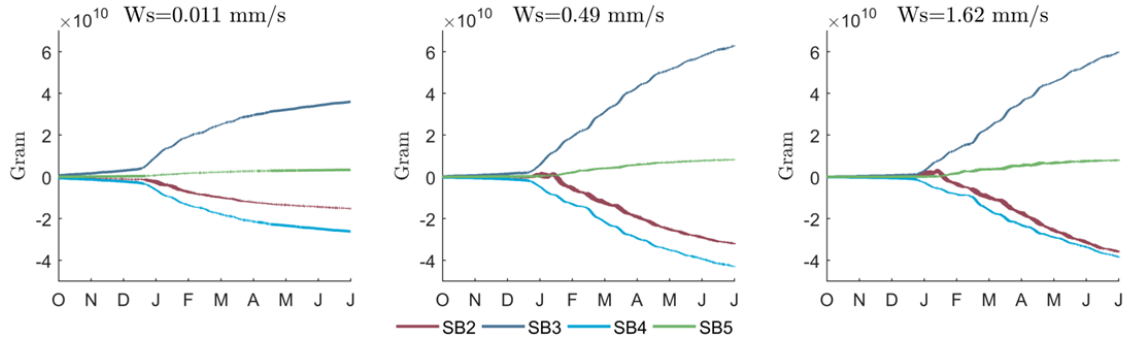

(b) The cumulative transport is shown for the transects between the channel and the west flat for WY2015

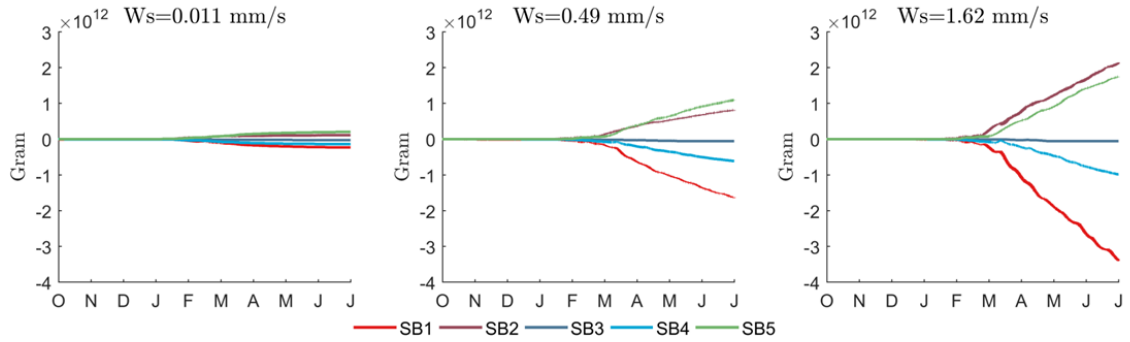

(c) The cumulative transport is shown for the transects between the channel and the east flat for WY2017

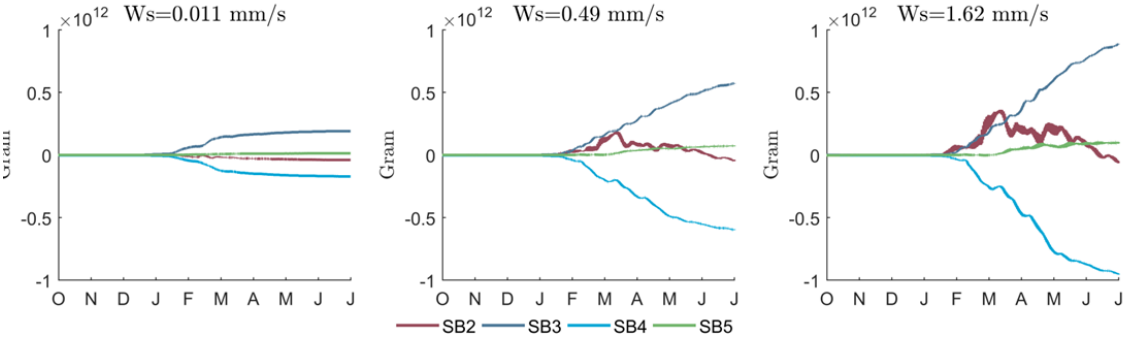

(d) The cumulative transport is shown for the transects between the channel and the west flat for WY2017

Figure 4.20: The computed cumulative transport is shown for three Delta sediment classes at cross-transects in South Bay in WY2015 and WY2017. Transport directed from the channel toward the flat has positive values, whereas transport directed from the flat towards the channel has negative values. Therefore, an increasing cumulative transport curve indicates transport from the channel to the flat, and a decreasing transport curve indicates transport from the flat to the channel. A constant cumulative transport implies no net transport

more substantial than the transport in the channel, resulting in a net transport of sediments north directed to Bay Bridge. The lag between the two pathways is more significant for sediment with the largest settling velocity than for lowest for sediment with the smallest settling velocity. The net transport for the sediment with the smallest settling velocity is directed northward earlier than the net transport for the sediment with largest settling velocity.

Different re-circulation patterns in South Bay facilitate the exchange between the channel and shoals. The transport is directed from the channel to the east and west shoal just north of Dumbarton Bridge (Fig 4.20a & 4.20b . The sediments move north over the shoals. The sediments on the east flat can then either follow the path on the shoal to the north or return to the channel. All sediments that move north on the west flat return to the channel. There are thus two circulation patterns in the southern part of South Bay, just north of Dumbarton Bridge. Another significant circulation cell can be observed just south of Dumbarton Bridge. This circulation cell is directed anti-clockwise. Sediments are transported from the channel to the shoal at SB2, to return at SB1 to the channel.

WY2017
The computed sediment pathways in South Bay in WY 2017 are quite similar to the computed sediment pathways just for WY 2015. However, some difference is notices, which will be elaborated.

An extremely wet period characterises WY2017. Three sediment pulses enter North Bay, of which the last two are significantly bigger than observed sediment pulses in a dry year such as WY2015. These sediments reach Central Bay, from where a fraction of sediments enter South Bay (Fig. 4.19a). The Delta discharge the first sediment pulse half December. A tiny pulse of sediment crosses Bay Bridge in December (Fig. 4.19a). The Delta discharge the substantially second sediment pulse and third sediment pulse respectively half January and half February. Two pulses of sediment with smallest fall velocity cross Bay Bridge half January and February. The transport of sediment with the smallest settling velocity (Ws= 0.011 mms^{-1}) into South Bay is small but more than during a dry year. The transport of these sediments are quickly reversed and the majority of the sediments is transported back to Central Bay around May.

A pulse of sediment with the larger fall velocity (Ws= 0.49 mms^{-1} & Ws= 1.62 mms^{-1}) crosses Bay Bridge mainly in March. After the three sediment pulses have quickly entered South Bay, the sediment transport reverses, resulting in a small net transport directed towards Central Bay at Bay Bridge. The sediment transport into South Bay is the biggest for the sediment with the largest fall velocity (Ws= 1.62 mms^{-1}) (Fig. 4.19a).

The sediments are transported down the estuary in the channel towards South Bay. One difference with the dry year is that the sediments reach Dumbarton Bride only after two to three months, in contrast to the delay of one month in the dry year. The sediment transport in the channel is from January to March relatively slow, to get a sudden increase around March (Fig. 4.19c). The sudden increase is substantial for sediment with the largest settling velocity(Ws= 1.62 mms^{-1}).

Sediments are transported to Lower South Bay from March, passing the cross-section at Dumbarton Bridge. Less than 20 percent reaches this cross-section. These sediments remain in Lower South Bay since the sediment flux at Dumbarton Bridge is always directed south (Fig. 4.18a). The lowest fall velocities particles do not reach the Dumbarton Cross-section. These sediments, together with the other 80 percent of the sediment with the larger fall velocity (Ws= 0.49 mms^{-1} and Ws= 1.62 mms^{-1}) are dispersed to the shoals.

The sediment transport is almost constant after March. The sediment transport at the east flat directed to the North is slightly higher than the sediment transport in the channel directed to the South. Therefore, a small net transport directed northward is observed.

Transport of local river sediments in South Bay
Sediments from local tributaries enter South Bay directly. The main local river sediment source is the Alameda Creek (Alameda), which discharges high peaks of sediments one or twice a year just North of Dumbarton Bridge. The east flat transports a substantial fraction of these sediments towards South Bay.

WY 2015
The Alameda Creek has a very high episodic sediment discharge into the Bay. It discharges almost all its annual sediment load in one day. In WY 2015, the Alameda has three sediment discharges events. Two occur in December, of which one is small, and the successive one is a substantially high sediment pulse. The third sediment pulse is a moderate pulse in February. The three sediment pulses are transported north and cross Bay Bridge within days leaving South Bay. The sediment with the larger settling velocities (Ws=0.49 mms^{-1} and Ws=1.62 mms^{-1}) are transported slower out of South Bay in contrast to the rapid transportation of the sediment with the smallest settling velocities (Ws=0.011 mms^{-1}) out of South Bay (Fig. 4.21a). A part of the sediment with the larger settling velocities seem to remain in South Bay in January and February.

A tiny fraction of sediments is transported south over the Dumbarton Bridge cross-section to Lower South Bay (Fig. 4.21a). The cumulative transport at Dumbarton bridge remains positive throughout the year. This suggests that more sediments are entering Lower South Bay than leaving. Lower South Bay is, therefore, an importing sub-embayment. The sediments that enter Lower South Bay (Guadalupe River and Coyote Creek) are likely to remain there and are not transported to South Bay.

The primary sediment pathway is located in the east flat and directed north to Bay Bridge (Fig. 4.21d). The sediments are dispersing from the east flat to the channel just at SB4 and SB1 (Fig. 4.22a & 4.22b). The sediments entering the channel in SB4 are either directed north or south. The sediments that are flowing south are transporting to Lower South Bay or are dispersed to the shoals, creating a re-circulation just north of Dumbarton Bridge. The other sediments that entered the channel at SB4 are transported north to Bay Bridge. This transport reverses around January (Fig. 4.21c), when the freshwater flow from the Delta is entering Bay Bridge (Fig. 4.8). From that moment, the sediments are transported south in the channel. The sediment pathway on the east flat remains north directed and dominant. Therefore does the net transport remains directed north, transporting sediments out of South Bay.

Four re-circulation cells can be observed in South Bay. Two anti-clock circulations are located on the east flat, one is just north of Dumbarton Bridge (SB4 and SB5), and the other is located just south of Dumbarton Bridge (SB1 and SB2) (Fig. 4.22a & 4.22b). Two circulation cells can be observed on the west flat, these circulations cell transport fewer sediments than the two circulation cells on the east flat. One circulation is located just north of Dumbarton Bridge and anti-clockwise (SB4 and SB5). The other circulation is clockwise, and is located north-west (SB2 and SB3)

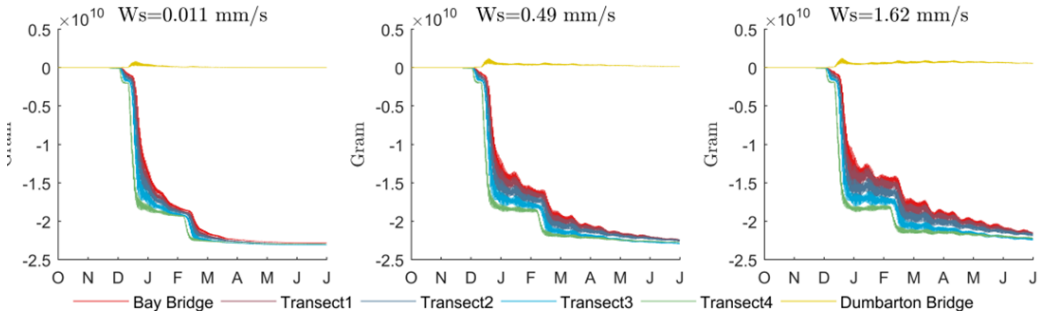

(a) The computed cumulative transport is shown for the transects that account for north/south transport over the complete transect in South Bay

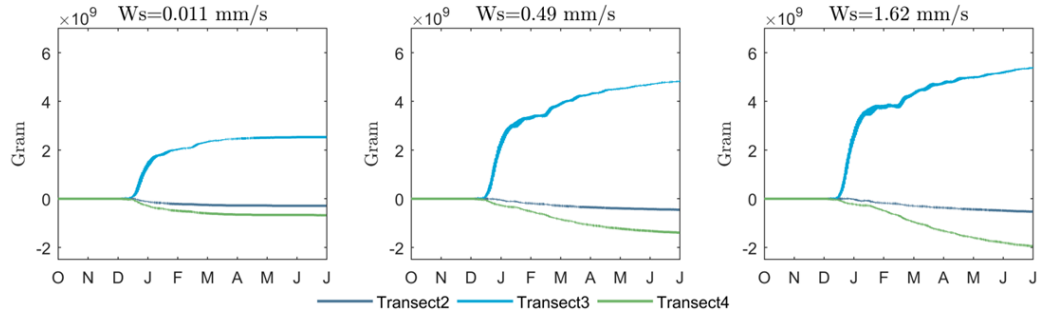

(b) The computed cumulative transport is shown for the transects that account for north/south transport over at west flat of South Bay

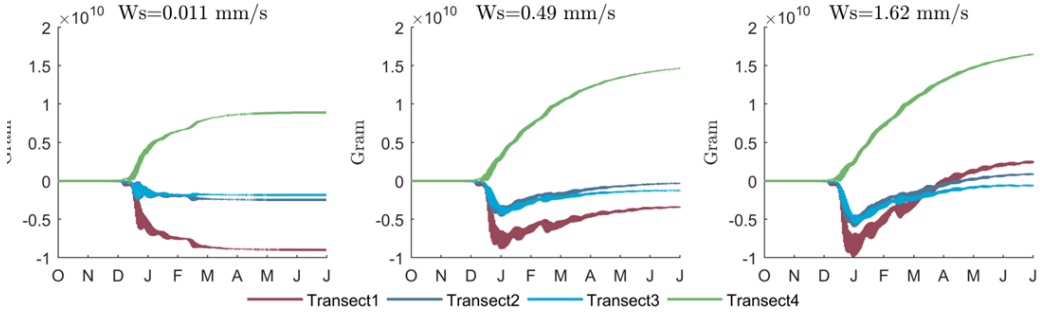

(c) The computed cumulative transport is shown for the transects that account for north/south transport over at the channel of South Bay

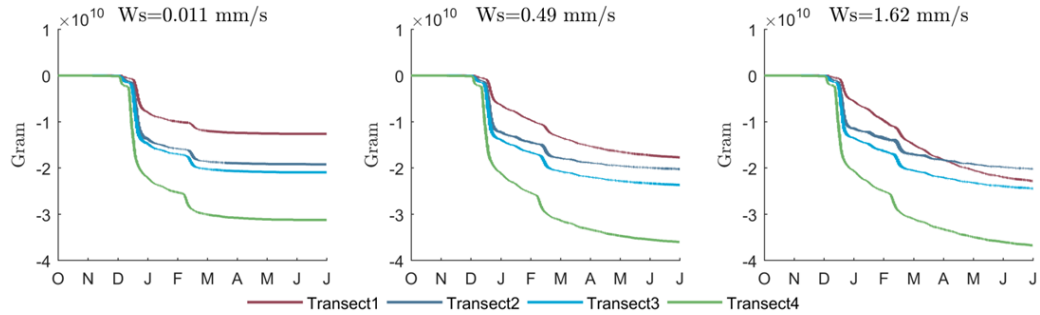

(d) The computed cumulative transport is shown for the transects that account for north/south transport over at the east flat of South Bay

Figure 4.21: The computed cumulative transport is shown for three local sediment classes at several transects in South Bay in WY2015. Transport directed south has positive values, whereas transport directed north has negative values. Therefore, an increasing cumulative transport curve indicates transport south and a decreasing transport curve indicates transport north. A constant cumulative transport implies no net transport

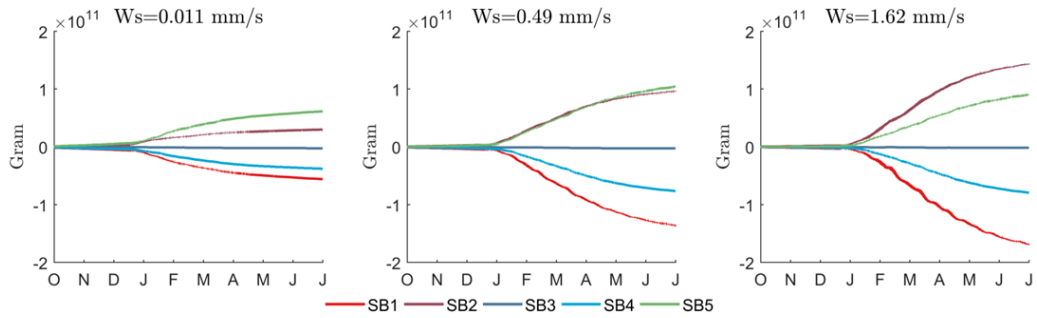

(a) The cumulative transport is shown for the transects between the channel and the east flat for WY2015

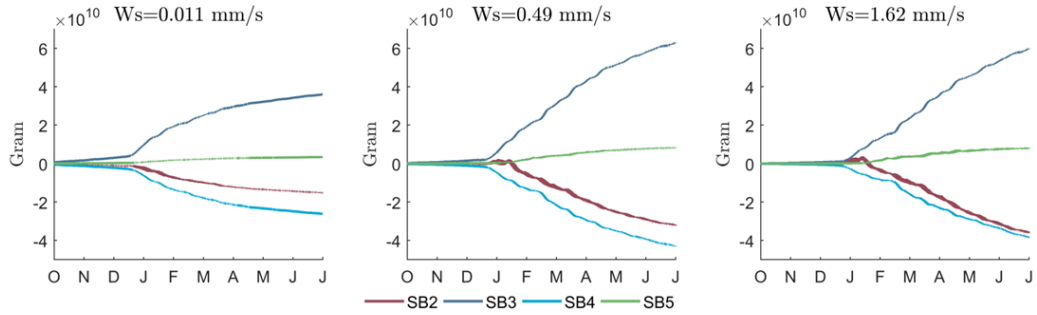

(b) The cumulative transport is shown for the transects between the channel and the west flat for WY2015

Figure 4.22: The computed cumulative transport is shown for three local sediment classes at cross-transects in South Bay in WY2015. Transport directed from the channel toward the flat has positive values, whereas transport directed from the flat towards the channel has negative values. Therefore, an increasing cumulative transport curve indicates transport from the channel to the flat, and a decreasing transport curve indicates transport from the flat to the channel. A constant cumulative transport implies no net transport

5

Discussion

The objective of this research is to create a better understanding of the sediment pathways in San Francisco South Bay. For this purpose, trends have been analysed using a new set of data (WY2015-WY2017) and sediment pathways in time and space have been investigated using a numerical model. In this model, the pathways of three sediment classes with different settling velocities are traced from its source throughout the Bay Area.

This chapter discusses the results per research question presented in §4. Firstly, the sediment sources of South Bay are discussed in §5.1. The primary sediment pathways in the Northern reach are considered in §5.2 and §5.3 discusses the dominant physical processes affecting the sediment exchange between Central Bay and South Bay. In §5.4, the primary sediment pathways in South Bay are touched upon, and lastly the limitations of the used methods are described.

5.1. Sediment sources of South Bay

The field data presented in §4.1.2 suggests a high sediment input from the Delta to South Bay. Comparison of the Suspended Sediment Concentration (SSC) at Pier17 (Measurement station at Bay Bridge) with Delta flow shows that the SSC measurements do reflect inputs from the Delta at high river flow rates ($Q_s > 3kg/s$). The correlation coefficient of the daily-averaged data yield r=0.4. At higher Delta flow rates ($Q_s > 300kg/s$), the SSC response is substantially more evident (r=0.75). These observations are in line with the findings of Erikson et al. (2013), who found that the response to the Delta flow of the SSC measurements at the nearby location Alcatraz, is correlated with the magnitude of the Delta flow.

A peak in sediment load from the Alameda river is observed before an increase in SSC at Pier17 in the time series presented in §4.1.2. However, the comparison of the SSC measurements at Pier17 with local tributaries flows does not show any relation between the measured SSC and sediment input from local tributaries. The very discrete data set (daily time step) of Alameda could be the reason that no relation appears. Additionally, the model results show that the sediment input from the Alameda contributes limitedly to the SSC at Pier17 during a period of high river flow rates($Q_s > 3kg/s$). This indicates that the Alameda river contributes only marginally to the SSC at Pier17 in the wet periods.

We find no contribution to the SSC of river outflow during the low river flow rates ($Q_s < 3kg/s$), as is shown in §4.1.2. The signal is masked by re-suspended material, sediment that is kept in suspension and transported due to persistent tidal and other currents ([Erikson et al., 2013]).

Shellenbarger et al. (2013) observed a spring sediment plume at Dumbarton Bridge in each spring period during WY2009-WY2011 and concluded that this increase in SSC is decoupled from tributary inflow. They proposed the idea that this increase in SSC was the result of local redistribution of re-suspended sediments due to wind-waves travelling over the flats, based on previous work on local wind-driven re-suspension by Brand et al.(2010). The results of the data analysis presented in §4.1.2 partially reinforces this theory, since a strong seasonal correlation (r=0.76) was observed between the wind speed and the SSC at Dumbarton Bridge.

However, the computed SSC of Delta sediments at Dumbarton Bridge also shows an increase in the spring period for a simulation without wind forcing. The same spring sediment plume, as observed by Schellerbarger et al.(2013), was predicted at Dumbarton Bridge. This model result suggests that the observed spring sediments plume at Dumbarton Bridge is a delayed response of Delta sediments entering South Bay and not a results of local redistribution or re-suspended sediment due to wind-waves.

Over larger time scales, previous studies indicated a downward trend of sediment load from the Delta. Wright and Schoellhamer (2004) found that the sediment input into San Francisco Bay has decreased by about one-half from 1957 to 2001. The estimated suspended sediment load from the Delta is found to be 1.2 ±0.4 Mt/y in the period between 1995-2003 [McKee et al., 2006]. Krone (1996) made a hypothesis that the total sediment load from the Delta to the Bay would decrease to 0.85 Mt/y by the year 2035. According to the observed data trends in this research, the decrease of the sediment load from the Delta could be even stronger. The sediment load of WY2015 and WY2016 are respectively 0.42 Mt/y and 0.53 Mt/y. The next years should be monitored to confirm the overall enhanced downward trend of the sediment load from the Delta. Because the yearly variability is significant, two years may not be representational covering a decadal trend.

In addition to Mckee et al. (2012), this study shows that a decrease in sediment load from the Delta increases the importance of the local tributaries as a sediment source for South Bay. The model results show that 0.04 Mt of the total 0.4 Mt of Delta sediments entering San Francisco Bay in WY2015 entered South Bay during the wet period (§4.2.4). The Delta input is only twice the sediment load from the Alameda that discharged 0.02 Mt into South Bay. This ratio indicates that a decrease in Delta sediment loads could lead to an equal sediment input of the Delta and the local tributaries in South Bay.

5.2. Primary sediment pathways in the Northern Reach

In this study, we find sediment pulses propagating from the Delta down the estuary towards Central Bay during periods of high river runoff (Fig. 5.1a). The found sediment pulses are in line with the aerial observations of turbid water plumes that extended from Suisun Bay to South Bay in period of high river flow [Carlson and McCulloch, 1974]. Two or three sediment pulses are observed each year, as is shown in the data presented in §4.1.1. The model results demonstrate that the pulses are delayed and diffuse while propagating down the northern reach, confirming the observation of diffusive pulses at five monitoring stations in the northern estuary by Downing-Kunz et al. (2016).

The cumulative transport curves of several transect at the northern reach, presented in §4.2.4, illustrate trans-

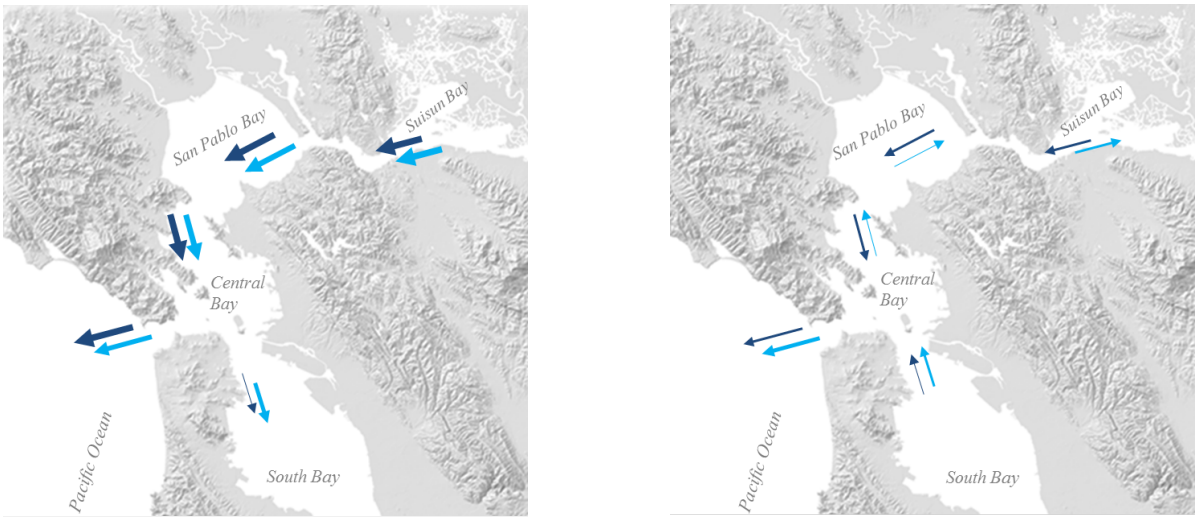

(a) Transport in periods of high Delta flow

(b) Transport in periods of low Delta flow

Figure 5.1: Schematisation of the sediment pathways of sediments in the northern reach dark blue arrow represents the lower fall velocity sediment particle and the light blue arrow the higher fall velocity sediment particles.

port upward for the higher settling fall velocity particles in periods of low flows (Fig. 5.1b). Around 0.09 Mt/y is transported landward in the low flow periods in WY2015. The landward transport is in agreement with the observed landward transport of 0.12 Mt/y in similar dry years (WY2001, WY2002) by Mckee et al. (2006). They concluded that tidal dispersive transport causes the upward transport. The model results show that the upward transport affects only the higher settling fall velocities.

The computed suspended sediment flux at the Golden Gate is persistently seaward directed throughout the year (Fig 5.1a and 5.1b). The seaward directed flux is in line with the field observations reported by Erikson et al. (2013) and Downing-Kunz et al. (2016) and the bed form asymmetry analysis done by Barnard et al. (2012). Hence, following the outcomes of these previous studies combined with the results from this study, it can be concluded that the Pacific acts as a sink for fine sediments.

In line with the outcomes from Carlson and McCulloch (1974), this research observes that Central Bay is turbid during the wet period, whereas it is less turbid in dry periods. It is shown that Central Bay accumulates sediments during periods of high river runoff and loses sediments during periods of low river flows (§4.2.5). Sediments accumulate in Central Bay because the pulsed sediment flux from the Delta exceeds the constant export towards the Pacific and South Bay. In periods of low Delta river runoff, the sediments are either transported to the Pacific and South Bay or up the northern reach by tidal dispersive transport.

5.3. Dominant processes affecting the sediment exchange at Bay Bridge

Previous studies found the tide and the baroclinic flows to be the governing forces for the exchange of water between Central Bay and South Bay at Bay Bridge [Conomos, 1979, McCulloch et al., 1970, Pubben, 2017]. In our study, we assess the effects of both the tide and the baroclinic flows on the sediment exchange. The model does not account for the slack duration asymmetry, due to the exclusion of the bed-interaction. Therefore only the diffusive effect of the tide, the asymmetry in mixing, and the baroclinic flows is reviewed (§3.2.3).

Three types of sediment exchange at Bay Bridge can be observed in the model results presented in §4.2.5. The first type is observed during a period of low river flow ($Q_{Delta} < 800 m^3/s$). The computed residual water flow at an observation point at Bay Bridge is seaward directed over the depth in this type. Sediments are slowly transported out of South Bay during this period. The second and third type are after respectively a moderate ($Q_{Delta} > 800 m^3/s$) and extreme river flow ($Q_{Delta} > 10,000 m^3/s$). These two types are discussed more extensively below.

Sediment exchange after a period of moderate Delta flow ($Q_{Delta} > 800 m^3/s$)
The field data presented in §4.1 show that Central Bay and South Bay are partially refreshed by a moderate Delta flow ($Q_{Delta} > 800 m^3/s$) in WY2015. The salinity of both bays drops to 25 PSU. The dilution of South Bay only lags a couple of days behind, creating a horizontal density difference of 2/3 PSU, where South Bay is more saline than Central Bay. Within this period, the model results show a reversed estuarine circulation flow at an observation point at Bay Bridge. The bottom currents are directed to sea and surface currents are directed to South Bay for some days. These currents reverse after a couple of days, and a classic estuarine circulation flow can locally be observed in the model for a two or three weeks. Although the horizontal density gradients persist throughout the year, the corresponding baroclinic flows are hardly observed for the most substantial part of the year. The computed residual flow in the channel at Bay Bridge of WY2015 is directed seaward over the depth (Fig. 5.2a).

The computed cumulative transport curves at Bay Bridge (§4.2.5) show that sediments are transported into South Bay while a seaward directed residual flow is locally observed. This suggests that the sediments are not transported into South Bay by a flow in the channel. The model results show, in addition to Carlson and McChulloch (1974), that Central Bay is more turbid than South Bay during the period that the net sediment transport is directed towards South Bay. Therefore, it is suggested that the transport of sediments into South Bay is governed by the diffusive transport of the tide after a moderate Delta flow.

The model results show that South Bay accumulates only marginally sediment in WY2015. However, the model overestimates the SSC gradient over Central Bay from South Bay. Therefore, the process governing the transport into South Bay is overestimated. It is therefore expected that South Bay loses sediment in WY2015.

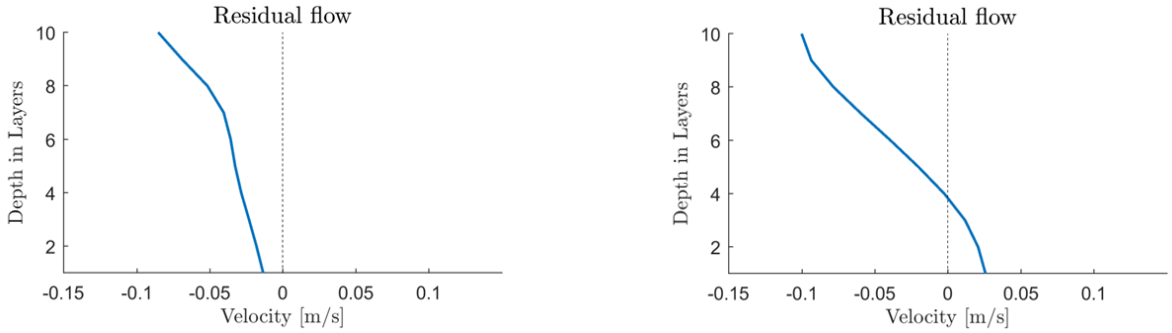

(a) WY2015 (b) WY2017

Figure 5.2: Residual water flow at an observation point in the channel at Bay Bridge (Fig. 3.5a) for a) WY 2015 and b) WY2017. Layer 10 is the surface, layer 1 is the bottom. Negative values indicate a flow directed to the sea, positive values indicate a flow directed to South Bay

Sediment exchange after a period of extreme Delta flow ($Q_{Delta} > 10,000m3/s$)
The results of the data analysis presented in §4.1, indicate that the high Delta flow ($Q_{Delta} > 10,000m3/s$) refreshes a large part of Central Bay and South Bay. In WY 2017, three water pulses can be observed, refreshing the Bay three times. The salinity of both bays drops to 12 PSU. The dilution of South Bay only lags a couple of days behind, creating a significant horizontal density difference of 4 PSU, where South Bay is more saline than Central Bay. Within this period, the model results show a locally reversed estuarine circulation, with bottom currents directed to sea and surface currents directed to South Bay. Then, the salinity in Central Bay increases due to the interaction with the more saline water of the Pacific, resulting in a slow increase in the salinity. The salinity of South Bay increases more gradual than the salinity at Central Bay, resulting in a significant horizontal salinity difference between the Bays (10 PSU). Central Bay is more saline than South Bay, which holds for a couple of months. During this period, the model results (§4.2.5) indicate a classic estuarine circulation, with bottom currents directed to South Bay and surface currents seaward directed. Moreover, the computed residual flow in the channel at Bay Bridge of WY2017 reflects the persistent baroclinic flows. The residual flow is directed seaward at the surface and directed landward at the bottom (Fig. 5.2b).

The computed cumulative transport curves at Bay Bridge (in §4.2) show that the net sediment transport of the larger settling velocities (Ws= 0.49 mms^{-1} and Ws= 1.62 mms^{-1}) is directed into South Bay during the period that a classic estuarine circulation is observed in the channel at Bay Bridge. These cumulative transport curves are zero in the period that a reversed estuarine circulation is observed. These model results indicate that sediment is only brought into South Bay through the bottom currents corresponding to the classic estuarine circulation. This suggest that the baroclinic flows are the governing forces for sediment exchange after a period of extreme Delta flow. Moreover, the model results show that South Bay accumulates sediment in WY2017.

Furthermore, The model results show that SSC of the smallest settling velocity (Ws= 0.011 mms^{-1}) at Bay Bridge is uniform over depth throughout the year. Therefore, the sediment transport of this sediment class is not governed by baroclinic flows. The model results suggest that the transport of the smallest settling velocity sediments into South Bay is governed by the diffusive transport of the tide.

5.4. Primary sediment pathways in South Bay

The sediment pathways presented in this study cover the whole Bay Area, whereas previous studies focused only on suspended sediment flux (SSF) measurements of one or two observation points for a month period of time. The model results show two significant pathways with opposite transport directions characterising the sediments pathways in South Bay. One pathway is located in the channel and is directed landward throughout the year. The second pathway is located on the extensive east flat and is directed seaward throughout the year.

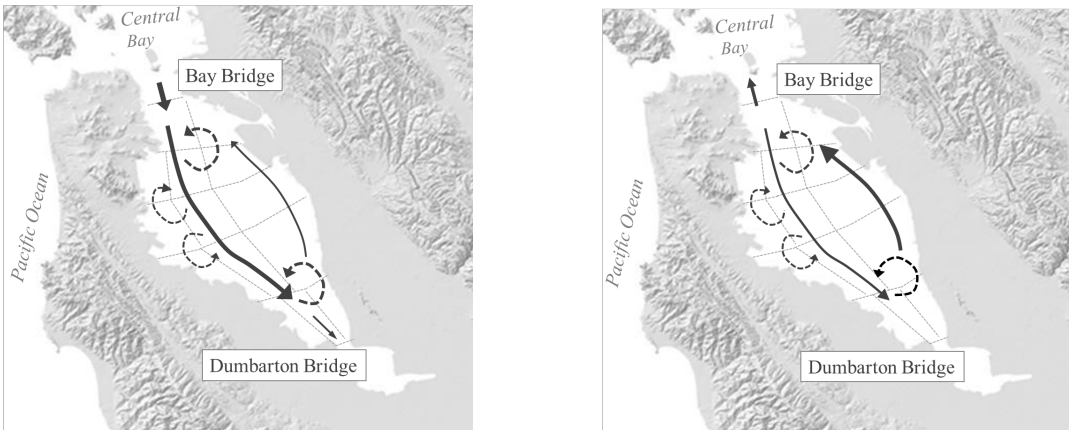

(a) Transport after a period of high river flow (3-4 months)

(b) Transport during period of low river flow (8-9 months)

Figure 5.3: Schematisation of the depth-averaged sediment pathways of Delta sediments in South Bay. The thickness of the black arrows displays the relative magnitude of the transport flow. The dotted lines represent the circulation cells.

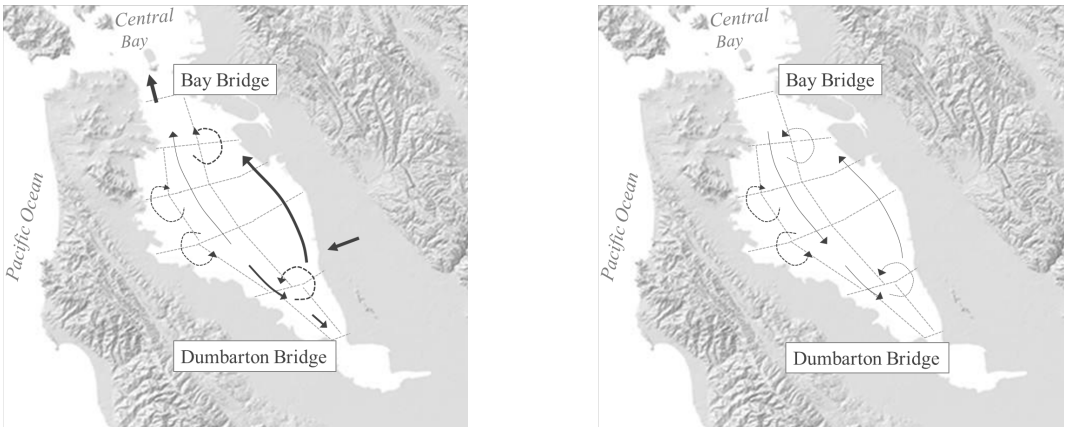

(a) Transport after a period of high river flow (3-4 months)

(b) Transport during period of low river flow (8-9 months)

Figure 5.4: Schematisation of depth-averaged sediment transport of Local river sediments in South Bay. The thickness of the black arrows displays the relative magnitude of the transport flow. The dotted lines represent the circulation cells.

Following the model results, the Delta sediments only enter South Bay after a high river flow at Bay Bridge (Fig. 5.3a). From there, the sediments are slowly brought down the estuary in the channel. The first sediments reach Dumbarton Bridge after a month in a dry year such as WY2015, corresponding to the tidally averaged velocity of 1 cm/s found in a field study [Carlson and McCulloch, 1974]. At the east flat, a seaward directed sediment transport brings the sediment back to Bay Bridge. After a period of high river flow, the sediment transport in the channel is larger than the sediment transport on the east flat, resulting in a net import of sediments (Fig. 5.3a). The found sediment transports are in line with the found SSF during a field study [Lacey et al., 2014].

In previous studies, there was not a discrimination between Delta and Alameda sediments. From this work we conclude that the Alameda sediments are mainly transported over the east flat, resulting in a net seaward transport (Fig. 5.4a). However, the transport of Alameda sediments is small in contrast to the transport of Delta sediments. The overall sediment transport remains landward.

A different behaviour than expected is observed for the dry summer period (Fig. 5.3b and 5.4b). According to Lacey (2014), the sediment transport is directed seaward in the channel and directed landward on the east flat. The unexpected transport pathways are most likely a consequence of the exclusion of the bed interaction

in the model. Brand (2010) found that the SSC is on average higher on the shallow flats during ebb, because the effect of the wind-waves on the bottom increases as the depth decreases. More sediments are in suspension during the flood tide than during the ebb tide, resulting in an asymmetrical sediment movement. More sediments are transported on the flood tide, leading to a land inward directed transport.

Apart from the two dominant sediment pathways, four re-circulation cells are found in the model results, that facilitate the exchange between the shoals and the channel. Two anti-clockwise circulation cells connect the two dominant transport pathways; one is located just north of Dumbarton Bridge, and the other is just south of Bay Bridge. The other two re-circulation cells are smaller and facilitate the circulation of sediments on the west flat. The northwest re-circulation cell is clockwise, and the southwest circulation cell is anti-clockwise. These circulation cells have not yet been observed in prior studies.

The modelled sediment transport flux at Dumbarton Bridge is directed south during periods of high river flow (Fig. 5.3a) and is insignificant during low river flow (Fig. 5.3b). This direction of transport is in line with SSF observations at Dumbarton Bridge [Schellenbarger et al., 2013] and deposition/erosional studies of Lower South Bay [Jaffe and Foxgrover, 2006a,b]. Hence, it can be concluded that Lower South Bay acts as a sink for fine sediments.

5.5. Research limitation

In this research, two types of limitations can be distinguished. The first limitation relates to the data analysis and the second to the model limitations. In this section, both will be described.

5.5.1. Limitations in the data analysis

As to the limitations in the data analysis, in the first place, it was found that there is a lack of data at the local rivers during extreme wet periods. The relation between precipitation and streamflow for these rivers is only of moderate strength [Schellenbarger et al., 2013], so these could not be constructed by other data.

Secondly, the data set contains only three years of SSC time series. The correlation found during the data analysis should therefore be evaluated with more data, when available.

5.5.2. Model limitations

A limitation concerning the model is that the temperature is not accounted for as a characteristic of this research. The model simulation shows an underestimation of the salinity levels during the dry summer months in a dry year such as WY2015. Pubben (2017) stated that the temperature is not dominant in the estuarine circulation. However, the computed salinity's values of Central Bay and South Bay presented in §4.2.5 deviate from the found salinity values in field measurements (§4.1.1) for WY2015. South Bay is more saline than Central Bay in the summer months of WY2015, according to the field measurements, whereas the model results show that Central Bay is more saline than South Bay throughout WY2015. This deviation during the summer months could possible lead to incorrect found baroclinic flows in WY2015.

Moreover, the local tributaries are simplified as three rivers that outflow in South Bay. This simplification leads to an underestimation of the contribution of the local tributaries. It shows an accurate hydrodynamic model, but it could be the case that some sediment sources are overlooked.

Lastly, due to the exclusion of the bed-interaction, the DelwaQ set-up used in this model does not include all essential processes for sediment transport. Consequently, the model does not account for net sediment transport that results from to slack duration asymmetry, peak velocity asymmetry and wind-wave induced re-suspension (§2). Additionally, sediments end up in the lowest layer of the water column instead of the bed since there is no bed-interaction. These sediments are transported by bottom currents, such as baroclinic flows (Fig. 3.4c). As a result, This model set-up overestimates sediment transport resulting from bottom currents

6

Conclusion and Recommendation

In this chapter, the conclusions and recommendations of this research are described. Section 6.1 includes the conclusions, followed by the recommendations in Section 6.2.

6.1. Conclusions

This study provides more insight into the sediment pathways in San Francisco South Bay. The Delta is found to have a high sediment input to South Bay. The suspended sediment concentration (SSC) at northern South Bay reflects input from the Delta during periods of high river flow. The input from the Delta is evident during periods of extreme high Delta river runoff. The SSC at the southern part of South Bay reflects input from the Delta during the spring period. A new theory opts that the observed spring sediments plume at Dumbarton Bridge is a delayed response of Delta sediments entering northern South Bay during periods of high river flow and not a results of local redistribution of re-suspended sediment due to wind-waves. Furthermore, the local tributaries contribute to a limited extent to the SSC of South Bay. The Alameda Creek is the largest of the local sources, and its sediment input contributes only marginally for a few days in the wet period.

According to the data used in this research, the decrease of the sediment load from the Delta could be even stronger than previously thought. With a decreasing sediment load from the Delta, the importance of the local tributaries as a sediment source for South Bay could increase. The model results show that the sediment input from the Delta to South Bay was only twice the sediment input from the local sources in WY 2015. With a further decreasing Delta load, the sediment load from the Delta could become equal to the sediment input from the local tributaries.

Following the model results in this research, Central Bay is accumulating sediments during periods of high river runoff and losing sediment during periods of low river flows. Sediment accumulates in Central Bay because the pulsed sediment flux from the Delta exceeds the constant exports towards the Pacific. In periods of low Delta river runoff, the sediments are either transported to the Pacific or up the northern reach by tidal dispersive transport.

In this research, three different types of sediment exchange between Central Bay and South Bay are observed. The first type is observed during periods of low river flows ($Q_{Delta} < 800 m^3/s$). A seaward directed residual flow is found in the channel at Bay Bridge. Sediments are slowly transported out of South Bay. The second type is observed after a period of moderate river flow ($Q_{Delta} > 800 m^3/s$). A pulsed sediment flux from the Delta increases the turbidity of Central Bay, resulting in a horizontal spatial variation in SSC from Central Bay to South Bay. The diffusive character of the tide transports the sediments slowly from the turbid Central Bay to the relatively clearer South Bay. The third sediment exchange type is observed after an extreme Delta river flow ($Q_{Delta} > 10,000 m^3/s$)). The extreme Delta flow refreshes a large part of Central Bay and South Bay. Then, the salinity in Central Bay increases due to the interaction with the more saline water of the Pacific, resulting in a slow increase in the salinity of Central Bay. The salinity of South Bay increases more gradual than the salinity at Central Bay, resulting in a significant horizontal salinity difference between the Bays. Central Bay is more saline than South Bay. It is during this period that a classic estuarine circulation can be found,

with bottom currents directed to South Bay and surface currents seaward directed. These bottom currents bring in the larger settling velocity sediments into South Bay.

South Bay is expected to lose sediments in dry years, such as WY2015. Sediments are transported seaward for the more prominent part of the year. Only after the episode of moderate river flow, sediments are transported limitedly into South Bay. South Bay is expected to accumulate sediments of the larger settling velocities during an exceptionally wet year, such as WY 2017. A classic estuarine circulation persist for several months. The bottom currents directed landward transport the sediments from Central Bay to South Bay.

Two dominant pathways with opposite transport direction characterise the sediment transport in South Bay. One pathway is located in the channel and is directed southward after periods of high river runoff. The second pathway is located on the extensive east flat and is directed northward after periods of high river runoff. The transport in the channel is dominant during the wet period, resulting in a net transport landward. Besides these two dominant pathways, four re-circulations cells are found, facilitating the exchange between the channel and the shoals.

In line with the outcomes of previous studies, this research found that the transport flux at Dumbarton Bridge is found to be directed south during periods of high river flow and insignificantly during low river flow. Hence, it can be concluded that Lower South Bay acts as a sink for fine sediments.

It is found that this model has incorporated the correct bed-shear stress for wind-waves. This model can be used as a start for modul simulations including bed-interaction.

6.2. Recommendation

As the yearly variability is considerable, it is possible that the timespan of three years does not represent a trend. To be able to confirm the trends found in the data analysis, it is therefore recommended to monitor the next few years.

Moreover, this study shows that a decrease in Delta sediment loads could lead to an equal sediment input of the Delta and the local tributaries into South Bay. This means that the contribution of the local tributaries could become more substantial. We, therefore, recommend to further analyse the local tributaries sediment trends and its influence on the SSC. Furthermore, only the three most prominent local tributaries (Guadalupe, Coyote and Alameda) are considered in this research. A reconsideration of to the most significant local tributaries is hence considered useful.

The next step in gaining more insight in sediment physics is to include the bed interaction in the model. A model simulation with bed interaction will be able to confirm the hypotheses proposed in this research. In the first place, it can be used to assess if the spring sediment plume at Dumbarton Bridge is a delayed response of Delta sediments or a result of local redistribution of re-suspended sediments due to wind waves travelling over the flats. Secondly, it can be used to analyse the effect of the asymmetry of erosion of the tide on the sediment pathways. Thirdly, the influence of the wind-wave re-suspension on the sediment pathways in a dry period could be evaluated using a model simulation with bed interaction.

In this research, the model was empty when sediments were entering from the boundary. The SSC gradient over Central Bay to South Bay is therefore overestimated. To accurately assess the impact of the SSC gradient on sediment transport, a simulation with an initial SSC in the model is recommended.

It is recommended to use the model as a tool to create scenarios to compare to one another rather than to use the model as a tool for deterministic prediction.

Bibliography

Achete, F., van der Wegen, M., Roelvink, J., and Jaffe, B. (2015). A 2-d process-based model for suspended sediment dynamics; a first step towards ecological modeling. *Hydrology and earth systems sciences*, 19:2837–2857.

Ariathurai1974 (1974). *A finite element model for sediment transport in estuaries*. PhD thesis, University of California Davis.

Barnard, P., Erikson, L., Elias, E., and Dartnell, P. (2012). Sediment transport patterns in the san francisco bay coastal system from cross-validation of bedform assymetry and modeld residual flux. *Marine Geology*, 345:72–95.

Barnard, P., Schoellhamer, D., Jaffe, B., and McKee, L. (2013). Sediment transport in the san francisco bay coastal system; an overview. *Marine Geology*, 345:3–17.

Bergamaschi, B., Kuivilia, K., and Fram, M. (2001). Pesticides associated with suspended sediments entering san francisco bay following the first major storm of water year 1996. *Estuaries*, 24:368–380.

Bosboom, J. and Stive, M. (2013). *Coastal Dynamics I, Lecuter notes CIE4305*. VSSD, Delft.

Brand, A., Lacy, J.R., H. K., Hoover, D., Gladding, S., and Stacey, M. (2010). Wind-enhanced resuspension in the shallow waters of south san francisco bay: Mechanisms and potential implications for cohesive sediment transport. *JOURNAL OF GEOPHYSICAL RESEARCH*, 115(C11024).

Brand, A., Lacy, J., Gladding, S., Holleman, R., and Stacey, M. (2015). Model-based interpretation of sediment concentration and vertical flux measurements in a shallow estuarine environment. *Limnology and Oceanography*, 60(2):463–481.

Bridger, A., Becker, A., Ludwig, F., and Endlich, R. (1994). Evaluation of the wocss wind analysis scheme for the san francico bay area. *Journal of Applied Meteorology*, 33:1210–1218.

Buchanan, P. and Schoellhamer, D. (1996). Summary of suspended-solid concentration data, san francisco bay california, water year 1995. *U.S. Geological Survey*, 40.

Carlson, P. and McCulloch, D. (1974). Aerial observations of suspended sediment plumes in san francisco bay and adjacent pacific ocean. *US Geol. Surv. Water-Resourc. Res.*, 2(5):519–526.

Cheng, T., Gartner, J., Cacchione, D., and Tate, G. (1998). Flow and suspended particulate transport in a tidal bottom layer, south san francisco bay california. *Physics of Estuaries and Coastal seas*, pages 3–13.

Chengt, R. and Gartner, J. (1985). Harmonic analysis of tides and tidal currents in south san francisco bay, california. *Estuarine, coastal an shelf science*, 21:57–74.

Cloern, J. (1984). Temporal dynamics and ecological significance of salinity stratification in an estuary. *Oceanologica Acta*, 7(1).

Cloern, J. and Schraga, T. (2016a). Usgs measurements of water quality in san francisco bay (ca). *1969-2015: U. S. Geological Survey data release*.

Cloern, J. and Schraga, T. (2016b). Usgs measurements of water quality in san francisco bay (ca). *U. S. Geological Survey data release*.

Conomos, T. (1979). Properties and circulation of san frnacisco bay waters. *American Association for the Advancement of Science*, pages 47–84.

Conomos, T. and Peterson, D. (1977). Suspended-particle transport and circulation in san francisco bay, an overview. *Estuar. Process.*, 2:82–97.

Conomos, T., Smith, R., and Gartner, J. (1985). Environmental setting of san francisco bay. *Hydrobiologia*, 129(1).

De Nijs, M. (2012). *On Sedimentation processes in a stratified estuarine system*. PhD thesis, Delft Technical University.

Deltares (16 December 2016a). D-water quality, user manual. *Deltares*, version 1.1, revision 48450.

Deltares (16 December 2016b). Delft 3d flexible mesh suite, technical reference manual. *Deltares*, version 1.1.0, revision 48665.

Deltares (17 June 2017). Delft 3d flexible mesh suite, user manual. *Deltares*, version 1.2.1, revision 51215.

Deltares (2014). Delft 3d flow, simulation of multi-dimensional hydrodynamic flows and transport phenomena, including sediments. *Deltares*, version 3.15.34158.

Downing-Kunz, M., Schoellhamer, D., and Work, P. (2016). Water and suspended-sediment flux measurements at the golden gate, 2016. *United States Geological Survey*.

Erikson, L., Wright, S., Elias, E., Hanes, D., Schoellhamer, D., and John, L. (2013). The use of modeling and suspended sediment concentration measurements for quantifying net suspended sediment transport through a large tidally dominated inlet. *Marine Geology*, 345:96–112.

Fofonoff, N. and Millard, R. (1983). Algorithms for computation of fundamental properties of seawater. *UNESCO Technical Papers in Marine Science*, 44(4):6–9.

Fong, S., Louie, S., Werner, I., Davis, J., and Connon, J. (2016). Contaminant effects on california bay-delta species and human health. *San Francisco Estuary and Watershed Science*, 14(4).

Friedrichs, C. (2011). Tidal flat morphodynamics: A synthesis. *Virgina Institute of Marine Science, Gloucester point, USA*.

Jaffe, B. and Foxgrover, A. (2006a). A history of tidal flat area in south san francisco bay, california, from 1858 to 2005. *U.S. Geological Open-File*, Open-File report 2006-1287(1262):32.

Jaffe, B. and Foxgrover, A. (2006b). Sediment deposition and erosion in south san francisco bay, california from 1956 to 2005. *U.S. Geological Survey Open-File*, Open-File report 2006-1287.

Jansen, P., van Bendegom, L., van den Berg, J., de Vries, M., and Zanen, A. (1997). *Principles of River Engineering The non -tidal alluvial river*. Pitman, London.

Kimmerer, W. (2002). Physical, biological, and management responses to variable freshwater flow into the san francisco estuary. *Estuaries*, 25:1275–1290.

Kimmerer, W. (2004). Open water processes of the san francisco estuary; from physical forcing to biological responses. *San Francisco Estuary and Watershed Science*, 2(1).

Krone, R. (1962). *Flume studies of the Transport of Sediment in Estuarial Shoaling processes*. University of California, Berkeley, California.

Krone, R. (1993). *Sedimentation in the San Francisco Bay System*. Pacific division, American Association for the Advancement of Science, San Francisco, California.

Krone, R. (1996). Recent sedimentation in the san francisco bay system in: Hollibaugh, j.t. (ed.), san francisco bay: the ecosystem further investigations into the natural history of the san francisco bay and delta with reference to the influence of man. *Pacific Division of the American Association for the Advancement of Science c/o California Academy of Sciences, San Francisco, California*, pages 63–67.

Lacey, J., Gladding, S., Brand, A., Collignon, A., and Stacey, M. (2014). Lateral baroclinic forcing enhances sediment transport from shallow to channel in an estuary. *Coastal and estuarine research federation*.

Lacy, J., Schoellhamer, D., and Burau, J. (1996). Suspended-solids flux at a shallow-water site in south san francisco bay, california. *Proceedings of the North American Water and Environment Congress, Anaheim.*, pages 3357–3362.

Lewis, E. and Perkin, R. (1981). The practical salinity scale 1978: conversion of existing data. *Deep-sea Research*, 28A(4):307–328.

MacAnally, W. and Mehta, A. (2001). *Coastal and estuarine fine sediment processes*. Elsevier, Amsterdam.

Maren, D. and van Winterwerp, J. (2013). The role of flow assymmetry and mud properties on tidal flat sedimentation. *Continental Shelf Research*, 60s:S71–S84.

Martyr-Koller, R., Kernkamp, H., van Dam, A., van der Wegen, M., Lucas, L., Knowles, N., Jaffe, B., and Fregoso, T. (2017). Application of an unstructured 3d finite volume numerical model to flows and salinity dynamics in the san francisco bay-delta. *Marine Ecology Progress Series*, 192:86–107.

McCulloch, D., Peterson, D., Carlson, P., and Conomos, T. (1970). *A preliminary study of the effects of water circulation in the San Francisco Bay Estuary; some effects of fresh-water inflow on the flushing of South San Francisco Bay*. U.S. Geological Survey Circular.

McKee, L., Ganju, N., and Schoellhamer, D. (2006). Estimates of suspended sediment entering san francisco bay from the sacramento and san joaquin delta, san francisco bay, california. *J. Hydrol.*, 323:335–352.

McKee, L., Lewicki, M., Schoellhamer, D., and Ganju, N. (2012). Comparison of sediment supply to san francisco bay from watersheds draining the bayarea and the central valley of california. *Marine Geology*, 345:47–62.

Monismith, S., Burau, J., and Stacey, M. (1996). *Stratification dynamics and gravitational circulation in northern San Francisco Bay*, pages 123–153. In: San Francisco Bay; the ecosystem. Pacific Division, American Association for the Advancement of Science, San Francisco, California.

NOAA (2017a). National data buoy center. *http://www.ndbc.noaa.gov/*.

NOAA (2017b). Noaa tides and currents. *https://tidesandcurrents.noaa.gov/*.

Pietrzak, J. (2016). *An Introduction to Stratified Flows for Civil and Offshore Engineers*. Delft University of Technology, Delft.

Prooijen, B. v. (2016). *River Engineering, classnotes for CIE4345*. Delft University of Technology, Delft.

Pubben, S. (2017). 3d mixing patterns in san francisco south bay. Master's thesis, Delft Technical University.

Rasmussen, P. P., Gray, J. R., Glysson, G. D., and Ziegler, A. C. (2013). uidelines and procedures for computing time-series suspended-sediment concentrations and loads from in-stream turbidity-sensor and streamflow data. *U.S. Geological Survey Techniques and Methods*, 345(3):52.

Rijn, L. v. (1993). *Principles of sediment transport in rivers, estuaries and coastal seas*. Aqua Publications, Amsterdam.

San Francisco Bay conservation, D. C. B. (2017). A san francisco bay plan.

Sanfoord, L. and Maa, P. (2001). A unified erosion formualtion for fine sediments. *Marine Geology*, 179:9–23.

Schellenbarger, G., Wright, S., and Schoellhamer, D. (2013). A sediment budget for the southern reach in san francisco bay, ca implications for habitat restoration. *Marine Geology*, 345:281–293.

Schettini, C., Jaffe, B., and Truccolo, E. (2017). Climatology of salinity and suspended particulate matter in san francisco bay. *USGS*.

Schoellhamer, D., Wright, S., Monismith, S., and Bergamachi, B. (2016). Recent advances in understanding flow dynamics and transport of water-quality constituents in the sacramento-san joaquin river delta. *San Francisco Estuary and Watershed Science*, 14(4).

Schoellhamer, D. H., Mumley, T. E., and Leatherbarrow, J. (2007). Suspended sediment and sediment-associated contaminants in san francisco bay. *Environ. Res.*, 105:119–131.

SFEI (2017). Sfei pilot erddap, easier acces to data. *http://sfbaynutrients.sfei.org/erddap/tabledap*.

Stacey, M., Monismith, S., and Burau, J. (1999). Observations of turbulence in a partially stratified estuary. *Journal of Physical Oceanography*, 25:1950–1970.

Swart, D. (1974). *Offshore sediment transport and equilibrium beach profiles*. PhD thesis, Delft Technical University.

University, D. M. . C. S. S. J. S. (2017). Wind data. *http://www.met.sjsu.edu/ sinton/winds/*.

USGS (2017). Nwis site information for usa: Site inventory. *https://maps.waterdata.usgs.gov/mapper/index.html?state=ca*.

van Rijn, L. (2006). *Principles of sediment transport in rivers, estuaries and coastal seas*. Aqua Publications, Amsterdam.

Wagner, R., Boulger, R., Oblinger, C., and Smith, B. (2006). Guidelines and standard procedures for continuous water-quality monitors— station operation, record computation, and data reporting. *U.S. Geological Survey Techniques and Methods*, 1–D3:51.

Walters, R., Cheng, R., and Conomos, T. (1985). Time scales of circulation and mixing processes of san francisco bay waters. *Hydrobiologia*, 1:13–26.

Winterwerp, J. and Prooijen, B. v. (2016). *Sediment Dynamics, classnotes for CIE4308*. Delft University of Technology, Delft.

Winterwerp, J. C., Manning, A. J., Martens, C., de Mulder, T., and Vanlede, J. (2006). A heuristic formula for turbulence-induced flocculation of cohesive sediment. *Estuar. Coast. Shelf Sci*, 68:195–207.

Wright, S. and Schoellhamer, D. (2004). Trends in the sediment yield of the sacramento river, california, 1957–2001. *San Francisco Estuary and Watershed Science*, 2(2).

Yuan, C. and Yamagat, T. (2014). California nino/nina. *Sci. Rep.*, 4(4801).

Zimmerman, J. R., Bricker, J. D., Jones, C., Dacunto, P. J., Street, R. L., and Luthy, R. G. (2008). The stability of marine sediments at a tidal basin in san francisco bay amended with activated carbon for sequestration of organic contaminants. *Water Res.*, 42:4133–4145.

A

Data Sources

In this appendix is an overview given of the available and used data sources in the area of interest. The figures below show the locations of multiple data resources, sorted to either the operator of the source or to what kind of data is available. In this appendix is for each figure below a more detailed description is given about what kind of data and operator.

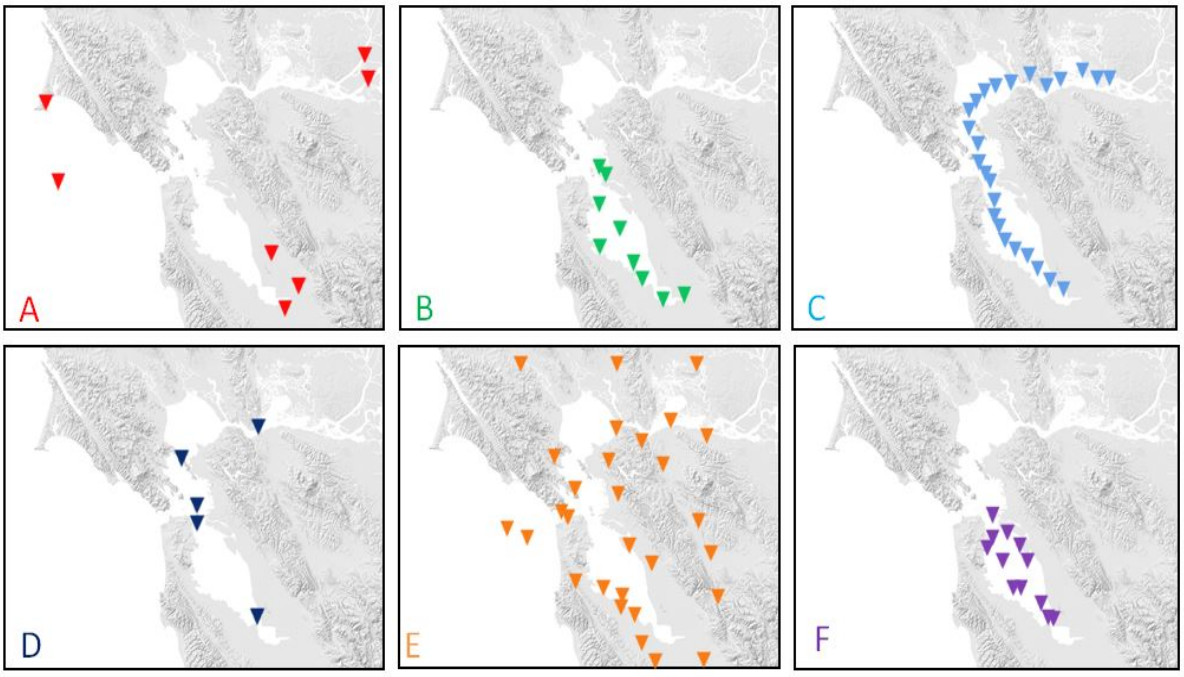

Figure A.1: The different plots show multiple data sources. A) In the upper left plot are data sources related to data about the rivers and the tides shown by red triangles. B) The upper middle plot shows in green the data locations regarding the waste-water treatment plants. C) In the upper right blow are the measurement locations during the Polaris cruise displayed in blue. D) The dark blue triangles in the lower left plot are the data sources related to observations buoys in the estuary. E) In the lower middle plot are the wind measurement locations shown in orange. F) The purple triangles in the lower right plot shows the measurement locations by the California Department for fish and wildlife.

A.1. Data sources regarding tides and rivers

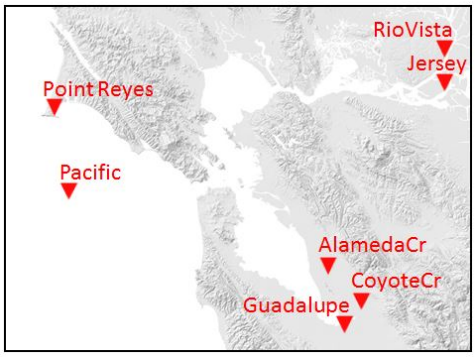

Figure A.2: Data Sources regarding tides and rivers

Location	Parameter	Data-Interval	Depth measurement	Monitoring site	Operator
RioVista	Discharge	15-minute	0 ft NAVD88	11455420 Sacramento R a Rio Vista CA	USGS
	Temperature	15-minute	0 ft NAVD88	11455420 Sacramento R a Rio Vista CA	USGS
	SSC	15-minute	0 ft NAVD88	11455420 Sacramento R a Rio Vista CA	USGS
Jersey	Discharge	15-minute	0 ft NAVD88	11337190 SAN JOAQUIN R A JERSEY POINT CA	USGS
	Temperature	15-minute	0 ft NAVD88	11337190 SAN JOAQUIN R A JERSEY POINT CA	USGS
	SSC	15-minute	0 ft NAVD88	11337190 SAN JOAQUIN R A JERSEY POINT CA	USGS
AlamedaCR	Discharge	15-minute	85 ft NGVD29	11179000 ALAMEDA C NR NILES CA	USGS
	Temperature	15-minute	85 ft NGVD29	11179000 ALAMEDA C NR NILES CA	USGS
	SSC	Random dates (min every month)	85 ft NGVD29	11179000 ALAMEDA C NR NILES CA	USGS
CoyoteCR	Discharge	15-minute	10 ft NGVD29	11172175 COYOTE CR C AB HWY 237 A MILPITAS CA	USGS
	Temperature	Random dates (min every month)	10 ft NGVD29	11172175 COYOTE CR C AB HWY 237 A MILPITAS CA	USGS
	SSC	Random dates (min every month)	10 ft NGVD29	11172175 COYOTE CR C AB HWY 237 A MILPITAS CA	USGS
Guadalupe	Discharge	15-minute	17 ft NAVD88	11169025 GUADALUPE R ABV HWY 101 A SAN JOSE CA	USGS
	Temperature	(min every month)	17 ft NAVD88	11169025 GUADALUPE R ABV HWY 101 A SAN JOSE CA	USGS
	SSC	Random dates (min every month)	17 ft NAVD88	11169025 GUADALUPE R ABV HWY 101 A SAN JOSE CA	USGS
Pacific	Temperature	(min every month)	-	46026 18 NM West of San Francisco, CA	NOAA
PointReyes	Waterlevel	hourly	-	9415020 Point Reyes, CA	NOAA

Table A.1: Data Sources regarding tides and rivers

A.2. Data sources observation points

Figure A.3: Data sources observation points

Location	Parameter	Data-Interval	Depth measurement	Monitoring site	Operator
Benicia	SSC	15-minute	10 ft NGVD29	11455780 SUISUN BAY A BENICIA BRIDGE NR BENICIA CA	USGS
Richmond-San Rafael Bridge	SSC [upper]	15-minute	30 ft from bed	376507122264701 SAN FRANCISCO BAY A RICHMOND-SAN RAFAEL BRIDGE CA	USGS
	SSC [Lower]	15-minute	5 ft from bed	376507122264701 SAN FRANCISCO BAY A RICHMOND-SAN RAFAEL BRIDGE CA	USGS
	Temperature [upper]	15-minute	30 ft from bed	376507122264701 SAN FRANCISCO BAY A RICHMOND-SAN RAFAEL BRIDGE CA	USGS
Alcatraz Island	Salinity	15-minute	12 ft above NGVD29	37493812251801 SAN FRANCISCO BAY A NE SHORE ALCATRAZ ISLAND CA	USGS
	Temperature	15-minute	12 ft above NGVD29	37493812251801 SAN FRANCISCO BAY A NE SHORE ALCATRAZ ISLAND CA	USGS
	SSC	15-minute	12 ft above NGVD29	37493812251801 SAN FRANCISCO BAY A NE SHORE ALCATRAZ ISLAND CA	USGS
Pier17	Salinity	15-minute	0 ft NGVD29	374811122235001 SAN FRANCISCO BAY A PIER 17 A SAN FRANCISCO CA	USGS
	Temperature	15-minute	0 ft NGVD29	374811122235001 SAN FRANCISCO BAY A PIER 17 A SAN FRANCISCO CA	USGS
	SSC	15-minute	0 ft NGVD29	374811122235001 SAN FRANCISCO BAY A PIER 17 A SAN FRANCISCO CA	USGS
Dumbarton Bridge	temperature [upper	15-minute	25ft from bed	373015122071000 SOUTH SAN FRANCISCO BAY AT DUMBARTON BRIDGE CA	USGS
	SSC [Upper]	15-minute	25ft from bed	373015122071000 SOUTH SAN FRANCISCO BAY AT DUMBARTON	USGS
	SSC [Lower]	15-minute	4ft from bed	373015122071000 SOUTH SAN FRANCISCO BAY AT DUMBARTON	USGS

Table A.2: Data Sources observation points

A.3. Data sources regarding Waste-Water treatment plants

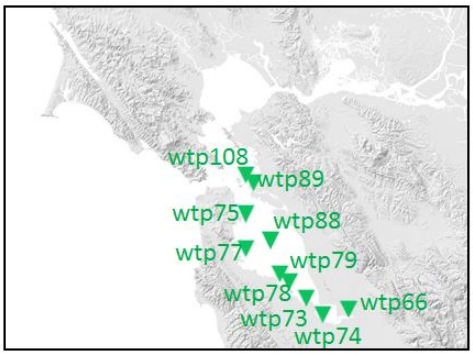

Figure A.4: Data Sources regarding Waste-Water treatment plants

Location	Parameter	Data-Interval	Operator
WTP 66-108	Discharge	once every day	SFEI
	Temperature	once every day	SFEI

Table A.3: Data Sources regarding Waste-Water treatment plants

A.4. Data sources Polaris cruise

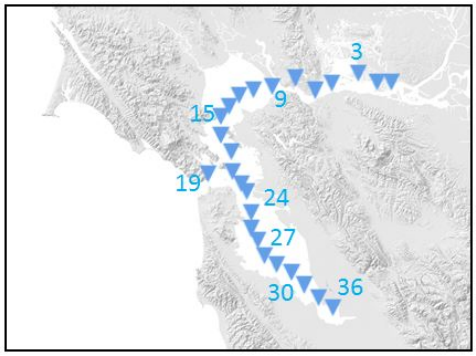

Figure A.5: Data sources Polaris cruise

Location	Parameter	Data-Interval	Depth measurement	Operator
Station 1-36	SSC [discrete]	random, once every month	1 m depth interval	USGS
	SSC [Calculated]	random, once every month	1 m depth interval	Cloern and Schraga
	Temperature	random, once every month	1 m depth interval	Cloern and Schraga
	Salinity	random, once every month	1 m depth interval	Cloern and Schraga

Table A.4: Data Sources regarding Polaris cruise

A.5. Data sources Wind

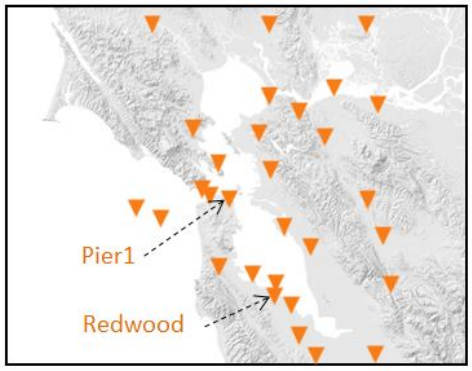

Figure A.6: Data sources wind

Location	Parameter	Data-Interval	Operator
Pier1	Wind speed	-	NOAA
	Wind direction	-	NOAA
Redwood	Wind speed	-	NOAA
	Wind direction	-	NOAA
Other	Wind speed	random dates	University
	Wind direction	random dates	University

Table A.5: Data sources wind

B

Bed shear stress due to wind in Delft3D FM

From the system analysis it became apparent that the wind could have a major influence in the re-suspension of the sediment in the water column. For that reason the some extra attention went to the modelling of the bed shear stress in Delft3D FM. The bed shear stress due to the stirring of wind waves was not included in the bed shear stress of former Delft3D versions.
Therefore the calculation of the bed shear stress according to Swart was included in the model, to incorporate the bed shear stress due to wind waves in the total bed shear stress. According to Swart (1974) the total bed shear stess is calculated as follows;

$$\tau_{totalbedshearstress} = \tau_{current} + \tau_{wave} \tag{B.1}$$

where $\tau_{current}$ is determined like;

$$\begin{aligned} \tau_{current} &= \rho * u^*_{current}2 \\ u^*_{current} &= \sqrt{c_f} * u \end{aligned} \tag{B.2}$$

and τ_{wave} is determine like ;

$$\begin{aligned} \tau_{wave} &= \rho * u^2_{wave} \\ u^*_{wave} &= 0.5 * f_w * u^2_{orb} \\ f_w &= 0.00251 * e^{(14/a)^{-0.19}} \\ a &= T_{sig} * u_{orb}/z_0 \\ z_0 &= 1/30 * k_{s_w ave} \end{aligned} \tag{B.3}$$

The two different manners of calculating the total bed shear stress are compared with each other, by modelling different wind scenarios with a small part of the model shown in figure 3.2. The most southern part of South Bay is used here. The grid is shown in figure B.1b and the bathymetry in figure B.1a. The small model used, has a deep channel and very shallow shoals, so the difference between two should be noticeable in the model runs.

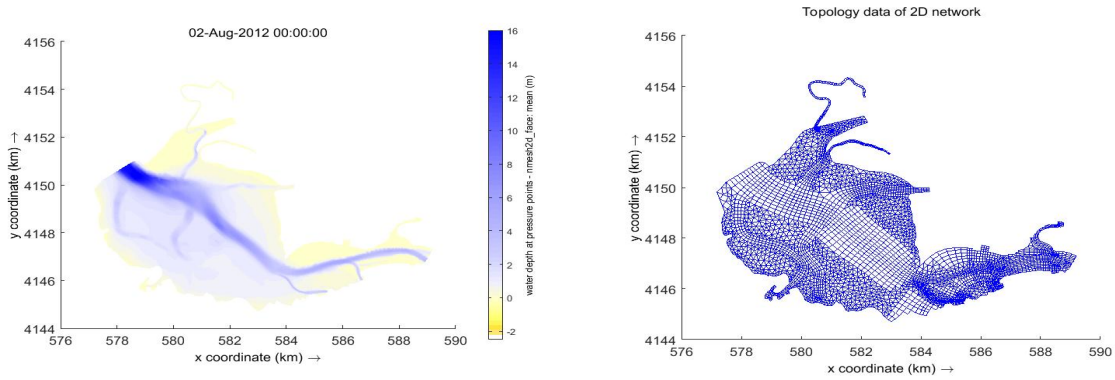

(a) Depth (b) Grid

Several scenario runs are done to asses if the models are correctly showing the total bed shear stress. Figure B.2 shows the wind magnitude and its direction in South Bay period for two distinct periods of time. In December the wind direction is highly fluctuating and the magnitude of the wind speed can be up to 10 m/s.

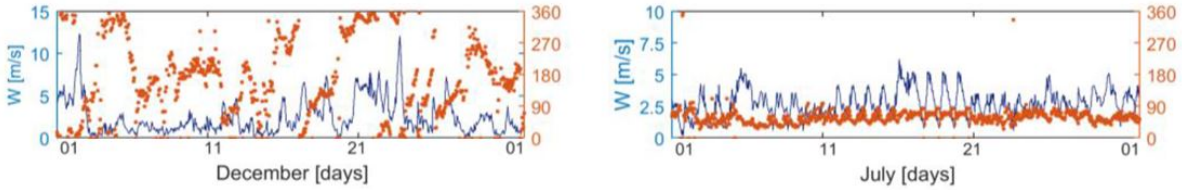

Figure B.2: The wind at South Bay

B.1. Over a tidal cycle

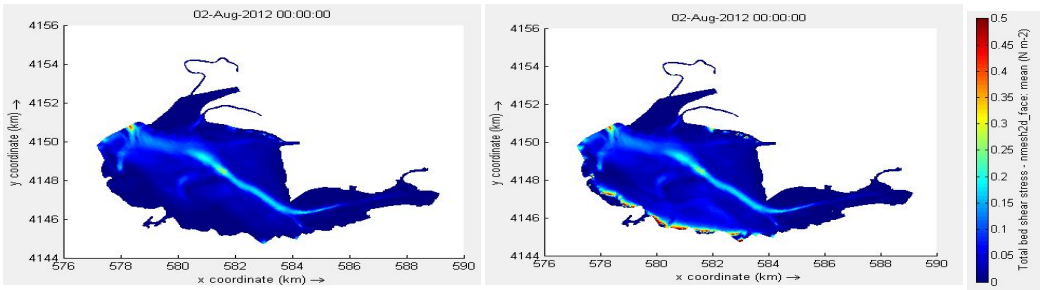

(a) Without wind waves(former FM coding) (b) With wind waves according to Swart

Figure B.3: Tau bed current for a windspeed of **2,5** m/s and a winddirection form the **North** at flood water.

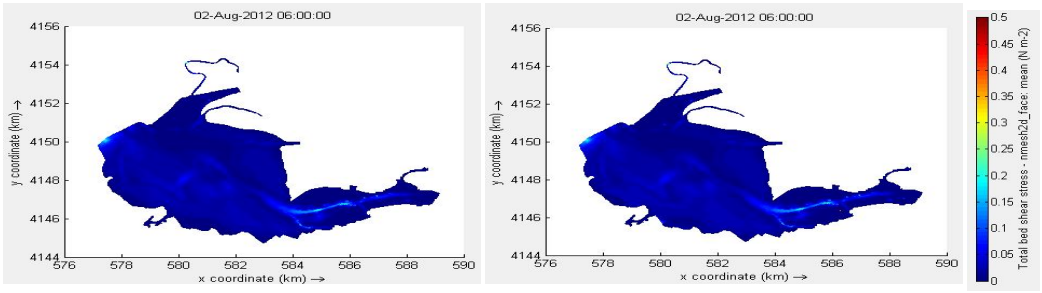

(a) Without wind waves(former FM coding) (b) With wind waves according to Swart

Figure B.4: Tau bed current for a windspeed of **2,5** m/s and a winddirection form the **North** at high water.

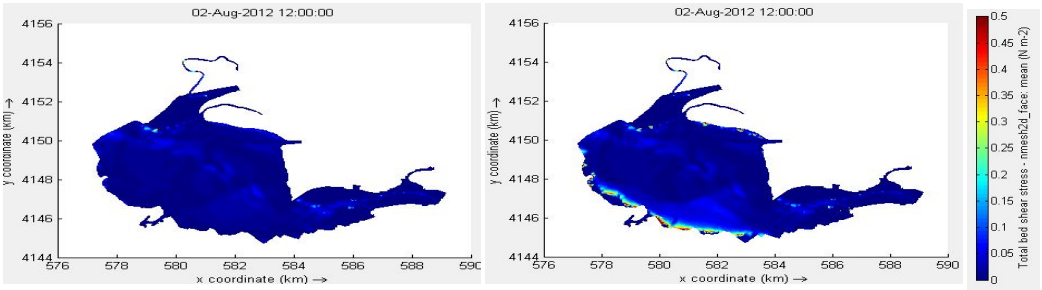

(a) Without wind waves(former FM coding) (b) With wind waves according to Swart

Figure B.5: Tau bed current for a windspeed of **2,5** m/s and a winddirection form the **North** at ebb.

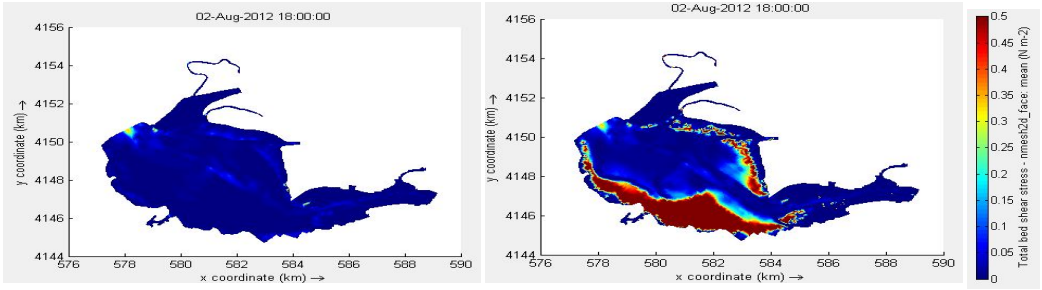

(a) Without wind waves(former FM coding) (b) With wind waves according to Swart

Figure B.6: Tau bed current for a windspeed of **2,5** m/s and a winddirection form the **North** at low water.

B.2. Different wind magnitudes

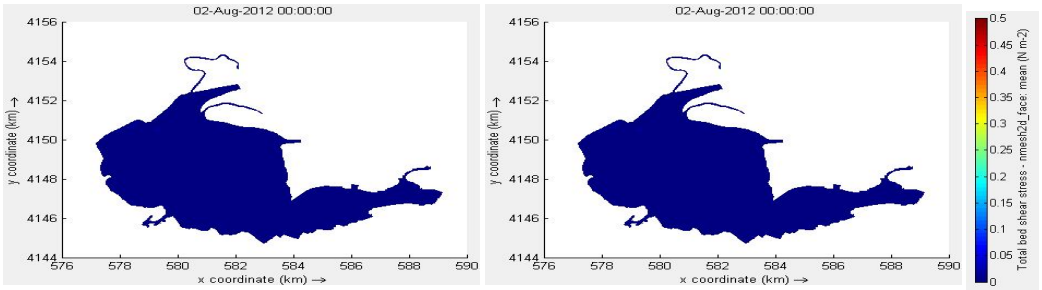

(a) Without wind waves(former FM coding) (b) With wind waves according to Swart

Figure B.7: Tau bed current for a windspeed of **2.5** m/s and a winddirection form the **north**.

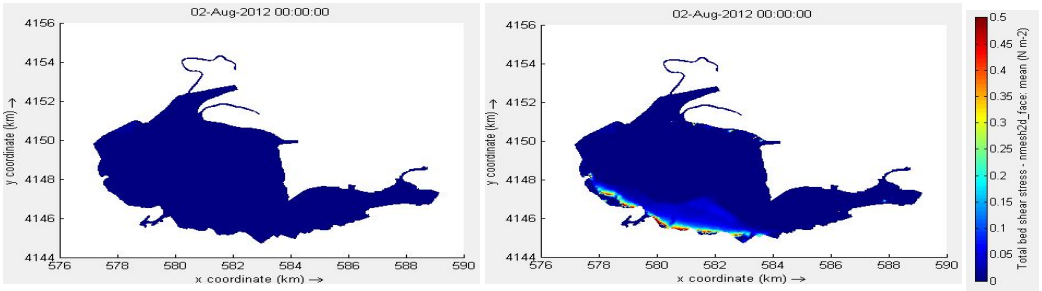

(a) Without wind waves(former FM coding) (b) With wind waves according to Swart

Figure B.8: Tau bed current for a windspeed of **5** m/s and a winddirection form the **north**.

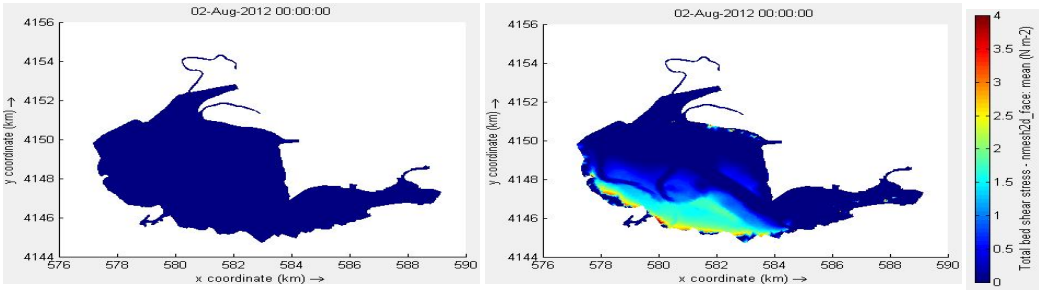

(a) Without wind waves(former FM coding) (b) With wind waves according to Swart

Figure B.9: Tau bed current for a windspeed of **10** m/s and a winddirection form the **north**.

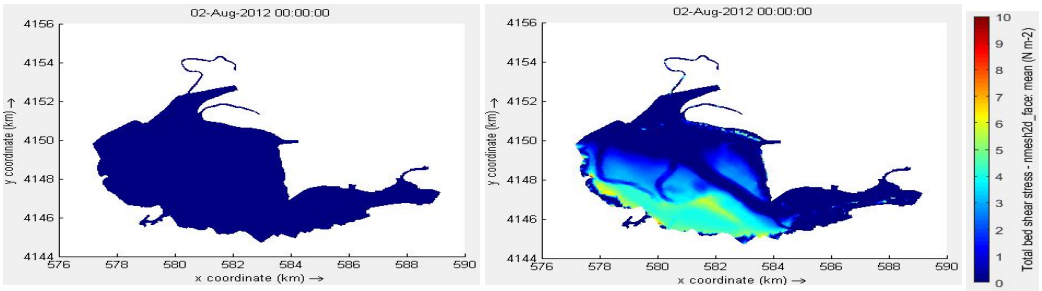

(a) Without wind waves(former FM coding) (b) With wind waves according to Swart

Figure B.10: Tau bed current for a windspeed of **0** m/s and a winddirection form the **north**.

B.3. Different wind directions

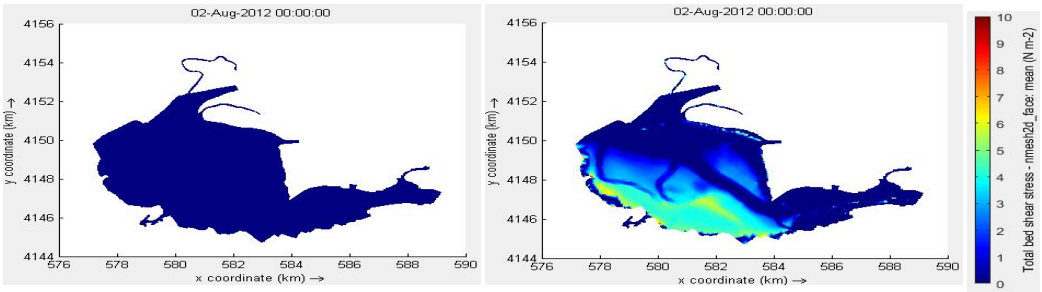

(a) Without wind waves(former FM coding) (b) With wind waves according to Swart

Figure B.11: Tau bed current for a windspeed of **10** m/s and a winddirection form the **North**.

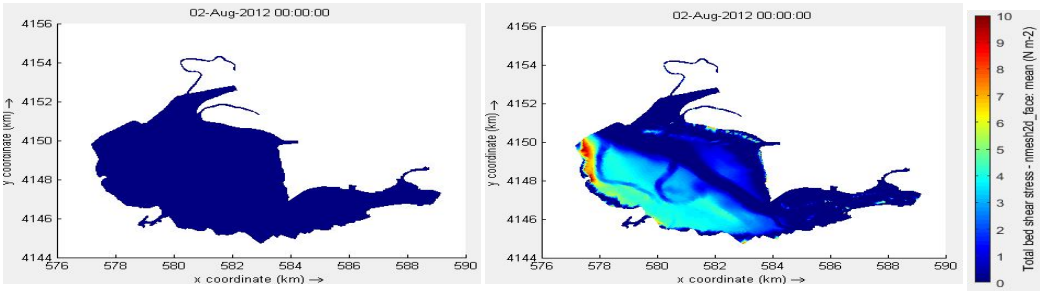

(a) Without wind waves(former FM coding) (b) With wind waves according to Swart

Figure B.12: Tau bed current for a windspeed of **10** m/s and a winddirection form the **East**.

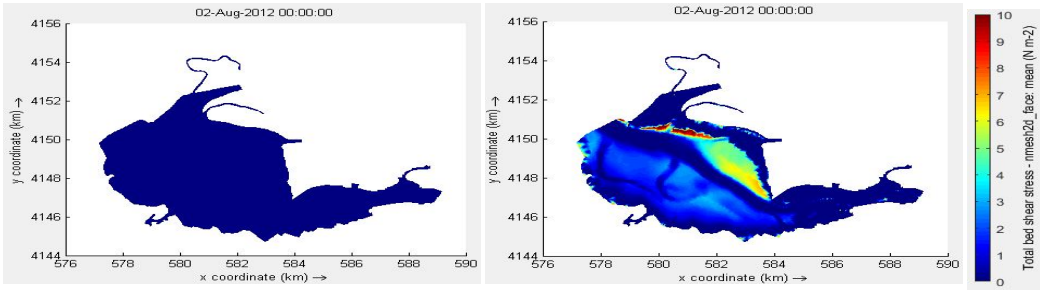

(a) Without wind waves(former FM coding) (b) With wind waves according to Swart

Figure B.13: Tau bed current for a windspeed of **10** m/s and a winddirection form the **South**.

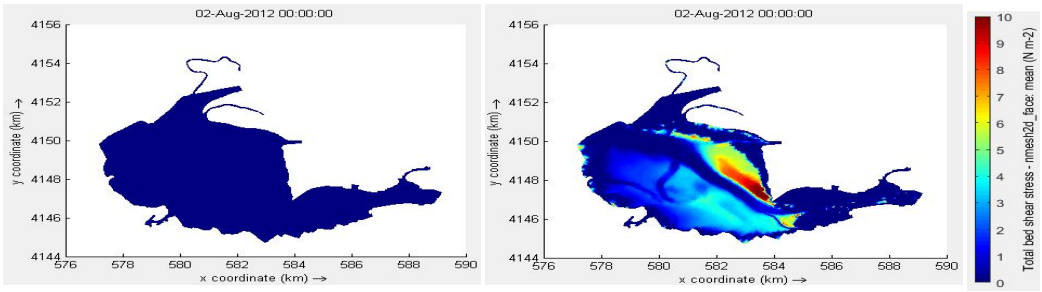

(a) Without wind waves(former FM coding) (b) With wind waves according to Swart

Figure B.14: Tau bed current for a windspeed of **10** m/s and a winddirection form the **West**.

C

Continuity

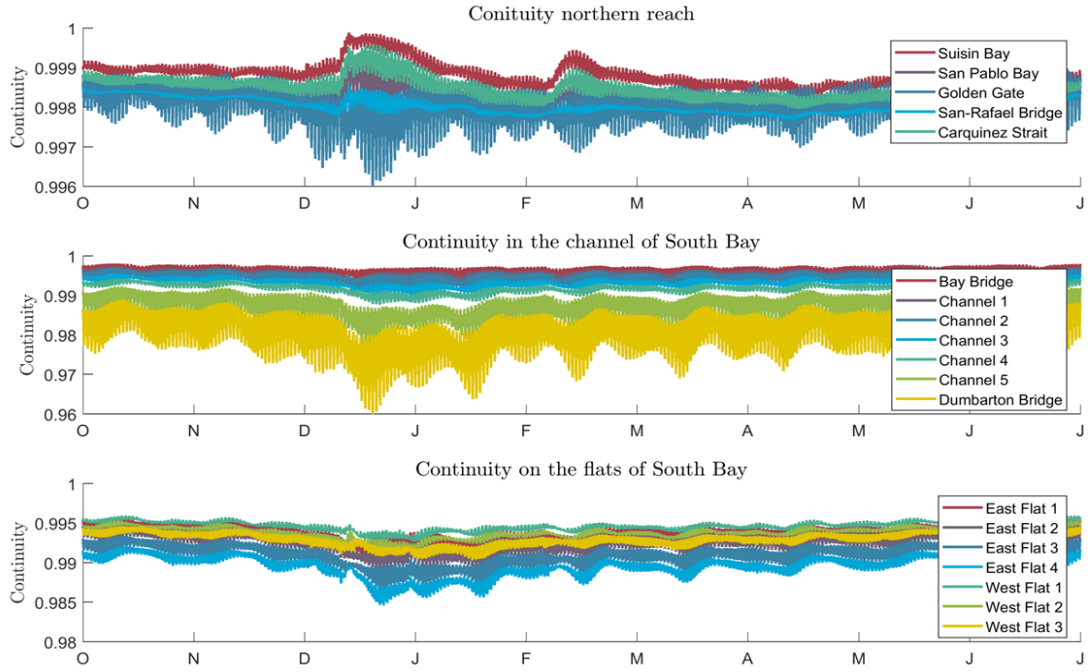

Figure C.1: This figure displays the Continuity over a simulation year for the northern reach (top plot), in the channel of South Bay (middle plot) and on the flats of South Bay (lower plot)

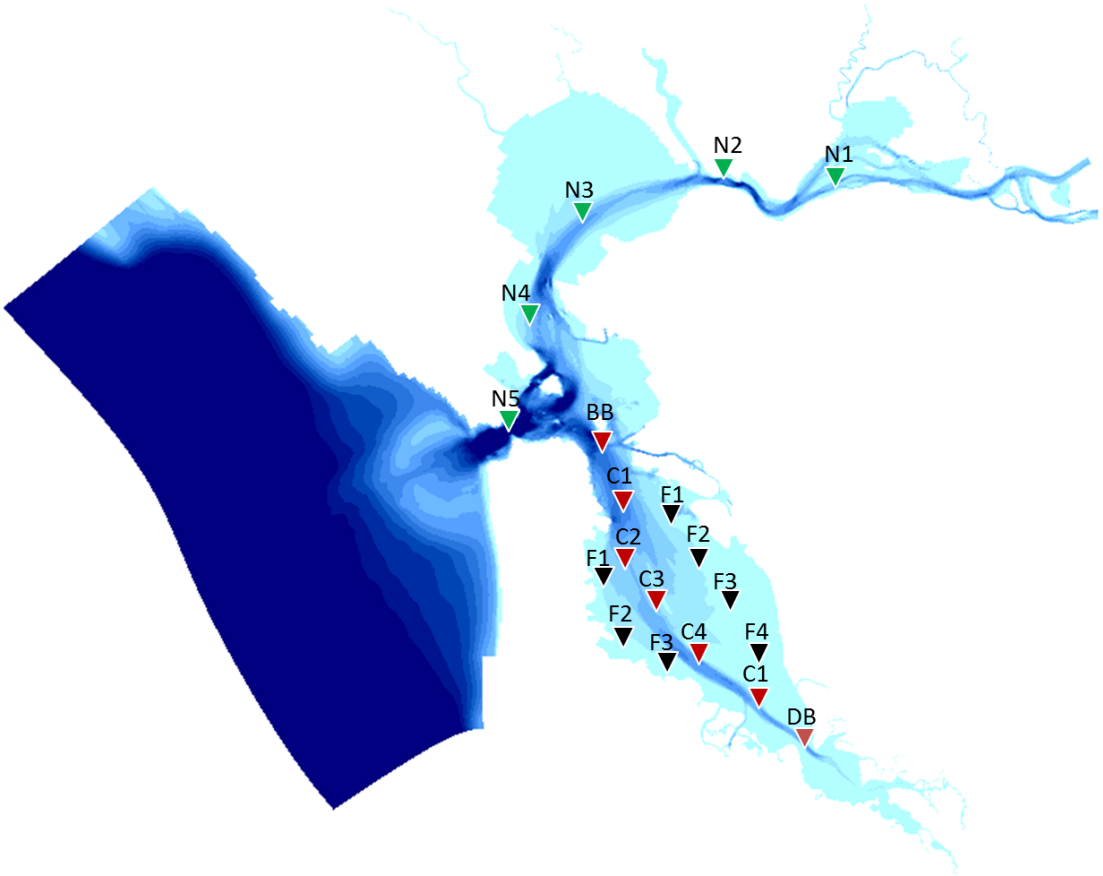

Figure C.2: The different plots show multiple data sources. A) In the upper left plot are data sources related to data about the rivers and the tides shown by red triangles. B) The upper middle plot shows in green the data locations regarding the waste-water treatment plants. C) In the upper right blow are the measurement locations during the Polaris cruise displayed in blue. D) The dark blue triangles in the lower left plot are the data sources related to observations buoys in the estuary. E) In the lower middle plot are the wind measurement locations shown in orange. F) The purple triangles in the lower right plot shows the measurement locations by the California Department for fish and wildlife.

Abbreviation		**Abbreviation**		**Abbreviation**	
N1	Suisin Bay	BB	Bay Bridge	F1	East Flat 1
N2	Carquinez Strait	C1	Channel 1	F2	East Flat 2
N3	San Pablo Bay	C2	Channel 2	F3	East Flat 3
N4	San-Radael Bridge	C3	Channel 3	F4	East Flat 4
N5	Golden Gate	C4	Channel 4	F5	West Flat 1
		C5	Channel 5	F6	West Flat 2
		DB	Dumbarton Bridge	F7	West Flat 3

Table C.1: Several settings of the DelwaQ module

D

Model Results

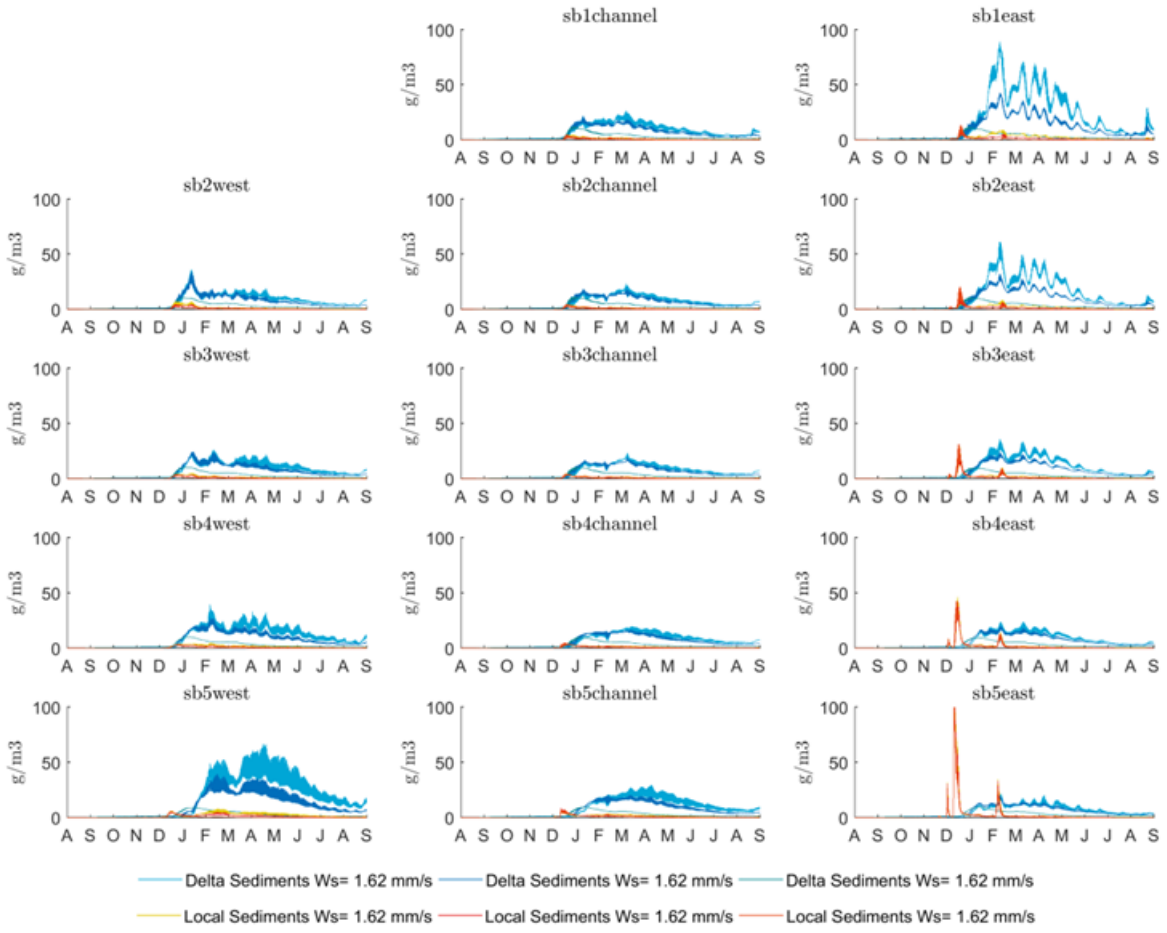

Figure D.1: The SSC at the sub-areas in South Bay in a dry year such as WY2015(a) are shown in the figure. The SSC is area- and depth averaged. The subareas are marked in Fig(3.5b). The dotted rectangle reflects the period of high river flows. The sediments from the Sacramento-San Joaquin Delta are labelled as Delta sediments. The sediments from the local tributaries are labelled as the local sediments.

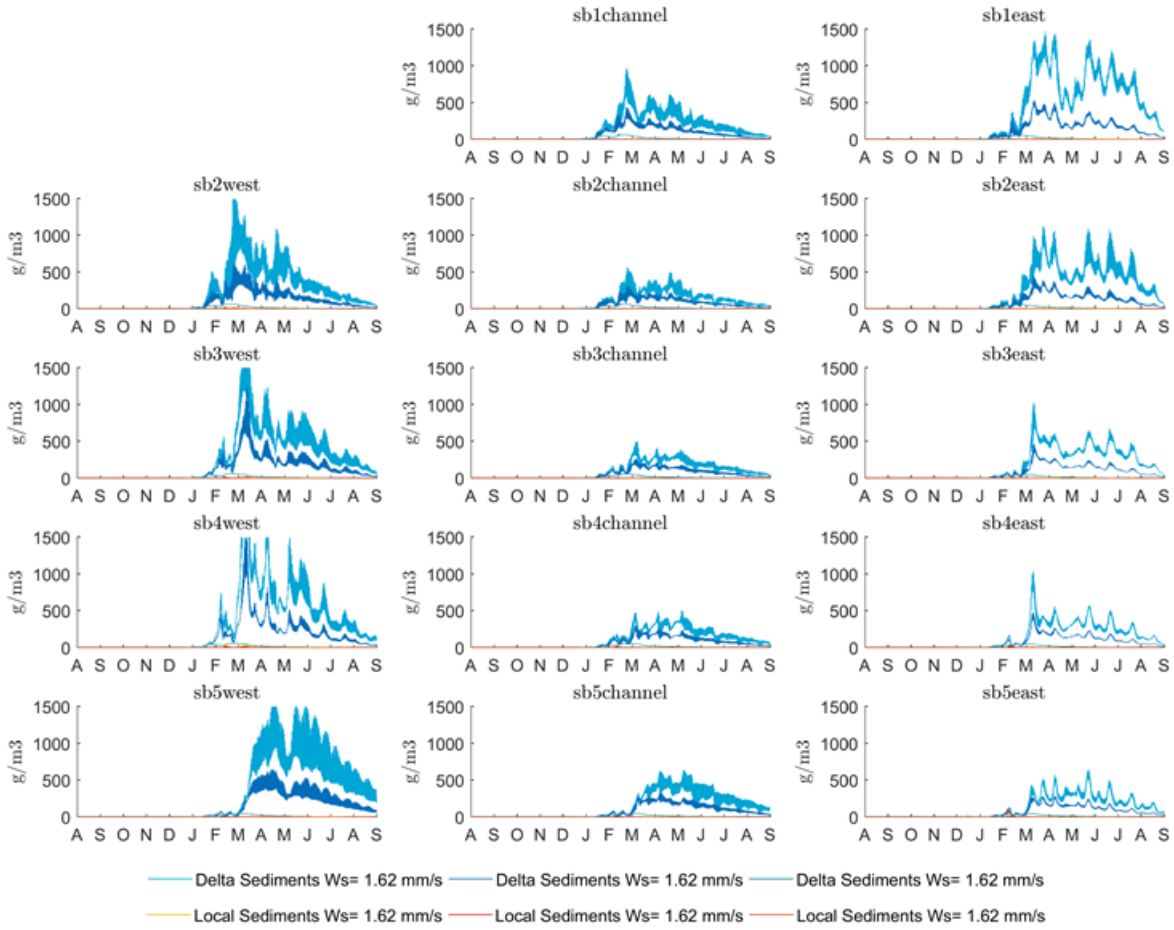

Figure D.2: The SSC at the sub areas in South Bay in a wet year such as WY2017(b) are shown in the figure. The SSC is area- and depth averaged. The subareas are marked in Fig(3.5b). The dotted rectangle reflects the period of high river flows. The sediments from the Sacramento-San Joaquin Delta are labelled as Delta sediments. The sediments from the local tributaries are labelled as the local sediments. There is no sediment data available for the local sediments during the WY2017. Therefore, the are no local sediments included in the simulation of WY2017.

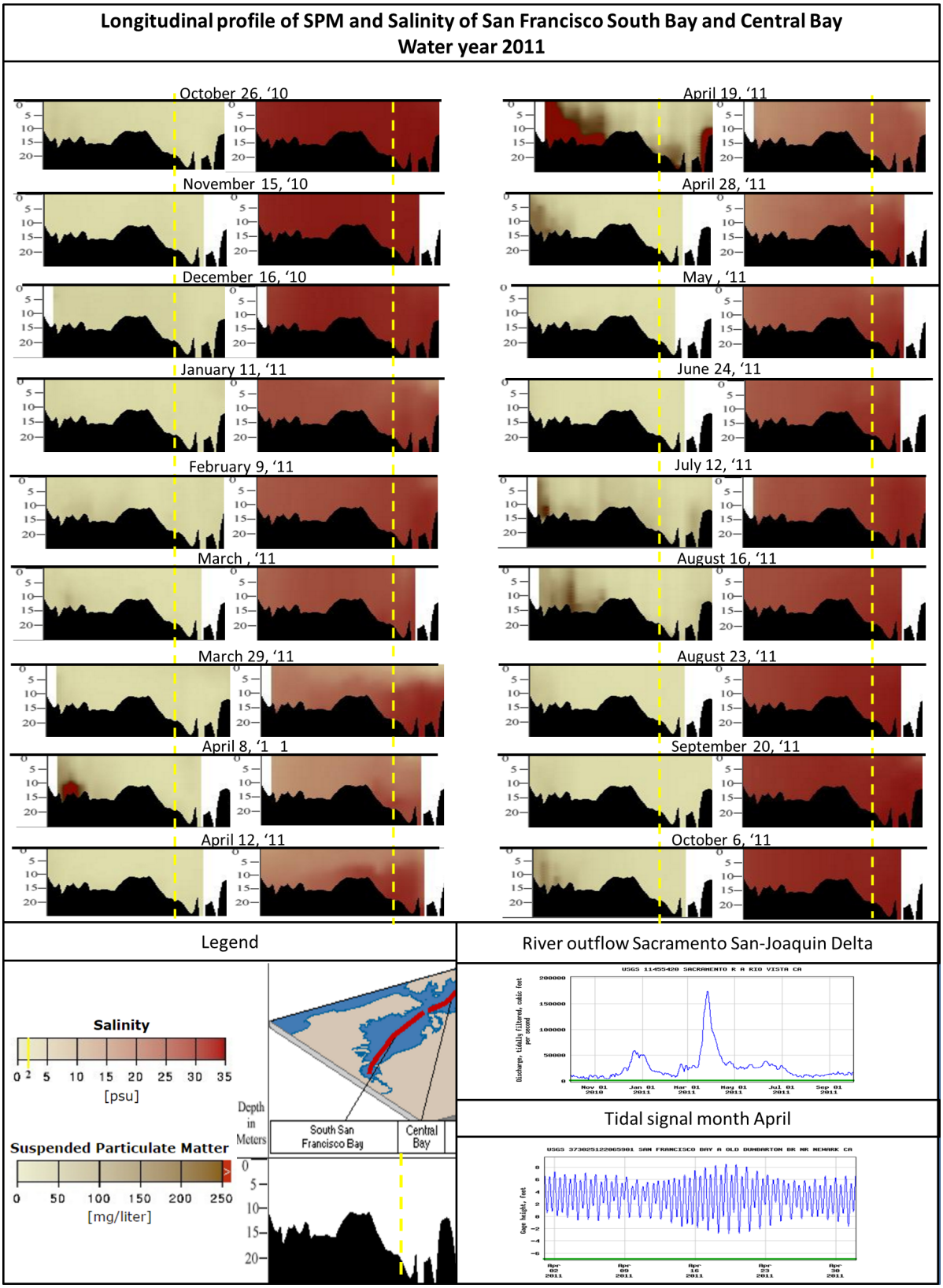

Figure D.3: Longitudinal profile of the SPM and salinity from the head of San Francisco (left) to Central Bay (right). The transition between the two bay's is marked with the dotted yellow line. The SPM is shown in mg/liter, the salinity is shown in PSU, as can be seen in the legend in the left lower corner. The profiles are from USGS, who measured the profiles during irregular measurements. All measurements done are shown with the date that they were observed. In the lower right corner some hydrodynamic forcings are plotted. The river outflow over the year from Sacramento river and the water elevation in South Bay in April of 2011 USGS [2017]

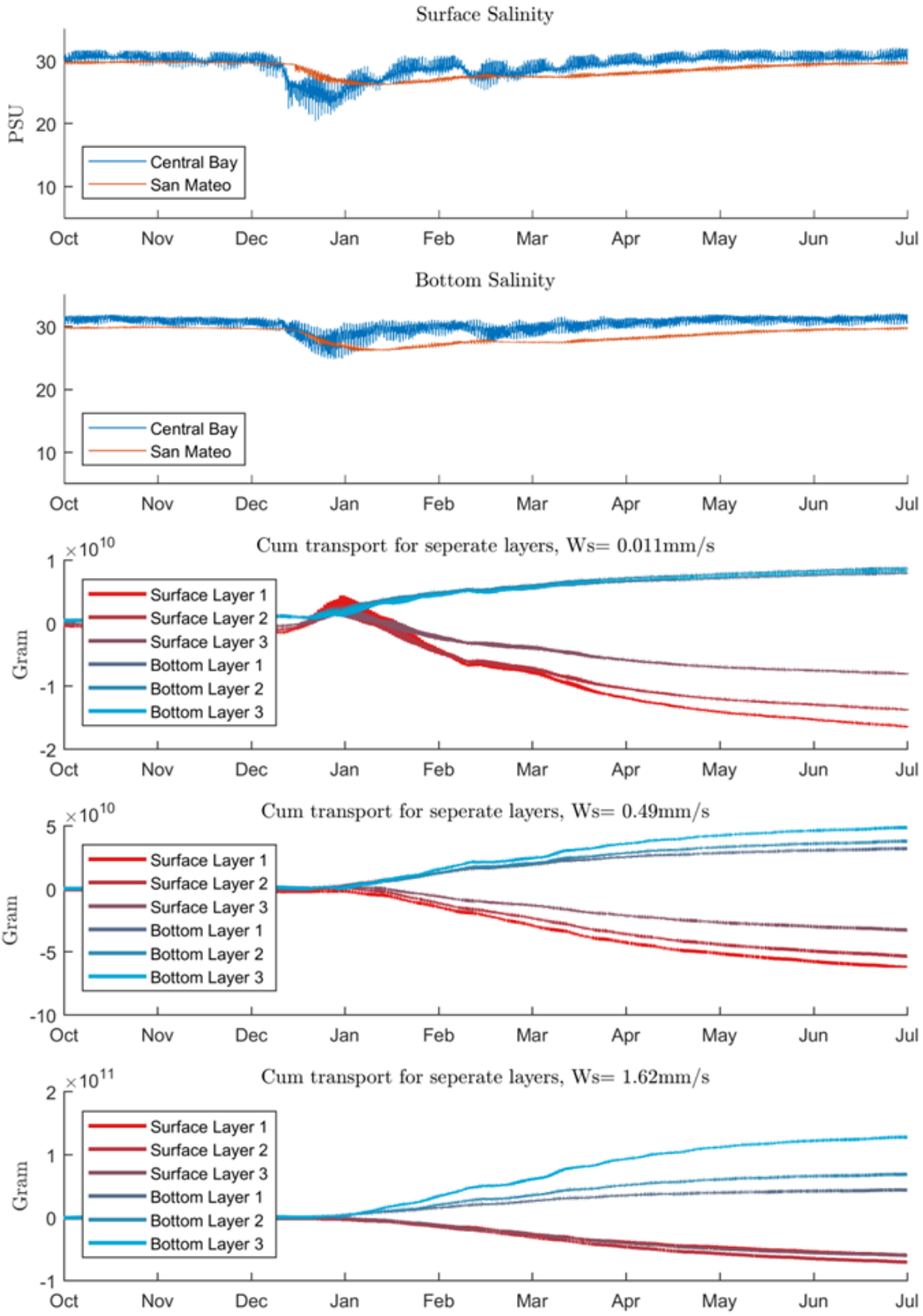

Figure D.4: This figures display the bottom and surface salinity's at Central Bay (blue line) and San Mateo (red line) in WY2015. The cumulative transport over the transect at Bay Bridge is given for the three sediment classes for the three upper (red lines) and three lowest layers (blue lines).

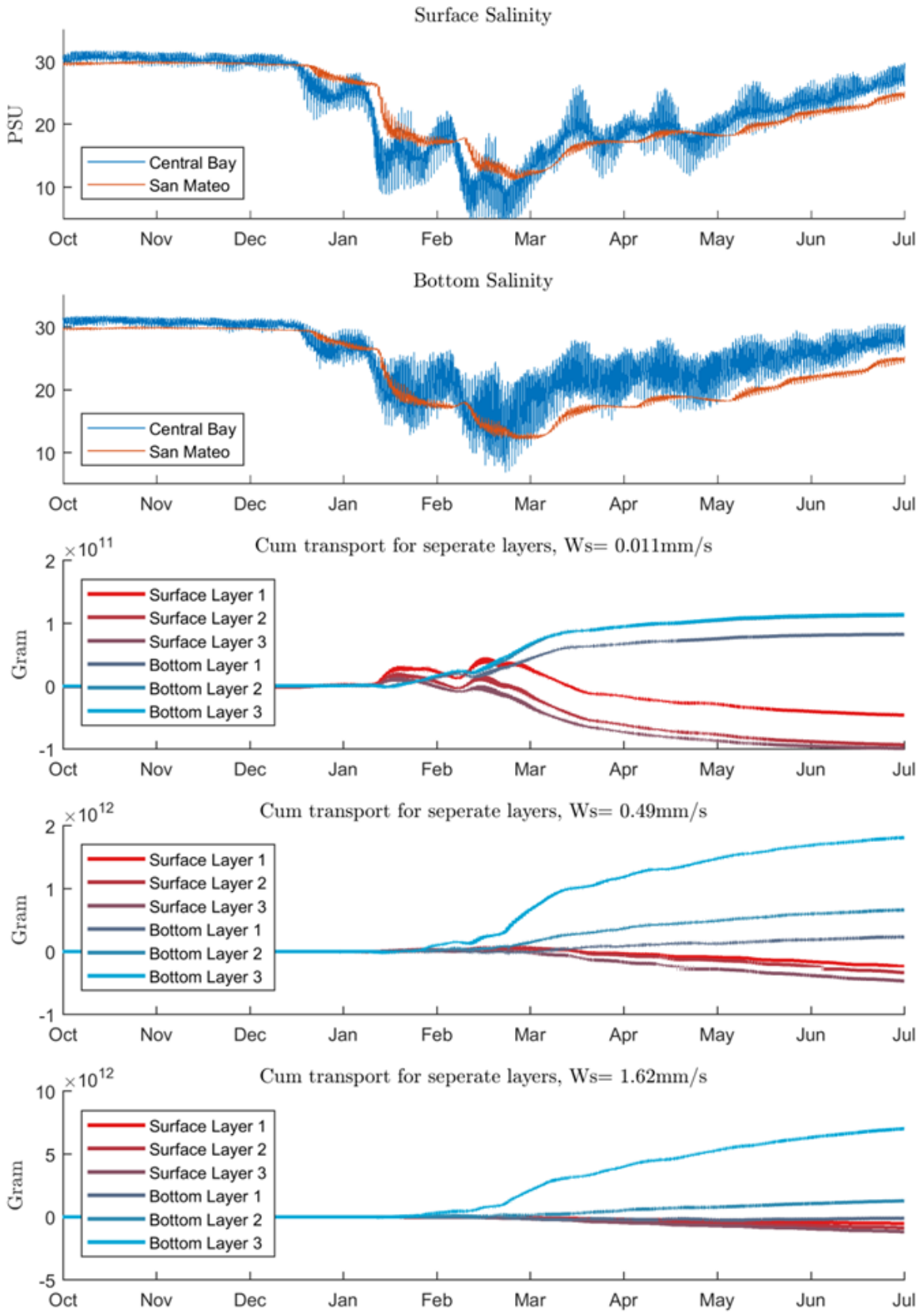

Figure D.5: This figures display the bottom and surface salinity's at Central Bay (blue line) and San Mateo (red line) in WY2017. The cumulative transport over the transect at Bay Bridge is given for the three sediment classes for the three upper (red lines) and three lowest layers (blue lines).